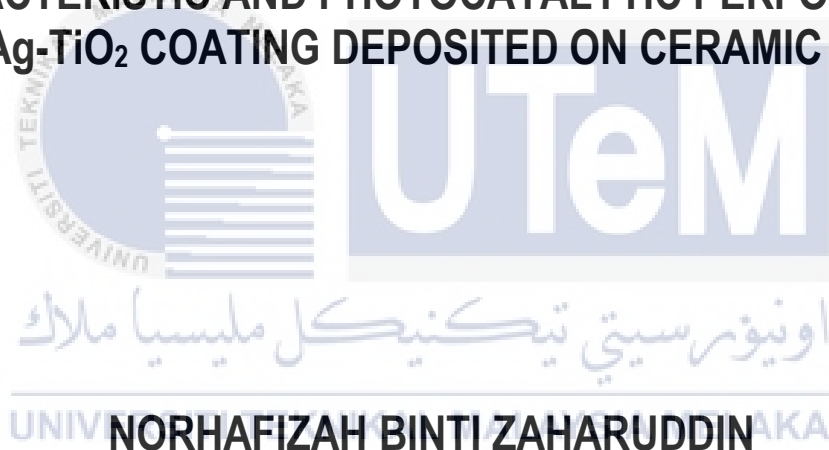UNIVERSITI TEKNIKAL MALAYSIA MELAKA

EFFECT OF DEGUSSA ADDITION AND Ag CONTENTS ON THE CHARACTERISTIC AND PHOTOCATALYTIC PERFORMANCE OF Ag-TiO$_2$ COATING DEPOSITED ON CERAMIC TILES

NORHAFIZAH BINTI ZAHARUDDIN

DOCTOR OF PHILOSOPHY

2024

Faculty of Industrial and Manufacturing Technology and Engineering

EFFECT OF DEGUSSA ADDITION AND Ag CONTENTS ON THE CHARACTERISTIC AND PHOTOCATALYTIC PERFORMANCE OF Ag-TiO$_2$ COATING DEPOSITED ON CERAMIC TILES
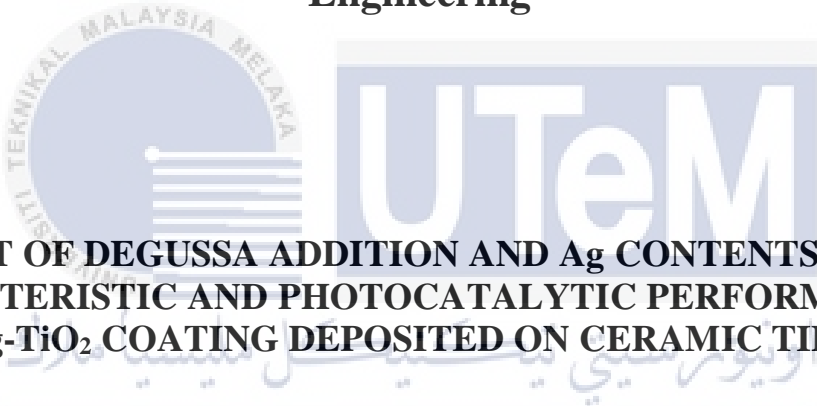
Norhafizah Binti Zaharuddin

Doctor of Philosophy

2024

EFFECT OF DEGUSSA ADDITION AND Ag CONTENTS ON THE CHARACTERISTIC AND PHOTOCATALYTIC PERFORMANCE OF Ag-TiO$_2$ COATING DEPOSITED ON CERAMIC TILES

NORHAFIZAH BINTI ZAHARUDDIN

**A thesis submitted
in fulfillment of the requirements for the degree of
Doctor of Philosophy**

Faculty of Industrial and Manufacturing Technology and Engineering

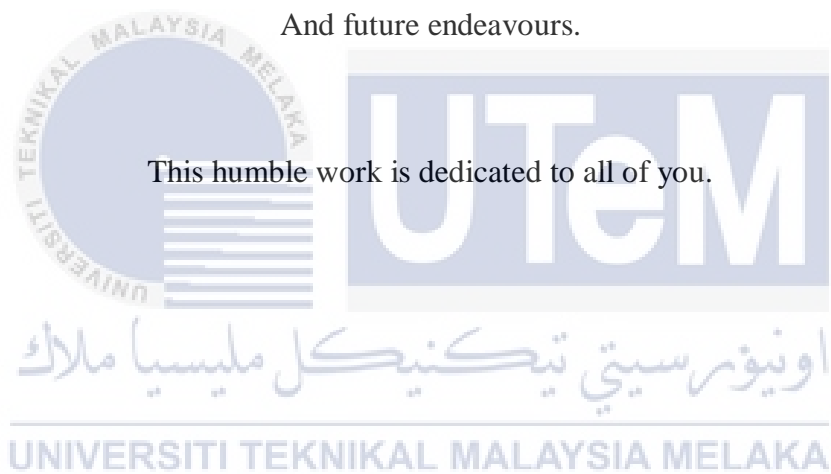**UNIVERSITI TEKNIKAL MALAYSIA MELAKA**

2024

DEDICATION

To my family member especially my beloved parents,

To the people who have supported me throughout the journey,

And future endeavours.

This humble work is dedicated to all of you.

ABSTRACT

TiO_2 coating has drawn great attention in various field of application including the ceramic industry. The limitation of TiO_2 photocatalytic activity that only reacts on short-wavelength ultraviolet irradiation has brought an effort to extend its potential to visible range by reducing the fast rate of electron-hole pair recombination. Hence, doping with semiconductor such as silver (Ag) incorporated TiO_2 is proposed. However, Ag incorporated TiO_2 had some issues where the use of Ag with high concentration decreases the surface charge that can cause an agglomeration of Ag species and reduction to Ag^o particles on TiO_2 surface. Lowering the amount of Ag concentration thereafter contributed to the formation of AgO, Ag_2O and Ag^o. The amount of Ag that can control the particles size, surface area, thermal stability and band gap that contributes towards good photocatalytic performance is still vague and continuously studied. Yet, the works of $Ag-TiO_2$ coating reported mostly on the surface of glass, metal and fabric instead of ceramic surfaces. Therefore, in this study, the deposition of $Ag-TiO_2$ coating was carried out on unglazed and glazed ceramic tiles. Firstly, the effect of Degussa P25 on the $Ag-TiO_2$ coating was studied to decide the needs of Degussa P25 in synthesizing $Ag-TiO_2$ sol formulation. Later, the effect of Ag content (2.5, 5.0 and 7.5 mol %) on the microstructure (crystalline phase, crystal size, elemental distribution, morphology and cross section surface) of the $Ag-TiO_2$ coated ceramic tiles (unglazed and glazed) were examined and its photocatalytic performance were tested. This yield to the self-cleaning properties of the intended antibacterial ceramic tiles application. The coatings were heat treated at 500 °C and characterized by Glancing angle X-ray diffraction (GAXRD) and Scanning electron microscopy (SEM), Field electron scanning microscopy (FESEM) coupled Energy-Dispersive X-ray Spectrometer (EDX) and further tested for environmental application using methylene blue degradation (MB) under ultraviolet (UV) and visible light irradiation. The results of the present study suggest that $Ag-TiO_2$ sol can be synthesized without the aid of Degussa P25 where Degussa P25 possibly hinders the formation of Ag metallic. $Ag-TiO_2$ coating deposited on the unglazed tile was observed sip into the pores of ceramic surfaces. The finding highlights that $Ag-TiO_2$ coating deposited on unglazed and glazed improved photocatalytic performances at 5.0 mol % Ag content under visible light irradiation. This is because 5.0 mol % Ag content presented uneven small density of cracks over the surface with more Ag demonstrated by surface morphology and elemental mapping. Also, it can be related to their active crystallites that react well upon visible irradiation. Hence it can be deduced that the amount of Ag needed for good photocatalytic performance needs to take into account the substrate and surrounding condition.

KESAN PENAMBAHAN DEGUSSA DAN KANDUNGAN Ag KE ATAS CIRI DAN PRESTASI PEMANGKIN-FOTO SALUTAN Ag-TiO₂ DIENDAPKAN PADA JUBIN SERAMIK

ABSTRAK

Salutan TiO_2 telah menarik perhatian pelbagai bidang aplikasi termasuk industri seramik. Had aktiviti fotobermangkin TiO_2 yang hanya bertindak balas pada penyinaran gelombang pendek ultraungu telah mencetuskan usaha untuk meluaskan potensinya pada gelombang julat boleh dilihat dengan cara mengurangkan kadar pantas penggabungan semula pasangan elektron-lubang. Oleh itu pengedopan dengan bahan separuh pengalir seperti perak (Ag) telah dicadangkan ke dalam TiO_2. Walau bagaimanapun, Ag yang dimasukkan ke dalam TiO_2 dengan kepekatan tinggi boleh mengurangkan cas permukaan yang akan menyebabkan penggumpalan spesies Ag dan penurunan kepada zarah Ag^o pada permukaan TiO_2. Sebaliknya, pengurangan jumlah kepekatan Ag menyumbang kepada pembentukan AgO, Ag_2O dan Ag^o. Jumlah Ag yang boleh mengawal saiz zarah, luas permukaan, kestabilan terma dan jurang jalur kearah prestasi fotobermangkin yang bagus masih kabur dan terus dikaji. Namun, kerja-kerja salutan Ag-TiO_2 yang dilaporkan kebanyakannya adalah pada permukaan kaca, logam dan fabrik dan bukannya permukaan seramik. Dalam kajian ini, pengendapan salutan Ag-TiO_2 telah dijalankan pada jubin seramik tidak berlicau dan licau. Pertama, kesan Degussa P25 pada salutan Ag-TiO_2 telah dikaji untuk menentukan keperluan Degussa P25 dalam mensintesis formulasi sol Ag-TiO_2. Kemudian, kesan kandungan Ag (2.5, 5.0 dan 7.5 mol %) ke atas mikrostruktur (fasa hablur, saiz kristal, taburan unsur, morfologi dan permukaan keratan rentas) jubin seramik tidak berlicau dan licau bersalut Ag-TiO_2 telah diperiksa dan prestasi fotobermangkinnya telah diuji. Ini menghasilkan sifat pembersihan kendiri bagi jubin seramik antibakteria. Salutan telah dirawat haba pada 500 ℃ dan dicirikan melalui sudut kerling pembelauan sinar-X (GAXRD) dan Mikroskop pengimbasan elektron (SEM), Mikroskop pancaran medan pengimbasan electron (FESEM) ditambah Spektrometer Serakan Tenaga Sinar-X (EDX) dan diuji untuk aplikasi alam sekitar menggunakan degradasi metilena biru (MB) di bawah sinaran ultraungu (UV) dan cahaya nampak. Keputusan kajian ini mencadangkan bahawa sol Ag-TiO_2 boleh disintesis tanpa bantuan Degussa P25 di mana Degussa P25 mungkin menghalang pembentukan logam Ag. Salutan Ag-TiO_2 yang dimendapkan pada jubin tidak berlicau meresap ke dalam liang permukaan seramik. Penemuan ini menyerlahkan bahawa salutan Ag-TiO_2 yang diendapkan pada jubin seramik tidak berlicau dan berlicau meningkatkan prestasi fotobermangkin pada 5.0 mol % Ag di bawah penyinaran cahaya boleh nampak. Ini kerana 5.0 mol % Ag menunjukkan kehadiran rekahan yang tidak sekata dengan ketumpatan kecil di atas permukaan dan lebih banyak Ag hadir pada morfologi permukaan. Ia juga dikaitkan dengan kumin hablur aktif yang bertindak balas dengan baik terhadap sinaran boleh nampak. Oleh itu, dapat disimpulkan bahawa jumlah Ag yang diperlukan untuk prestasi fotobermangkin yang baik perlu mengambil kira substrat dan keadaan sekeliling.

ACKNOWLEDGEMENTS

In the Name of Allah, the Most Gracious, the Most Merciful

Alhamdullillah, praise to Allah that I am finally able to complete this thesis writing for the requirement of Doctor of Philosophy. First and foremost, I would like to acknowledge and express my sincere gratitude to my main supervisor, Assoc. Prof Dr. Jariah Mohamad Juoi for the great moral support, advices and guidance given to me to complete this research. I would also like to thank to my co-supervisor, Assoc. Prof Ts. Dr. Zulkifli Rosli for the invaluable advice and financial support through the journey.

My special thanks to my family members especially my beloved parents, Mr. Zaharuddin and Mrs. Norhayati for their endless prayer, encouragement and support. My genuine gratitude to my uncle, Mr. Rozaideen for the continuous motivation and financial support given that make me manage to complete the thesis. I also would like to express my warmth gratitude to all the staff of Faculty of Industrial and Manufacturing Engineering, Universiti Teknikal Malaysia Melaka that involved directly or indirectly during the research.

Last but not least, I am very grateful to my colleagues, in particular Amalina, Dalilah, Izyanie, Najwa and Maula for the knowledge, skills, cooperation and inspiration. Thank to them that I manage to handle the experiment well. I really owed them a lot. Completing this journey was like a dream that I never imagined. Without them, this thesis would never been possible. My gratitude was never enough and I hope that this thesis can be a proof for all the support given.

TABLE OF CONTENTS

LIST OF TABLES

LIST OF FIGURES

xi

LIST OF ABBREVIATIONS

A	-	Ampere
Ag	-	Silver
Au	-	Gold
Al	-	Aluminium
$AgNO_3$	-	Silver nitrate
Ag/TiO_2	-	Silver doped TiO_2
Ba	-	Barium
Ca	-	Calcium
Cl	-	Chlorine
CuO	-	Copper oxide
DI	-	Dionised
DSCCs	-	Dye Sensitized Solar Cells
EDX	-	Energy dispersive X-ray spectroscopy
EtOH	-	Ethanol
Fe	-	Ferum
FWHM	-	Full width half maximum
GAXRD	-	Glancing Angle X-ray diffraction
HCl	-	Hydrochloric acid
H_2O	-	Water
ITO	-	Indium tin oxide
ISO	-	International Organization for Standard
JCPDS	-	Joint committee on powder diffraction standards
K	-	Potassium
MB	-	Methylene Blue
Mg	-	Magnesium
MWCNT	-	Multi-Walled Carbon Nanotubes
N	-	Nitrogen
O	-	Oxygen
PAD	-	Photo-Assisted Deposition

Pt	-	Platinum
pH	-	Potential Hydrogen
ppm	-	Part per million
P25	-	Degussa 25
rpm	-	Revolution per minute
ROS	-	Reactive Oxygen Species
SEM	-	Scanning Electron Microscope
SPR	-	Surface resonance
Sn	-	Tin
Si	-	Silicon
Ti	-	Titanium
TiO_2	-	Titanium dioxide
TTiP	-	Titanium tetraisopropoxide
TBOT	-	Tetrabutyl orthotitanate
UV	-	Ultra-violet
UV-Vis	-	Ultra-violet visible
VOC	-	Volatile organic compound
Wt	-	weight
XRD	-	X-ray Diffraction
Zn	-	Zinc
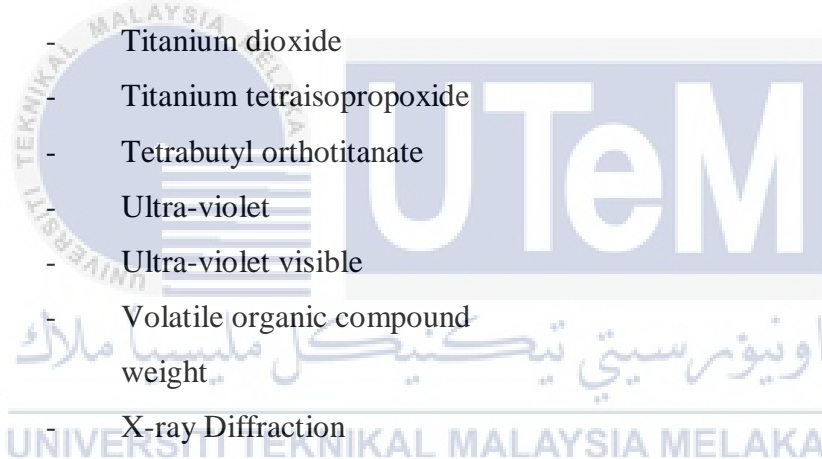
LIST OF SYMBOLS

A	-	Absorbance
cm	-	Centimeter
ca.	-	Circa/approximately
D, d	-	Diameter
e.g	-	Exempli gratia
E_P		Radiation intensity
eV	-	Electron volt
g	-	Gram
k	-	Scherrer coefficient
M	-	Molarity
m	-	Meter
ml	-	Milliliter
mm	-	Millimeter
n	-	Nano
nm	-	Nanometer
P_{MB}	-	Specific photocatalytic activity
ppm	-	Parts per million
R	-	Specific degradation rate
R_a	-	Surface roughness
s	-	Second
t_{ave}	-	Average thickness
V	-	Volume
W	-	Watt
ζ_{MB}	-	Photonic efficiency
μ	-	Micro
λ	-	Wavelength
º	-	Degree
ºC	-	Degree celcius
%	-	Percentage
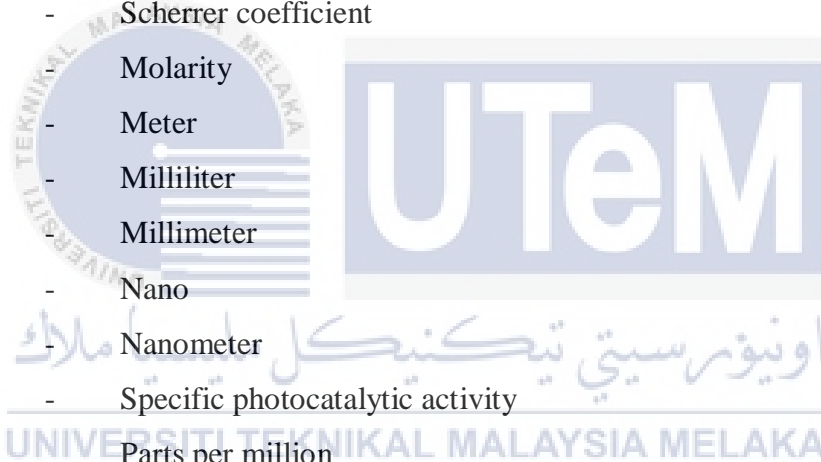
θ	-	Bragg angle
≥	-	More than or equal to
≤	-	Less than or equal to
±	-	Plus minus
ΔA_{λ}		Absorption difference

LIST OF APPENDICES

LIST OF PUBLICATIONS

Journals

1. **Hafizah, N. Z.,** Juoi, J. M., Zulkifli, M. R., and Musa, M.A, 2020. Effect of Silver Content on the Crystalline Phase and Microstructure of TiO_2 Coating Deposited on Unglazed Ceramics Tile. *International Journal of Automotive and Mechanical Engineering (IJAME),* 17(3), pp. 8179 – 8185.

2. **Hafizah**, N. Z., Juoi, J. M., Zulkifli, M. R., and Johari, N. D., 2023. Effect of Silver Doping on the Microstructure and Photocatalytic Performance of Ag-TiO_2 Coatings on Unglazed Ceramic. *Journal of Advanced Research in Micro and Nano Engineering*, 15(3) - accepted and submitted to publication 2024.

Conferences and Proceedings

1. **Hafizah, N. Z.,** Juoi, J.M., Zulkifli, M. R., Musa, M.A., 2019. Investigation on the Method of Ag Addition into TiO_2 Coating Deposited on Unglazed Ceramic Tile. *Proceedings of Innovative Research and Industrial Dialogue 2018* (IRID'18), pp. 142 – 143.

2. Paper presentation: Effect of Silver Content on the Crystalline Phase and Microstructure of TiO_2 Coating Deposited on Unglazed Ceramics Tiles. **In** *11th Malaysian Technical Universities Conference on Engineering & Technology "Communitising Technology in the Context of Industrial Revolution 4.0"*(MUCET 2019). 19 – 22 November 2019. Bukit Gambang Resort City, Kuantan.

Exhibitions

1. Poster presentation: Addition of Ag into TiO_2 Coating via Dipping and Precursor Method. **In** *Research Showcase of Innovative Research and Industrial Dialogue 2018* (IRID'18). 18 July 2018. Block B, FKP and PPS Auditorium

CHAPTER 1

INTRODUCTION

1.1 Background

Ceramic materials are one of the widely use material in various different field. It includes such as automotive, military, refractory, biotechnology, electrical, electronic and magnetic fields. The applications select its own appropriate property from ceramic materials and that's why ceramic are used in almost every field. In military, ceramic was used for making weapons, missile guidance and defence system because of the hardness and nonreactive properties. A certain use of refractories involved high technology ceramic and for biotechnology to strengthen tissues organ (Dash et al., 2023). The application of ceramic has been well developed and proposed frequently. The product of ceramic tile meanwhile is gaining popularity in both residential and commercial use because of its limitless potential. Tile is the most favourite use design materials for both in dry and wet area. Often can be seen in kitchen and bathroom renovation. The requirement of clean surfaces in every edge of our everyday live is a priority need because it involves our healthy lifestyle. Therefore, the simple easy cleaning or self-cleaning surfaces has been under the focus of nanotechnology.

Surfaces of different structure and nanocoating had become an interest among the researcher. Coating is priority in the furnishing process of a product. It was done on most of the surfaces such as ceramics, metals, polymers and wooden surfaces. There are two types of surface coating that are liquid base coating and powder coating. Both of them have different purposes and benefits. Liquid base surface coating mainly focus on corrosion

1

protection, environmental protection, increased longevity and durability, higher resale value and reduced maintenance costs of structure. Meanwhile, powder base coating generally promote less volatile organic compounds (VOC), environmental friendly, energy and material efficient.

Generally, ceramic tiles often faced with grout issues and microorganisms attack. Even so, the approach of antimicrobial and biocompatibility surfaces properties for ceramic is still rare due to the lack of experimental condition. In the unprotected ceramic surfaces, microbes are actively attack and react easily with the surfaces and leading to their growth. This arise the risk of society health and safety. Therefore, effort on developing a highly photocatalyst ability of ceramic tile for the purpose of antimicrobial ceramic surface will greatly contribute to disinfection efficiency.

Thus, nanocoating technology was introduced on metal, polymer, ceramic, wood, and even fabric surfaces. In between those surfaces, coating on ceramic surfaces is not widely reported. Ceramic materials were extensively used in both indoor and outdoor application and frequently found is ceramic tile. Ceramic tile can be classified into unglazed and glazed ceramic tile surfaces. The glazed ceramic surfaces are easily cleaned using common household cleaning supplies compare to the unglazed ceramic tile which is more prone to microorganism attack. However, both ceramic tiles surface were still in risk of microbes attack especially in moist condition due to the presence of water molecule which invited bacterial growth on the tiles surfaces (Bok and Johansson, 2020). An effort to prevent the bacterial growth was given a priority and coating was one of the alternative ways that has attracted researcher interest. The photocatalytic coatings of ceramic tile display outstanding performance for example in industrial domestic cleaning rooms, hospital operating theatres and sewage purification facilities (Zhang et al., 2022c).

Titanium dioxide (TiO_2) is one of the coating material used widely in industrial area due to its availability and properties of highly efficient, cheap, non-toxic, chemically and biologically inert and photo stable which highly reactivity under ultraviolet (UV) light irradiation (Abdellah et al., 2018, Canbaz et al., 2019, Lu et al., 2019, Kamrosni et al., 2022). However, the efficiency of TiO_2 photocatalytic is low due to restriction that it is only shows high photocatalytic reaction on UV light causing other factors such as preparation process, crystallite size and anatase-rutile ratio had a great effect on the activity. Hence, it is necessary to shift the TiO_2 absorption spectrum toward the visible region to fully harness the advantage of sunlight as an inexpensive and renewable energy source (Chakhtouna et al., 2021).

Eventhough TiO_2 demonstrates good properties as a photocatalyst; it cannot be denied that TiO_2 ability is quite limited. It can only respond to solar light from the earth surface at about 2 - 3% as the electron photogenerated of TiO_2 happened under shorter wavelengths of less than 380 nm. Beyond that, the recombination of hole–electron pairs happened within nanoseconds which results into low quantum yield (Grabowska et al., 2013). This has brought many studies on introducing metal and metal oxide such as Fe, Pt, Au, CuO, and Ag into TiO_2 particles (Meydanju et al., 2022, Cherif et al., 2023). Variety of approach has been done and in between those metals, it was found that silver (Ag) is the most promising metal ions collaborated with TiO_2 because the ability of silver to initiate surface plasmons resonance at the higher wavelength of light (Hidayat et al., 2021, Kamat, 2002). The surface plasmon resonance occurs when a photon of incident light strikes a metal surface and a portion of light energy interacts with the metal surface at a specific angle of incidence. The incident photons transfer energy to the free electrons present within the metal lattice and electrons move freely due to excitation. This free electrons movement known as plasmon and undergo a collective oscillation, resulting in the formation of surface plasmons.

3

The surface plasmon resonance angle shifts when biomolecules bind to the surface and change the mass of the surface layer (Nguyen et al., 2015).

The uses of Ag in coating have been known as an effective antimicrobial material with a broad spectrum of bactericidal activity. Based on the wide band gap of TiO_2 which are 3.0 eV for rutile and 3.2 eV for anatase, the photocatalytic activity of TiO_2 only taking place under UV light irradiation (Mahdieh et al., 2021). For example, in order to make TiO_2 applicable on solar energy, the deposition of metal ion Ag is commonly applied to TiO_2 because of the ability to narrow down the band gap up between 2.9 eV to 2.7 eV respectively. Unlike TiO_2, Ag has the ability as antibacterial agent even in the dark (Pohan et al., 2020). Thus, the presence of Ag in TiO_2 film improved photocatalytic activity where it serves as electron trap that promote increased in electron-hole separation (Mahdieh et al., 2021). The addition of metallic Ag successfully broadens the photoresponse range from UV region to visible light region. The additional absorption of Ag/TiO_2 in visible region was attributed to the plasmonic absorption of Ag (Zheng et al., 2019). The plasmon resonance of Ag extends the wavelength absorbance from UV spectrum to the visible light spectrum. Instead, it decrease the recombination rate of TiO_2 which increasing the electron-hole separation (Mahdieh et al., 2021).

Onna et al. (2018) studied tungsten loaded TiO_2 (W-TiO_2) coating synthesized via surface sol gel on glazed ceramic tiles as self-cleaning and antimicrobial surfaces for indoor applications. It was found that W-TiO_2 synthesis by sol-gel coated on glazed tile in the acid media was reliable to be used by the factory for tile's processing. While, Ashraf et al. (2019) developed a strategy to boost the photocatalytic performance via well distribution of Ag nanoparticles between graphene sheets. Graphene/Ag-doped TiO_2 nanocomposite prepared using Hummer's method through harsh oxidation of graphite. The amount of 0.1 g Ag nitrate added to the Ag/TiO_2 sol solution performed in the dark condition for the conversion of Ag^+

4

to Ag nanoparticles. The combination of sonochemical and freeze-drying methods did give a higher photocatalytic activity than the conventional dried nanocomposite itself.

Photocatalyst of pure TiO_2 and Ag-TiO_2 powder synthesized by sol-gel route were studied by Abbad et al. (2020). Similar Ag source obtained from reduction of Ag nitrate with amounts at 1 %, 5 % and 10 % was added. The results from the finding stated that the optimal 10 % of Ag dopant significantly had improved photocatalytic activity of Ag-TiO_2 which it lowers the band gap energy from 3.22 eV to 2.67 eV. In this research, the main focus is to study the effects of Ag content on the microstructure and photocatalytic performance of Ag-TiO_2 coating deposited on both unglazed and glazed ceramic tile substrates.

1.2   Problem Statement

TiO_2 in the form of powder and thin film were both restrain application to the UV region of the electromagnetic spectrum that is $\lambda \leq 365nm$. Beyond the spectrum region, the role of TiO_2 was no longer function. Though there are many benefits given by TiO_2 itself compared to other semiconductor photocatalyst, its high band gap 3.2 eV energy hinder the functionality as photocatalyst at variety of irradiation. In fact TiO_2 cannot react actively with the absence of light. The photocatalytic of TiO_2 strongly influenced by the surface rearrangement potential and lifespan of the electron-hole pair generated (Meydanju et al., 2022). Due to this, in order to maximize the potential of TiO_2, the needs to reduce the fast rate of electron-hole pair recombination is very important. Variety of efforts has been made to modified TiO_2 particles that can active under visible light irradiation such as doping with metal (e.g., silver, copper, platinum, chromium and ferum) and nonmetallic elements (e.g., nitrogen, sulphur and carbon).

Photocatalytic properties of TiO_2 are very essential because TiO_2 was widely used in our live without we realized. Recently, the effort to break through the development of new photovoltaic cells by doping TiO_2 with semiconductor on photosensitized solar cell market became popular issued among researchers. Hence, this technologies is to turn solar power directly into electricity through solar cells (Rheima et al., 2020). In textile industry, Ag-TiO_2 coated on fabric as for the purpose of antibacterial and there was a critical concentration of Ag dopant creating an optimized photocatalytic property. Mahdieh et al. (2021) studied the effect of Ag concentration on Ag-TiO_2 nanoparticles coated on polyester/cellulose fabric by comparing the in situ and ex situ method. Kamrosni et al. (2022) works on Ag-TiO_2 with 0.1 ml of 0.1 M Ag concentration used and deposited on glass substrate via spin coating method. Abbad et al. (2020) studied about the effect of Ag doping on the photocatalytic activity of TiO_2 nanopowder by adding 1 %, 5 % and 10 % of Ag. It is stated that 10 % Ag give improvement to the photocatalytic activity by having band gap 2.67 eV despite its appearance in brookite phase.

Mostly researcher works on improved TiO_2 in terms of its photocatalytic and antibacterial activity. It can be seen that, most of the works reported on Ag-TiO_2 deposited on glass, metal and fabric substrate rather than ceramic. Details study on Ag presence in TiO_2 and deposited onto ceramic substrate are still lack of explanation. Since the ceramic has different type of surfaces which are unglazed and glazed, the deposition of Ag-TiO_2 coating on ceramic surfaces may require different sol gel formulation. It is either the use of precursor TiO_2 or without the TiO_2 precursor is necessary for deposition of Ag-TiO_2 coating on ceramic surfaces. The TiO_2 precursor such as Degussa P25 had already composed a certain ratio of anatase to rutile which is 70:30. Therefore, it is suggested that by the aid of TiO_2 precursor in the sol formulation can simply generate high amount of anatase phase that

6

can significantly enhanced the photocatalytic properties of Ag-TiO$_2$ coating (Ningthoukhongjam and Nair, 2019).

The use of dopant such as Ag with high concentration will decrease the surface charge which attributed to agglomeration of Ag species and reduction to Ag^0 particles on TiO$_2$ surface (Mogal Sajid et al., 2014). In contrast, with lower concentration of Ag content, Ag species exist as AgO, Ag$_2$O and Ag^0. However, the exact amount of Ag that can effectively enhance the characteristics such as the particle growth, surface area, thermal stability and band gap energy are still vague and inconclusive. Therefore, the Ag interaction with TiO$_2$ and amount of Ag used that affect the coating characteristics and catalytic performance of the coated ceramic tiles is of interest in this study. Study is then discussing on how the characteristics of Ag-TiO$_2$ coating influences the photocatalytic performances.

1.3   Research Objectives

i. To identify the crystalline phase of Ag-TiO$_2$ coating (with and without commercial Degussa P25 addition) deposited on ceramic tiles.

ii. To assess the effect of Ag content on the microstructure (crystalline phase, crystal size, elemental distribution, morphology and cross section surface) of Ag-TiO$_2$ coated on ceramic tiles using GAXRD, SEM/EDX and FESEM/EDX.

iii. To evaluate the influence of Ag content on the photocatalytic performance of Ag-TiO$_2$ coated on ceramic tiles

1.4   Scope of Research

The scope of this research starts on examine the deposition of Ag-TiO$_2$ coating on unglazed and glazed ceramic tiles substrate. Here, the effect of using nano powder TiO$_2$

precursor which is Degussa P25 during the synthesis of Ag-TiO$_2$ sol gel was investigated. In this study, 22 nm of Degussa P25 has been used. Ag-TiO$_2$ coating was prepared by using sol gel method and deposited on ceramic tiles by dip coating technique. Due to the potential developmental toxicity effect of Ag nanoparticles to human that was reported by Hu et al. (2020), precursor AgNO$_3$ is preferable in replacing Ag nanoparticles. The precursor AgNO$_3$ needs to undergo several steps during mixing so that to obtain Ag particles. Besides, there were several variables taken into account when preparing the coating solution. The amount of 2.5, 5.0 and 7.5 mol % Ag content for each solution and the final Ag content would affect the ratio of Ag to TiO$_2$. The influence of Ag content on microstructure formation of the deposited Ag-TiO$_2$ coating was studied. The resulting microstructure would affect the photocatalytic performances and Ti, O and Ag elements distribution of the produced coating. The characteristics include the type of phases, elements distribution and sizes as well as surface morphology were observed. These criteria may contribute to the mechanism of photocatalytic of the Ag-TiO$_2$ coating on the ceramic tile. The samples then subjected to GAXRD, SEM/EDX and FESEM/EDX respectively. The photocatalytic performances were evaluated by studying the degradation of methylene blue under UV and visible light irradiation for 5 hours exposure. The optimize performance of Ag-TiO$_2$ coated on ceramic tile were finally determined.

1.5 Contribution of Research

This research contributes to the needs of work in ceramic tiles industry for producing photocatalytic self-cleaning ceramic tiles. Unlike others substrates, Ag-TiO$_2$ coating on ceramic substrate was given less attentive and basically limited on TiO$_2$ only. In order to deposit Ag-TiO$_2$ coating on ceramic tile, the amount of Ag content required for the coating

8

is then suggested to be applied for future ceramic coating on the unglazed and glazed ceramic tiles. The suitable amount of Ag content for Ag-TiO$_2$ coating on ceramic is related to the good microstructure and efficient photocatalytic surfaces observed during the study. This enable the wide use of Ag-TiO$_2$ coating on ceramic tiles hence will reduce the effort for cleaning service in domestic application and wastewater treatment in the ponds supporting green technology. The findings are not only limited on ceramic tiles but also applicable on the other ceramic substrate. Moreover, these findings also contributed to the potential of Ag-TiO$_2$ usability and paving the way for designing new ceramic tile with excellent antimicrobial activity. Hence, it can reduce the bacterial infection problems related to exposed surface.

1.6   Thesis Outline

This thesis is consists of five (5) chapters. Chapter 1 describes a brief introduction that consist of background of the study, research problems, objectives, scopes, contributions and significance of the research work. Chapter 2 discuss a comprehensive literature review of TiO$_2$ and Ag-TiO$_2$ principle of photocatalyst. The fabrication and modification made of TiO$_2$ by incorporating noble metal, metal ion and anion doping in TiO$_2$ system coating by previous study were presented in this chapter. Then the choices of Ag as promising metal dopant was judged according to the reported criteria. The method of Ag-TiO$_2$ and its utilization for coating deposition or nanoparticles were discussed. Later, this chapter presents overview of the Ag-TiO$_2$ effect on microstucture and photocatalytic performances.

Chapter 3 elaborates the details of methodology conducted to produce Ag-TiO$_2$ sol and coated on ceramic tile. This includes the preparation and synthesis of Ag-TiO$_2$ sol as

well as coating procedure. In addition, characterization and analyses were describes in details including the characterization equipment, handling procedure and samples preparation.

Chapter 4 covers the results and discussion of uncoated ceramic tiles and Ag-TiO$_2$ coating deposited on unglazed and glazed ceramic tiles. Throughout this chapter, the characterization of uncoated ceramic tiles and Ag-TiO$_2$ coating on ceramic tile were discussed and its photocatalytic performances being verified. This chapter was organized accordingly by:

i. The crystalline phase and surface morphology of uncoated ceramic tile

ii. Characterization of Ag-TiO$_2$ coating with and without the addition of Degussa P25 coated on ceramic tiles.

iii. The charcterization of Ag-TiO$_2$ coating with varied Ag content on uglazed and glazed ceramic tiles.

iv. Effect of Ag content on the photocatalytic performances of Ag-TiO$_2$ coating on ceramic tiles

Lastly, chapter 5 made up of conclusions and recommendations for the future research work. This chapter summarizes the main conclusions as well as achievements of the work undertaken in this research and suggests areas for the next future research to work on Ag-TiO$_2$ deposition on ceramic substrate.

CHAPTER 2

LITERATURE REVIEW

2.1 Introduction

This chapter briefly introduce the materials of titanium dioxide (TiO_2) involving its modification and photocatalytic properties. Then, it discusses the enhancement of TiO_2 photocatalytic properties, Ag-TiO_2 coating and sol-gel derived Ag-TiO_2 coating. The preparation of Ag-TiO_2 sol gel involving its formulation and the Ag-TiO_2 sol gel reaction are also explained. Later on, the various deposition methods, different types of substrates and the deposition of Ag-TiO_2 on ceramic substrate studied by previous researchers are reviewed. After that, the effect of Ag content on the crystalline phase, microstructure, and photocatalytic performances including degradation under UV and visible light irradiation of Ag-TiO_2 coating are discussed.

2.2 Titanium Dioxide (TiO_2)

Titanium dioxide (TiO_2) has been known as one of the semiconductor that widely used in several environmental applications such as photocatalysis, separations, paints, sensor devices and dye-synthesized solar cells (Coronado et al., 2008). These was due to its potential of having higher photocatalytic performances towards different organic pollutants, pharmaceutical compounds, photo induced bacterial and virus disinfections and self-cleaning properties (Chakhtouna et al., 2021, Prakash et al., 2022). TiO_2 semiconductor having advantages in terms of availability, stability, photoactivity and low cost materials makes it demandable especially in coating industrial application (Chakhtouna et al., 2021). It also having high efficiency in hydrogen generation and high photostability in an aqueous

11

solution that beneficial for use as photocatalysts, bactericides, and photoanodes (Choi et al., 2018). In spite, it also excellent in optical, electrical, and photoelectrochemical properties which attracted the interest of industry professionals (Mîndroiu et al., 2023).

Table 2.1 summarize the crystallographic properties of TiO_2. The crystalline structure of TiO_2 can be easily converted from amorphous to anatase by annealing it in air at temperatures between 350 - 450°C in air. The anatase structure provides a potentially unique ion-accommodation mechanism, allowing a tiny ion to enter the system (Li et al., 2018). The benefits of ion mobility in TiO_2 anatase structure have been suitably constructed as TiO_2 nanotube electrode. Rutile, in the other hand is known as the most stable polymorph at various temperatures because of its lower free energy than anatase and brookite. It also has photochemical ability but unfortunately it possessed lower photocatalytic properties than anatase when exposed under UV light irradiation (Xu et al., 2011, Kien et al., 2023). The rutile fast recombination rate and low charge carriers generated causing the electron unable to participate in reactive oxygen species on the catalyst surface (Žerjav et al., 2022). Brookite meanwhile having band gap energy ranging around 3.1 to 3.4 eV and brookite nanoparticles could be separated by selective precipitation of rutile (Coronado et al., 2008).

Table 2.1: The crystallographic properties of rutile, anatase and brookite (Zhang et al., 2018)

Crystal structure	Density (g/cm)	System
Rutile	4.240	Tetragonal
Anatase	3.830	Tetragonal
Brookite	4.170	Rhombohedral

The process of TiO_2 synthesis by industrial was originated from mineral ores ilmenite ($FeTiO_3$) and rutile (TiO_2). Purification and refinement of mineral ores process to obtained white powder TiO_2 depends on the quality of the mineral ores itself. Low grade is refined by the sulphate process and higher grade rutile, is refined by the chloride process. Both process

12

did not involve the use of concentrated sulphuric acid (Page, 2009). Figure 2.1 and 2.2 summarize the process involved:
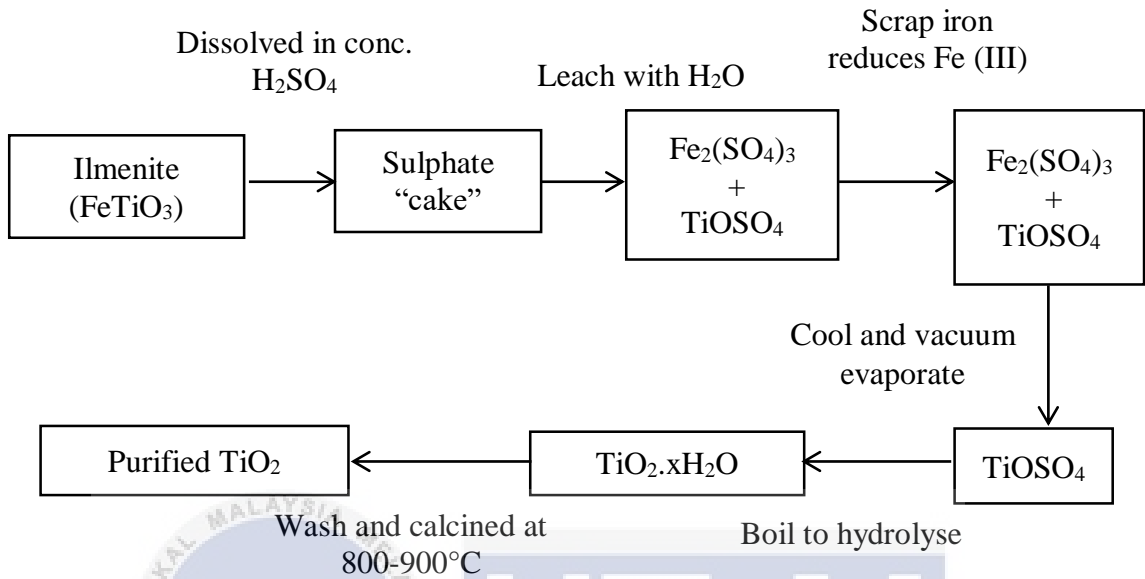
Figure 2.1: Refinement of TiO_2 by sulphate procress (Greenwood and Earnshaw, 1997)
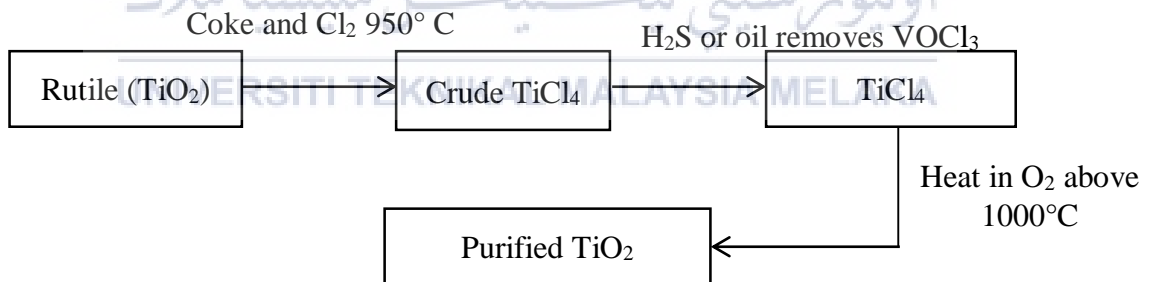
Figure 2.2: Refinement of TiO_2 by chloride process (Greenwood and Earnshaw, 1997)

Basically there are many methods available to fabricate TiO_2 in forms of nanorods, nanoparticles, nanotubes, nanofibers, and film. The employed method plays an important role on determining the optical, electronic as well as chemical properties of TiO_2 nanostructures. Some of the common method used such as vapor deposition, sonochemical,

13

hydrothermal, wet chemical and sol-gel method. The availability of different method in synthesizing TiO_2 will produce either single or mixed phase crystals dependent on the preparation method. The different preparation methods will contribute to the change of structure and properties of TiO_2 crystals. Hence, the mixed-phase ratio, morphology and surface properties of photocatalyst are controllable via optimizing the synthesis parameter such as calcination temperature, pressure, concentration and types of reagents use (Zhang et al., 2018). Some of the common examples of the TiO_2 synthesis method shown in Table 2.2.

Table 2.2: Different synthesis method of TiO_2

Method	TiO_2 precursor	Calcination Temperature	Author
Sol gel	Titanium tetra iso-propoxide (TTiP)	400, 500, and 600 °C) for 4 h	Mogal Sajid et al. (2014)
		400 °C for 5 hours	Lidiaine et al. (2015)
		300°C for 2 hours	Sharma et al. (2019)
		400 °C for 2 h	Sangchay and Rattanakun (2018)
		900, 1000 and 1100 °C	Evcin et al. (2017)
Photo-Assisted Deposition	TiO_2 P25	Not stated	Saraswati et al. (2019)
Hydrothermal	Tetrabutyl titanate (TBOT)	450°C for 2 h	Noreena et al. (2019)
		180°C for 48 h	Zheng et al. (2019)
Co-precipitation and one pot synthesized	Titanium (IV) - (triethanolaminato) isopropoxide	450 °C for 3 h	Hidayat et al. (2021)

In between all those methods, sol gel is considering the most reliable which produce thin, transparent, homogenous, multi component oxide layers of many compositions on various substrate at low cost and it allows the choice of refractive index and thickness of the layer by changing the preparation conditions (Mechiakh et al., 2007, Sangchay et al., 2018).

14

Even so, the photocatalytic properties of TiO_2 has often changes from one sample to another depending on the preparation method under various conditions (Cong and Xu, 2011).

Instead of synthesizing own TiO_2, the new era nowadays has developed a commercial TiO_2 which available in market. Some of the examples of commercial TiO_2 are Degussa-P25, TiO_2/P90 and millennium (Nour et al., 2017, Dontsova et al., 2021). The commercial TiO_2 however was quite expensive and this gain researcher interest in developing friendly economical TiO_2 photocatalyst.

2.3   Modification of TiO_2 coating

Despite of the good properties of TiO_2, there are some disability and weakness that restricted TiO_2 application. The wide band gap value of TiO_2 that is 3.2 eV (Thamer and Hatem, 2022) together with high recombination rate photoelectrons and holes (Zheng et al., 2019, Kamrosni et al., 2019) makes it negligible under visible light irradiation. The TiO_2 can absorb only 2 - 3% of solar radiation from the earth's surface because it can only be stimulated at shorter wavelength that is below 380 nm (Nagaraj et al., 2023). Hence, TiO_2 modification in several ways has been studies and explore throughout the research field to enhanced the efficacy of titania surface. The reaction of dopants towards TiO_2 depends on the semiconductor behave upon UV or visible light. In addition, the particle size significantly gave high impact on the structure and properties of TiO_2 and preferably small particles size due to high surface area which improved the contact area (Thamer and Hatem, 2022). Photoactivity of titanium dioxide to the visible light spectrum has been extended by plasmonic photocatalysis due to the collective oscillations of conduction electron induced by the electric field of incident visible light photon and inhibit the fast rate recombination of electron-holes pairs (Leong et al., 2014).

The modification of TiO_2 is either introducing transition metal or nonmetal ions into its lattice. Metal acts as electron acceptor and form special structure known as "Schottky Barrier" which capture photo-induced electrons (Zheng et al., 2019). However, the presence of the dopant leads to an increase in the system disorder due to a higher concentration of oxygen vacancies (Lidiaine et al., 2015). Doping TiO_2 with transition metals are expected to tunes the electronic structure and extends the absorption light from UV to visible light (Sharma et al., 2019). Interstitial doping often occurred on the TiO_2 surface, while substitutional doping included replacing Ti^{4+} ions with cations, resulting in an oxygen vacancy. Anion dopants other than cations, such as carbon, nitrogen, and sulphur, replace O^{2-} ions correspondingly. Nitrogen was the most frequent non-metal dopant due to its low ionisation energy and smaller atomic size compared to oxygen (Rtimi, 2017, Milošević et al., 2018). Noreena et al. (2019) experiment about the effect of silver nanoparticles together with graphene addition on the broad spectrum antibacterial ability of TiO_2 to inhibit the growth of bacteria Campylobacter jejuni under visible light.

The latest being studied recently by researchers were dopant with nanocomposite coating. For examples, Ag-doped SnO_2/TiO_2 photoanode were synthesized by Khojasteh et al. (2021) to improve performance of dye synthesized solar cells photovoltaic. The Ag-doped SnO_2/TiO_2 photoanode rated 6.93 % photon to electron conversion efficiency which was the highest value compared to TiO_2 photoanode alone. Such dopant with nanocomposite for solar cells photovoltaic had lower the charge transfer resistance, recombination and higher short-circuit photocurrent.

2.3.1 Photocatalytic properties

In recent years, TiO_2 has been commonly used in gaining photocatalytic properties especially in construction and building area. In between rutile, anatase and brookite crystal structure, it was highlighted that anatase crystal structure of TiO_2 having the greatest

16

photocatalytic activity than the other type of TiO_2 polymorphs (Simona et al., 2013). Figure 2.3 shows the TiO_2 crystal structure of rutile, anatase and brookite.

((a)
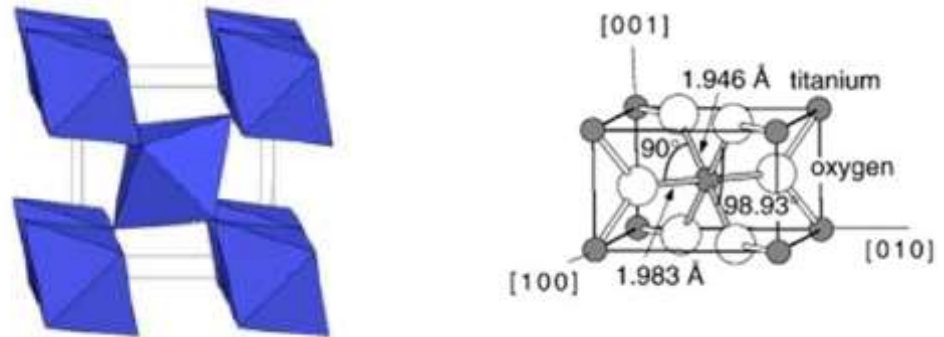
((b)
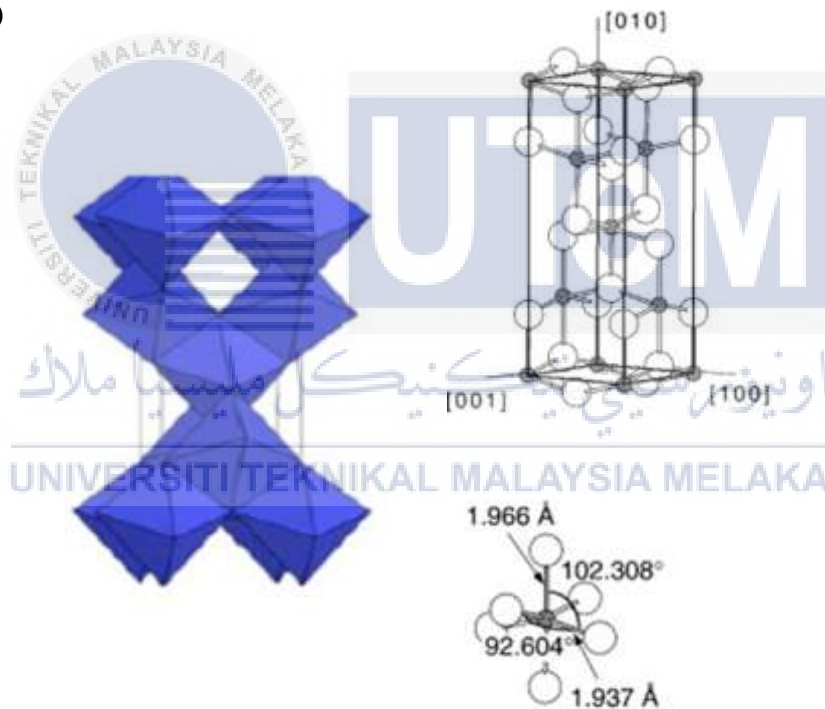
((c)
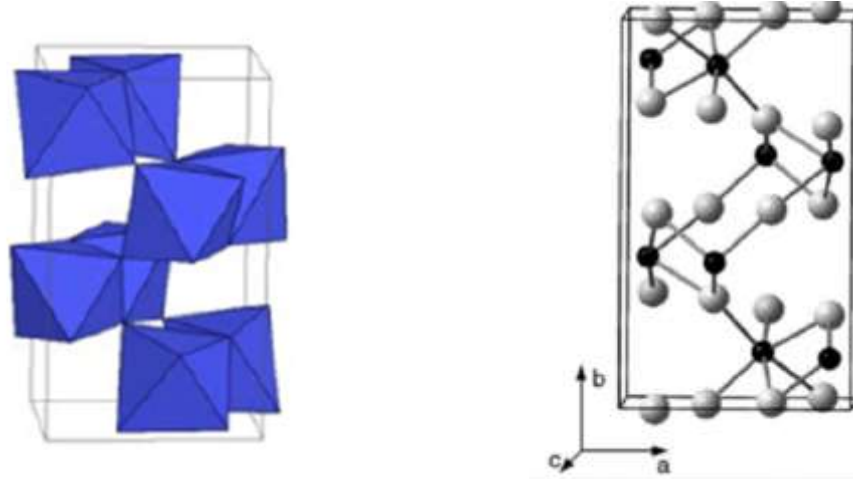
Figure 2.3: TiO$_2$ crystal structure of (a) rutile, (b) anatase and (c) brookite phase structure (Ulrike, 2003, Regonini et al., 2013, Sze-Mun et al., 2014)

Commonly, anatase has been showing highest photocatalytic properties due to the following properties (Simona et al., 2013):

i.   The high band gap energy of anatase which is 3.19 ~ 3.2 eV compared to rutile, 3.0 eV and brookite, 3.11 eV tends to make the electron-hole of anatase more positive or negative potential attraction. The large band gap of anatase tends to raise the valence band maximum to higher levels by facilitate the electron from TiO$_2$ to adsorbed molecules (Luttrell et al., 2014).

ii. Stronger adsorption ability of H$_2$O, O$_2$ and OH that boost the adsorption capacity during photocatalytic reaction.

iii. Smaller grain size of anatase compared to rutile and brookite and larger specific surface area which are helpful during crystallization process.

In addition, the nanostructures of TiO$_2$ for example nanotubes, nanocables and nanobelts had also attracted researcher interest due to their performance as effective catalyst in increased electron transfer. Among them, TiO$_2$ nanotubes had gave special attention

18

because of the photocatalytic activity, ion-exchange capacity, large surface area and multilayer wall structure (Thamer and Hatem, 2022). Moreover, the grain size, pore volume, structure, specific surface area and microstructural growth of TiO_2 thin film also need to be taken into account as it affect its photocatalytic performance (Halin et al., 2021). Due to photocatalytic potential in both science and practical application, TiO_2 was utilized for the destruction of recalcitrant organic pollutants in water and air, sterilizing, self-cleaning process, antibacterial effect, as cement mortar, in exterior tiles, paving blocks, glass, PVC fabrication and protect the Cultural Heritage surfaces (Šauta et al., 2008, Simona et al., 2013).

TiO$_2$ catalyst can be found in readily made which is in commercial form or either a mixture in sol. The three main aspects of TiO_2 photocatalytic technology were (Ju, 2019):

  i.   The basic theory of photocatalysis, which includes the mechanism and kinetics of photocatalytic reactions at the solid-liquid interface

  ii. Rules of photoelectron and mobile hole movement and complexion, provides a theoretical foundation for increasing photocatalytic activity and the potential for exploring new photocatalytic reaction systems

  iii. TiO_2 photocatalytic activity enhancement, including methodology for increasing TiO_2 photocatalytic activity and discovering more efficient photocatalyst; TiO_2 preparation, including bearing TiO_2 on solid materials and film preparation, and expanding the range of coated film substrate

2.3.1.1 Photocatalytic reaction of TiO$_2$

Photocatalysis is a reaction that takes place when the absorption of light having energy greater than or equal to the band gap energy of the photocatalyst. The energy difference between the highest filled energy level called valence band and lowest vacant

19

energy level, conduction band of photocatalytic substance is known as band gap energy. This photoinduced excitation generates a positive hole (h^+) in the valence band and electrons (e^-) in conduction band of the substance. The positive holes and electron may either recombine and energy released in the form of heat or takes part in reactions and initiates a series of redox reactions called photocatalytic reactions. However, the recombination of positive holes and electrons must be avoided for the photocatalytic reaction to occur. In order to favour the photocatalytic reactions, the positive holes and electrons must be able to react with the reductants and oxidants to produce oxidized and reduced products (Haq et al., 2022). Figure 2.4 illustrates the photocatalytic reaction mechanism of TiO_2 in the presence of light. Initially the photocatalytic reaction of TiO_2 takes place when the light is absorbed, then electron will excited from valence band to conduction band. The electron-hole generated recombine at surface and redox reaction occur. The transfer of electrons from O^{2-} to valence band and from metal to H^+ ions reduction will then generated hydrogen (H_2) and oxygen (O_2). Since the Gibbs free energy per electron is 1.23 eV corresponds to the frequency of light 1008 nm that required for water splitting, the photocatalyst band gap energy must be bigger than 1.23 eV for the photocatalytic reaction to occur. Instead, if the energy of the photocatalyst is lower that the electrons will unable to start the reaction. Hence, to improve the electronic properties of TiO_2, the modifications must be made to help in reduce self-decomposition and backward reactions in semiconductor photocatalyst (Irfan et al., 2022).
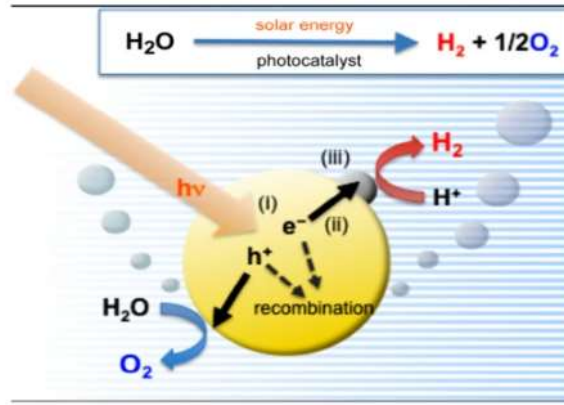
Figure 2.4: Photocatalytic reaction of TiO_2 water splitting (Irfan et al., 2022)

2.3.2 Enhancement of TiO_2 photocatalytic properties

The photocatalytic properties of TiO_2 determined its potential to be used in certain area. The drawbacks of TiO_2 such as weak light capture ability and small specific surface area limits its field to acts as photocatalyst as well as antibacterial capability. Hence, to overcome these drawbacks, the quality of the metal–semiconductor system plays a key role in enhancing the photocatalytic properties (Bao et al., 2023). Although many researchers have shown that addition of Ag into TiO_2 increases its photocatalytic activity, there exist several cases that prove Ag loading content can actually promotes as well as inhibit photocatalytic activity of TiO_2 (Nyankson et al., 2022, Cherif et al., 2023). This is because too much of Ag content may result in a photohole trapping effect which reduces the photocatalytic activity. According to work done by (Zheng et al., 2019) this trapping effect is negligible for Ag content below 0.5 molar %. On the other hand, the highest photocatalytic activity of film done by Ubonchonlakat et al. (2008) was obtain using 1 mol % Ag doped TiO_2 sintered at 500˚C, while Xin et al. (2005) shows 5 mol % as the optimum Ag content sintered at 400 ˚C for 4 hours.

Photocatalytic activity known to be the function of their surface properties for examples the surface area increase, the number of the active sites also increases. High surface

area gives better photocatalytic efficiency (Suwarnkar et al., 2013). The appropriate amount of Ag doped TiO_2 can effectively capture the photoinduced electron; photoinduced electron can be immediately transferred to oxygen adsorbed on the surface of TiO_2 and the amount of surface hydroxyl radical is increased (Sobana et al., 2006). The photocatalytic activity of TiO_2-Ag particles calcined at 500 ˚C was highest and decreased with increasing calcinations temperature up to 800 ˚C (Harikishore et al., 2014). Annealing at very high temperatures increases the particle size and decreases the surface area and favors the phase transformation from anatase to rutile.

The TiO_2 photocatalyst can be enhanced by combining other materials making it binary or ternary composite. For example, Bao et al. (2023) prepared Ag-TiO_2/ ZIF-8 ternary composite by solvothermal to study the antibacterial activity of E.coli and B. subtilis. The Ag-TiO_2/ ZIF-8 released Ag^+ and Zn^{2+} with low toxic that destroyed the proteins in bacteria's cell walls and membranes. Kien et al. (2023) synthesized TiO_2 - SiO_2 from tetra-n-butyl orthotitanate and tetraethyl orthosilicate to by sol gel method and applied on the ceramic surface. The amorphous SiO_2 prevented the transformation of anatase to rutile hence proving that the TiO_2 - SiO_2 coating became one of the photocatalyst materials. Cherif et al. (2023) doped Ag/TiO_2 for waste water treatment and hydrogen gas generation under natural sunlight and 1 wt % Ag content was 60 % higher photocatalytic activity than the pristine TiO_2 where it can remove 99% of 0.01g/L paracetamol in 120 minutes.

Choi et al. (2018) studied Ag-TiO_2/Nitrogen-Doped Graphene Oxide Nanocomposites for improvement of hydrophilicity and photocatalytic performances of TiO_2 and 80 % of methylene blue degraded at 6 hours irradiation. On the other hand, Chakhtouna et al. (2021) discussed the important role of Ag nanoparticles in enhancing the removal capacity and antibacterial performances of the Ag/TiO_2 photocatalysts while Noreena et al. (2019) proposed that silver-graphene TiO_2 composites was effective as

antimicrobial agents to control the spread of C. jejuni by preventing both bacterial growth and biofilm formation. Table 2.3 summarized the type of materials that aided in performance of better TiO_2 photocatalyst.

Table 2.3: Example of TiO_2 photocatalyst aided in photocatalytic properties

Photocatalyst composite	Precursor/Additive	Phase	Authors
Ag-TiO₂/ZIF-8	AgNO₃ and ZnNO₃•6H₂O	Anatase	Bao et al. (2023)
TiO₂-SiO₂	Tetraethyl orthosilicate (TEOS– Si(OC₂H₆)₄	Rutile and anatase	Kien et al. (2023)
Ag/TiO₂	AgNO₃	Anatase	Cherif et al. (2023)
Ag-TiO₂/graphene oxide (GO	AgNO₃ and ammonia	Ag metal	Choi et al. (2018)
Ag/TiO₂	AgNO₃	Tetragonal anatase structure	Chakhtouna et al. (2021)
Ag/TiO₂/graphene	AgNO₃	Anatase	Noreena et al. (2019)

2.4 Ag-TiO₂ coating

Ag-TiO₂ photocatalyst commonly has been found reported by many researchers because of its good potential in photocatalytic and antibacterial properties. The photocatalyst was either in form of nanoparticles powder state, liquid sol medium or vapour was extensively applied on different substrate such as glass, wood, metal, polymer and also ceramic substrate depending on the purpose of application. The Ag-TiO₂ can exhibited higher visible light photocatalytic activity under visible light region. This is because Ag 4d's isolated energy level contributes to visible light absorption, and the metallic silver on the surface helps to effectively separate electrons and holes (Nagaraj et al., 2023). Table 2.4 shows the examples of Ag-TiO₂ coating deposited on various substrates.

Table 2.4: Deposition of Ag-TiO$_2$ coating on different types of substrate

Type of substrate	Deposition method	Authors
ITO glass	Spin coating	Kamrosni et al. (2022)
	Co-precipitation and one pot synthesized	Hidayat et al. (2021)
Polyethylene	Poured into PE container	Meydanju et al. (2022)
Ag-doped TiO$_2$ nanoparticles	Hydrolysis of Ti(IV) isopropoxide	Lidiaine et al. (2015)
cotton fabrics	Photo-Assisted Deposition (PAD) method.	Saraswati et al. (2019)
Carbon substrate	Microwave-assisted hydrothermal	Choi et al. (2018)
Glass	Sol-gel spin coating	Halin et al. (2018)

Though coating on multiple types of surfaces has been studied years ago, it was rarely found that coating done on ceramic surface. Often we can found that the coating practically applied onto glass and metal instead of ceramic substrate. Ag-TiO$_2$ films coated on surface roughened Ti–6Al–4V alloy to improve the adhesion and integrity of the sol gel films studied by Fu et al. (2015). Albert et al. (2015) did Ag-TiO$_2$ coating on Si substrate to reveal the connection between applied silver-doping method, nature and structural properties of the composite. Shakeri et al. (2018) explore the technique to coat TiO$_2$ nanoparticles on ceramic tiles for the self-cleaning purposes. A single heat treatment step and (3-Aminopropyl) triethoxysilane (APTES) treatment technique to create a stable covalent coating of TiO$_2$ nanoparticles onto ceramic tiles. Both revealed that the photocatalytic power of particles was preserved, the coating was stable, and the surfaces were able to thoroughly degrade the dye that was used as an organic pollutant.

2.4.1 Application of Ag-TiO$_2$ as photocatalyst

Photocatalyst of TiO$_2$ has been extensively used as white pigment and the addition of inorganic compound such silver forming Ag-TiO$_2$ has wider the applications leading a global titanium dioxide pigment sales is continuing over the recent years (Braun et al., 1992). As pigment, it involved in coating application, plastics application, inks applications, paper industry and colouring products in pharmaceuticals and cosmetics industries (Linak and Inoguchi, 2005, Brown, 2014). In energy generation and storage, the Ag-TiO$_2$ can be found in dye-sensitized solar cell (DSSC), photocatalytic hydrogen production and lithium battery (Smestad et al., 1994, Kay and Grätzel, 1996, Yiming et al., 2009). In the area of environment protection, Ag-TiO$_2$ applied for self-clean and antibacterial and water treatment. In spite of that, it also one of the potential catalyst to induce the reductive chemical transformations such as reduction of carbonyl compounds (Wu, 2021).

Further, in health and biomedicine, the Ag-TiO$_2$ composite usually can be found in sunscreen ingredient because it absorbs strongly the UV (most often UVB) and physical filters (Dondi et al., 2006, Mansoori et al., 2007, Michela d'Alessandro et al., 2016, Nicoara et al., 2020). In biomedicine, Ag therapeutic potential of TiO$_2$ lies in the ability of these particles in response to light to produce reactive oxygen species (ROS). Production of ROS is the main factor in causing detrimental effects on cells (Cai et al., 1991). Therefore, it can be stated that Ag-TiO$_2$ was continuously applied in various big industrial areas because it enhance the photocatalytic properties along with the antibacterial and subjected to several different environmental applications. Herein, Table 2.5 shows some of the example worked of Ag-TiO$_2$ composite studied in different application.

25

Table 2.5: Several types of application of Ag-TiO₂ coating

Application	Authors
Fabric	Saraswati et al. (2019) Mahdieh et al. (2021)
Biomedical	Cotolan et al. (2016) Bao et al. (2023) Nyankson et al. (2022) Vladkova et al. (2020)
Self-cleaning surface	Kien et al. (2023) Razak et al. (2020) Shakeri et al. (2018) Silva et al. (2017)
Water treatment	Cherif et al. (2023) Aliyu et al. (2023) Pohan et al. (2020)
Solar cell	Vitanov et al. (2023) Supriyanto et al. (2021) Hidayat et al. (2021) Khojasteh et al. (2021) Rheima et al. (2020)
Antibacterial	Moongraksathuma and Chen (2018) Zhang et al. (2022a)

2.5   Sol gel derived Ag-TiO₂ coating

Sol gel is one of the promising method because it has the advantages in producing thin layer, transparent, homogenous, multi component oxide layers of many compositions on various substrate at low cost and it allows the choice of refractive index and thickness of the layer by changing preparation condition (Mechiakh et al., 2007, Sangchay et al., 2018). The final product's purity and homogeneity, as well as the growth and size of the particles, as well as the flexibility of adding high concentrations of doping agent, can all be controlled through the use of this low-cost and environmentally friendly method (Chakhtouna et al., 2021).

26

The process converts monomers into Sol, a colloidal solution, which is then transformed into gel. The transformation process was divided into two stages: sol (solution) and gel. The Sol undergoes hydrolysis and condensation polymerization during the activation phase before transform into gel. Then, the gel is applied to the substrate and dried to form a hard, glossy film. Without the use of fluoropolymers, sol-gel has the strength of silica as well as excellent release and smoothness. These coatings' release or nonstick properties are an inherent feature. As a result, sol-gel technology is very popular. Many studied report on the preparation of TiO_2 sol. Prepared sol gave almost the same result as commercial TiO_2 respectively. Eventhough the method required more materials, but it was the best way to reduce the cost with maximum advantages.

Thus, TiO_2 synthesis by sol gel method has become popular among the researches instead of using other method such as co-precipitation, hydrothermal crystallization, mechanochemical technique and chemical vapor deposition. Sol gel was the simplest method to produce supported or unsupported undoped and doped TiO_2-based photocatalysts which offers the ability to go all the way from molecular precursor to the product, controllable nanoparticles growth, reduce processing time and lower temperature, better homogeneity, higher purity, accurate control of composition as well as cost friendly (Abbad et al., 2020). It is also possible for coating on different substrate materials and complex geometries (Tung-Yueh et al., 2016).

The sol–gel process is comprised of a series of sequential steps, which are as follows (Chakhtouna et al., 2021):

1. Hydrolysis to convert alkoxides into metal hydroxides

2. Condensation to form gels

3. The drying process, which is necessary in order to acquire metal-doped TiO_2 nanoparticles

27

Sol gel route technique is reported to adhere strongly to substrates with an oxide layer because of the presence of functionalized, hydroxyl groups on the surface of the oxide. The polymer species or macroclusters that form in the sol gel solution during hydrolysation of the organic metallic precursors are able to react with these surface hydroxyl groups and form strong bonds. Surface hydroxyl groups are also present on the surface of ceramic powders. Thus, when powder such as zirconia or mixed into sol gel solution, strong bonds are formed between sol, ceramic powder and the substrate. This thick film process is in fact composed of many thin films which make up the bricks in a wall. The fact that films do not crack during processing can be attributed to two factors (Barrow et al., 1995):

1. The film forms a strongly bonded network with a sol gel film firmly bonded between ceramic particles, making it less likely that the film will crack during processing

2. Because of the presence of a significant amount of ceramic powder, the percentage of sol gel in the film is decreased and less shrinkage occurs when the film is processed.

2.5.1 Ag-TiO₂ Sol gel Preparation

Even though TiO_2 modified silver can increase its lifetime of photo-excited electrons and holes, silver also can give a negative effect. The increased in mobility and diffusion of Ag during annealing process may improve either deteriorate TiO_2 properties (Fakhouri et al., 2015). Instead, whatever process or method applied for Ag in modifying TiO_2, silver still diffuses to the surface through adjacent layers and form islands after annealing at 100 °C to 400 °C (Kulczyk-Malecka et al., 2014). Despite acting as electron acceptor centers, both Ag nanoparticles and ions exhibit a strong antibacterial activity and promoted the electron-hole pair separation of TiO_2 (Thi-Tuyet et al., 2016). Hence, decreasing the charge recombination, $Ag^°$ clusters exhibit strong visible light absorption on the oxide surface due

28

to the so called surface plasmon resonance (SPR) effect (Lidiaine et al., 2015). The SPR of Ag promote the light absorption to the visible region (Ling et al., 2019). Thus, Ag_+ is getting more attention than others because of its capability as followed (Abbad et al., 2020):

a) to bind, damage, and change the functions of the bacterial cell wall membrane, which are slightly negative

b) to interact with protein thiol groups, which are important for bacterial respiration and the transport of important substances through the cell.

c) improve electron-hole separation by serving as electron traps

d) to activate visible light excitation of TiO_2 and enhance surface electron excitation by visible light-excited plasmon resonances

e) alter the surface properties of photocatalysts

Silver also contributed to the band gap energy reduction. This reported by (Zheng et al., 2019) where the band gap energy of pure TiO_2 from 3.15 eV has reduced to 2.7 eV by deposition of metallic Ag.

2.5.2 Preparation method and formulation of Ag-TiO₂ coating

It can't be denial that the characteristic and performances of coating materials depends on many parameter such as materials used, shapes, chemical compositions and method preparation. Preparing Ag-TiO_2 sol can also be done easily by using the commercial TiO_2 and Ag nanoparticles. Somehow, due to the current unstable world economic issues nowadays, the production of inexpensive cost saving coating has become a competitive. Various way of coating with low cost has been developed.

2.5.2.1 The use of Degussa P25 as TiO₂ precursor

Degussa (Evonik, Germany) P25 is a type of commercial TiO_2 nanopowder known as Titania P25, Evonik 25, AEROPERL and Aeroxide P25 (Wang et al., 2019, Markowska-Szczupak et al., 2020). It was reported that Degussa P25 composed of mixed phase of anatase and rutile phase with typical ratio of 70:30 or 80:20 respectively (Guo et al., 2018, He et al., 2019) . The band gap of Degussa P25 stated 3.2 eV and 3.0 eV for both anatase and rutile phase with surface area measured 50 m^2/gm (Das et al., 2018) . It is the most efficient photocatalytical material compared to commercial TiO_2 of Millennium PCs which having only pure anatase phase (Bouanimba et al., 2017). Generally, the works on synthesizing TiO_2 solution used Degussa directly to produce TiO_2 sol or as an additive into self-prepared TiO_2 sol. The TiO_2 sol that used Degussa P25 typically possess thicker suspension rather than the derived TiO_2 from alkoxide sol via sol-gel process.

There have been several studies in the literature of Degussa P25 reporting on photocatalyst to degrade organic pollutant. Rejek et al. (2021) studied the different methods for immobilization of titanium dioxide P25 onto chitosan surface to be applied for water purification. Bessergenev et al. (2015) investigated the photocatalytic activities of Degussa P25 powders annealed at various temperatures in vacuum and air. The aim was to compare the oxygen vacancies generated by annealing in vacuum and to compare the results with annealing in air. Supriyanto et al. (2021) in their interest of developing high magnitude dye-sensitized solar cell used direct form of commercial TiO_2 and Ag nanoparticles. The Degussa P25 catalyst in aqueous solution for degradation of alachlor (organo chlorine herbicide) has been done by Malini et al. (2016) and the effect of temperature, pH, radiant flux, TiO_2 loading, presence of various cations, anions and surfactants were being considered. Wang et al. (2012) reported that the calcination treatment influenced the microstructures and photocatalytic activity of the Degussa P25 powders. The photocatalytic activity of calcined Degussa P25 powders was two times higher than uncalcined which it enhanced the anatase

crystallization respectively. Figure 2.5 illustrated the surface morphology of Degussa P25 nanopowder.
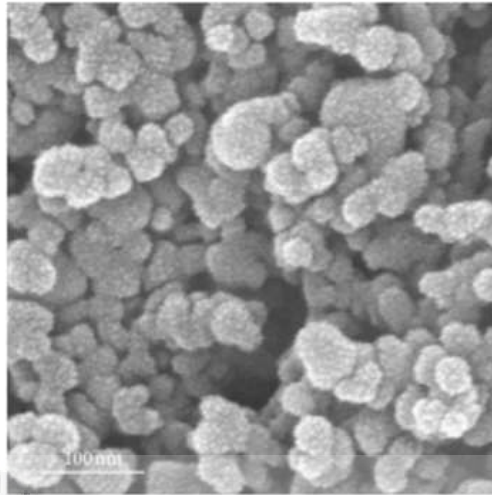
Figure 2.5: Surface morphology of Degussa P25 powders (Wang et al., 2012)

Sreethawong et al. (2014) worked on incorporation small content commercial Degussa P25 powder (3 – 7 wt % P25) into self-synthesized TiO_2 calcined at 400 °C deposited on glass substrate. It has been found that the specific surface area of the P-25 TiO_2-incorporated mesoporous-assembled TiO_2 photocatalyst (~127 m^2/g) decrease with increasing the incorporated P-25 TiO_2 content (~65 m^2/g). Despite, the mean mesopore diameter tended to conversely increase. The role of P25 TiO_2 assists in increasing the thickness of the mesoporous-assembled TiO_2. The average particle sizes of the mesoporous-assembled TiO_2 and Degussa P25 incorporated TiO_2 photocatalyst were in the range of 5-10 and 15-25 nm, respectively. The incorporation of Degussa P25 into mesoporous-assembled TiO_2 films exhibited only detected anatase phase even the phase of Degussa P25 consists of anatase and rutile.

2.5.2.2 The use of AgNO$_3$ as Ag precursor

Silver nanoparticles (AgNPs) were one of the attractive nanomaterials and has been popular among researcher due to its unique properties such as size and shape depending on optical, catalytical, antimicrobial, and electrical properties (Bachhav et al., 2020) . It has been applied in many different field of applications such as engineering, biomedical and agricultural sciences (Bamsaoud et al., 2021). There were various numbers of reported methodologies and methods for the synthesis of silver nanoparticles using chemical, physical, photochemical, and biological pathways (Vasileva et al., 2011, Bachhav et al., 2020). The physical methods involved condensation, evaporation and Laser ablation. As for the chemical methods used such as chemical reduction, microwave assisted synthesis, photo induced reduction and micro emulsion techniques. While, for the biological methods involves the use of plant parts, bacteria, algae and fungi for the synthesis of AgNPs (Bachhav et al., 2020). In this worked, AgNO$_3$ was used as Ag precursor to synthesized Ag nanoparticles doped on TiO$_2$ coating.

Silver doped titanium dioxide (Ag/TiO$_2$) thin film was prepared by the sol-gel method through the hydrolysis of titanium tetra-isopropoxide and silver nitrate solution performed by Kamrosni et al. (2022). The TiO$_2$/ZnO-Ag@TiO$_2$ multilayer nanocomposite for the purpose to create an organic dye sensitized solar cell photoanaode worked by Hidayat et al. (2021) applied one-pot synthesid method. The titanium (IV)-(triethanolaminato) isopropoxide (TTEAIP, 99.9%, Sigma Aldrich), and silver nitrate were mixed together in an Erlenmeyer. Meanwhile, Khojasteh et al. (2021) synthesized the dye sensitized solar cells by preparing solar cell photoanode , cathode electrode and electrolyte injection. The worked focussed on the effects of doped nanoparticles and different nanocomposites such as SnO$_2$/TiO$_2$ nanocomposites, Ni doped TiO$_2$ nanoparticles, Ag-doped TiO$_2$ nano particles and Ag-doped SnO$_2$/TiO$_2$ nanocomposites as photoanode on the performance of dye synthesized

solar cells using hydrothermal and sol gel method. In the experiment, the source of TiO_2 and Ag were obtained from TTiP and $AgNO_3$ respectively.

The synthesized of TiO_2 and silver doped nanoparticles by sol gel method using tetrabutyl titanate as titanium precursor and $AgNO_3$ as silver precursor and then Silver-Graphene-TiO_2 nanocomposites along with TiO_2, TiO_2-Graphene and TiO_2-silver nanocomposites were prepared by using hydrothermal method by Noreena et al. (2019). Zhang et al. (2022b) investigated 2D polystyrene spheres array composed of TiO_2 and Ag prepared by co-sputtering technique. In the deposition process the properties of the composites were affected by the sputtering power of TiO_2. The applied sputtering TiO_2 power was 10W, 20 W, 40W, and 60 W. At the highest power, 60 W increased size Ag-TiO_2 nanoparticles were observed that lead to the increased surrounding Ag-TiO_2 bilayer film dielectrics.

A homogenous, simple and fast method to synthesis Ag doped TiO_2 semiconductor by using sonochemical method was applied by Aini et al. (2019).Various amount of silver content of $AgNO_3$ was introduced into homogenous mixture of TiO_2 generated from TTiP as precursor. Ag-modified TiO_2 nanotube has been fabricated via alkaline hydrothermal process using commercial TiO_2 and $AgNO_3$ studied by Tsai et al. (2019). Table 2.6 shows few examples of synthesis method and formulation used to produce TiO_2 and Ag-TiO_2 composite.

Table 2.6: Different preparation method and formulation of Ag-TiO_2 photocatalyst

Method	Precurcor	Substrate	Authors
Sol gel spin coating	Ag doped TiO_2 (TTiP)	Si	Demircia et al. (2016)

	TTiP	Carbon steel	El-Katoria et al. (2019)
	Ag doped TiO$_2$ (P25)	Monolith granule	Thi-Tuyet and Van (2015)
	TTiP	Glass	Halin et al. (2018)
Sol gel	TTiP + AgNO$_3$	ITO	Kamrosni et al. (2022)
	TTiP	-	Sangchay et al. (2012)
	Ti(OC$_3$H7)$_4$ + AgNO$_3$	Nanoparticles powder	Evcin et al. (2017)
	TTiP + Ag nanoparticles	Glass	Li et al. (2016)
	TiCl$_4$ + AgNO$_3$	Titanium	Cotolan et al. (2016)
	TTiP + AgNO$_3$	Glass	Silva et al. (2017)
	TTiP + AgNO$_3$	Silicon wafer	Yu et al. (2011)
Peroxide sol gel and microwave assisted	TiCl$_4$	Ceramic plate	Shieh et al. (2015)
Photo reduction	TiO$_2$	Nanoparticles	Ling et al. (2019)
Conventional sol gel	Tetrabutylorthoti nate	Light ceramic	Ju (2019)

After all, it can be simplified that most of the studied use sol gel method and TTiP as titanium precursor to produce TiO$_2$ sol and AgNO$_3$ to yield into AgTiO$_2$ sol. It was reported that this method was effective and cost friendly along exhibited good properties as well as better performances of photocatalytic activity (Wang and Bierwagen, 2009, Silva et al., 2017).

2.5.3 Ag-TiO₂ sol gel reaction

Sol gel of Ag-TiO$_2$ usually formed by using titanium precursor such as titanium tetraisopropoxide (TTiP), tetrabutyl orthotitanate (TBOT), or titanium tetrachloride (TiCl$_4$) mixed with silver precursor commonly used was silver nitrate, followed by hydrolysis performed at low temperature (does not exceed 100 °C). During the synthesis, the pH must be controlled to ensure uniformity of properties followed by calcination at high temperature for further crystallization. The calcination temperature applied defined whether the composite sol produces amorphous or low crystalline (Sharma et al., 2018). The silver-doped titanium dioxide nanoparticles synthesis using ethanol as solvent described as followed (Chakhtouna et al., 2021):

$$Ti\,(OH)_4 + C_2H_5O - Ag \longrightarrow Ti(OH)_3 - Ag + C_2H_5OH \tag{2.1}$$

$$4Ti(OH)_3 - Ag + O_2 \longrightarrow 4TiO_2 - AgNP + 6H_2O \tag{2.2}$$
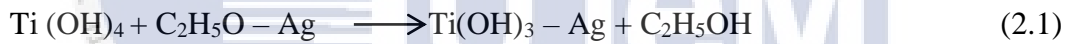
When Ag is doped into TiO$_2$ lattice, Ag atom will occupy substitutional site rather than interstitial site since the radius of Ag$^+$ (129 pm) is larger than that of Ti^{4+} (74.5 pm) (Mogal Sajid et al., 2014, Vakhrushev et al., 2017). Then, oxygen vacancy wil be generated to favour the structure reorganization and keep an overall neutral charge after Ti^{4+} in TiO crystal is replaced by Ag$^+$. The defect reaction equation can be expressed as follows:

$$4Ag^+ + 2O^{2-}_{anatase} \longrightarrow 4Ag^o \text{ (or Ag }_{cluster}) + O_2 + \text{oxygen vacancy} \tag{2.3}$$

When silver in contact with TiO$_2$, electron from TiO$_2$ will transfer from TiO$_2$ to silver. These electron then loads on silver surface and scavenged by the electron acceptor. The recombination between electrons and holes will eventually decrease. Thereby, Silver atom acts as electron traps which facilitate the transport of more holes to the surface. The

redistribution of atoms and phase transformation become vigorously favourable. Oxygen vacancies then diffuse to the bulk of anatase and initiate changes in its crystal lattice resulting silver clusters form silver nanoparticles in the bulk of TiO_2 matrix.

$$4Ag^o \longrightarrow Ag_{cluster}$$
$$nAg_{cluster} \longrightarrow Ag_{nanoparticle.}$$

(2.4)

2.5.4 Deposition method of Ag-TiO₂ coating

There were many types of deposition method applied to coat a substrate producing either thin film or coating layer. It depends on coating thickness to call it as thin film or coating layer. The TiO_2 thin films layer formed on FTO substrate by dip coating method and the optimal number of dip coating layer was determined worked by Mîndroiu et al. (2023). Kamrosni et al. (2022) producing Ag/TiO_2 thin film deposited on ITO glass substrate by using spin coating method that was conducted at 100 rpm for 10 s. Supriyanto et al. (2021) studied on solar cell with high-efficiency magnitudes by introducing different Ag concentration into dye-sensitized solar cells using spin coating technique deposition method. Similar with Hidayat et al. (2021) also investigated TiO_2/ZnO-Ag@TiO_2 nanocomposite as working layer of organic dye sensitized solar cell but via co-precipitation method. The deposition of Ag-TiO_2 composite on two dimensional (2D) polystyrene sphere array via co-sputtering technique was done by Zhang et al. (2022b) and it believed that Ag and TiO_2 co-sputtering can reduce the aggregation of silver nanoparticles. Table 2.7 presents the type of deposition method and coating speed that commonly used depending on the interval and the thickness of the produced coating.

Table 2.7: Different deposition method of Ag-TiO₂ coating

Deposition method	Coating Speed	Thickness	Authors

	3 cm/min	0.674± 1.945µm	Mîndroiu et al. (2023)
	Not stated	Controlled thickness	Silva et al. (2017)
Dip coating	12 cm/min and 2cm/min	96 nm	Albert et al. (2015)
	30 cm/min	300-350 nm	Moongraksathuma and Chen (2018)
Dip coating and magnetron sputtering	Not stated	~200 nm.	Li et al. (2016)
	2000 rpm/30 seconds	120-140 nm,	Cotolan et al. (2016)
Spin coating	2500 rpm	370 nm	Yu et al. (2011)
	100 rpm/10 s 2000 rpm/30 s	Not stated	Kamrosni et al. (2022)
	1000 rpm/30 s	300 nm	Supriyanto et al. (2021)
Co- sputtering	1.5 keVAr atoms at 45∘	~ 90- 95 nm	Singh et al. (2017)
	20 – 60 W	Not stated	Zhang et al. (2022b)
Physical vapour deposition (PVD)	25 mA, and the exposure time was 10–80 s.	Not stated	Barrientos et al. (2018)

2.6   Ag-TiO$_2$ coating on different substrate

Ag-TiO$_2$ ability to act as self-cleaning and antimicrobial has been explored on different kinds of surfaces for its application. Saraswati et al. (2019) applied Ag-TiO$_2$ nanocomposite coated on cotton fabric. The purpose was to form an antimicrobial and self - cleaning footwear cotton fabric. Cotolan et al. (2016) studied Ag-TiO$_2$ coating on titanium substrate for corrosion resistance and bacterial reduction, while coating on silicon substrate studied by Singh et al. (2017). It is mostly found that Ag-TiO$_2$ coating deposited on glass substrate has been explored continuously and dominated most of the research compared to

37

other substrates. Table 2.8 presents types of various substrates worked studied for Ag-TiO$_2$ deposition.

Table 2.8: Ag-TiO$_2$ coating on different substrate

Types of substrate	Authors
Glass	Albert et al. (2015) Tallósy et al. (2016) Li et al. (2016) Silva et al. (2017) Moongraksathuma and Chen (2018) Mîndroiu et al. (2023)
Fabric	Saraswati et al. (2019)
Titanium	Cotolan et al. (2016)
Si	Yu et al. (2011) Singh et al. (2017)
Bifunctional surface modifier: mercaptoacetic acid (HOOCCH2SH).	Barrientos et al. (2018)
Ceramic	Loffler (2000) Aazam (2014) Shieh et al. (2015) Hasmaliza et al. (2016)

2.6.1 Deposition of Ag-TiO$_2$ on a ceramic substrate

At present, although there was various depositions method has been applied to deposit Ag-TiO$_2$ coating on various substrates, only few works were reported studying on a ceramic substrate. Table 2.9 shows examples of deposition techniques that involved Ag-TiO$_2$ coating deposition on ceramic substrate.

Table 2.9: Examples of deposition technique on ceramic substrate

Deposition method	Ceramic substrate	Author
co-sputtering	Si(100)	Singh et al. (2017)
Spray coating	Concrete	Tryba et al. (2010)
	Clay roofing tile	Ranogajec et al. (2010)
	Glazed tile	Zhang et al. (2022c)
Spin coating	Silicon wafer	Yu et al. (2011)
Dip coating	Ceramic plate	Shieh et al. (2015)
	Floor ceramic tile	Golshan et al. (2022)

Singh et al. (2017) applied co-sputtering of Ag and TiO_2 on cleaned Si (100) substrates with different Ag concentration to enhance the photocatalytic properties. Tryba et al. (2010) directly used titania slurry with doped Ag and sprayed it on the concrete of the house for the purpose of self-cleaning and fungicidal effects. Zhang et al. (2022c) implemented Ag-TiO_2 coating deposited onto glazed ceramic tiles by a sol-gel and spraying method at high temperatures to determine if this method could produce TiO_2 coatings with simultaneously good adhesion and antibacterial properties. Nevertheless, Golshan et al. (2022) further carried out work on Ag-TiO_2 nanofilms for self-cleaning surface of industrial floor ceramic tiles by dip coating method to improve the antibacterial and hydrophobicity activity of floor tiles.

It can be seen that to produce Ag-TiO_2 surface coating that provide self-sterilisation and self-cleaning properties when exposed to light (Tryba et al., 2010), many deposition technique deployed to coat Ag-TiO_2 onto substrate for example physical vapour deposition (PVD), chemical vapour deposition (CVD), iron beam co-sputtering, spin coating and dip coating depends on the application criteria. Among those depositions, dip coating reported a promising technique (Abd Samat and Mohd Saad, 2016, Guo et al., 2018). Dip coating is a process which the substrate was immersed in sol medium for certain period and withdrawal

from the sol. These process were repeated to obtain specific thickness needed ranging from nanometer to hundreds of micrometer (Scandola et al., 2019, Away et al., 2021). Hence, dip coating technique considerably used for the preparation of $Ag\text{-}TiO_2$ sol in order to form uniform and continuous layer. This was due to its reliable and low cost effective easy method compared to other method.

2.6.2   Effect of Degussa P25 addition on the crystalline phases and microstructure

Degussa P25 is a type of commercial TiO_2 and frequently used by researchers as the source of TiO_2 to produce composite coating or thin film. It was widely used to produce nanocomposite TiO_2 since it can reduce the step in producing any type of TiO_2 composite materials. Saraswati et al. (2019) prepared Ag/TiO_2 nanocomposite through photo-assisted deposition synthesis using TiO_2 P25 powder. From the investigation, XRD pattern only clarified anatase and rutile phase crystalline with no peak of Ag. It stated that Ag is attached to the crystal matrix of TiO_2 because the percentage of TiO_2 is greater than Ag and the size of crystallite was 34 nm for anatase and 39 nm for rutile. EDX analyses shows that Ag was well dispersed on the surface of TiO_2 but element of Ag is not found on the TiO_2 P25.

Most of the finding reported by the XRD pattern is that there is no Ag phase detected. In contrast, Tsai et al. (2019) had worked on Ag-modified titanium dioxide nanotube (TNT) which revealed intrinsic peaks of AgCl and Ag co-existing are presence in the XRD pattern of the Ag-modified TNT sample. Gyorgyey et al. (2016) explored deposition of TiO_2/Ag photocatalyst onto the surface of titanium disc using Degussa P25 as the source of TiO_2. The amount of Degussa P25 did not being mentioned and based on the SEM done, it was found that rounded grains of Ag present on the surfaces of the discs that were coated with the silver photocatalyst containing copolymer film.

2.7   Effect of Ag content on the crystalline phase of Ag-TiO$_2$ coating

The amount of Ag doped in the TiO$_2$ film has been shown to affect the phase transformation and grain growth of sol-gel titania, which has a direct impact on the TiO$_2$ film's photocatalytic activity and antimicrobial performance. Ag doping promotes the anatase to rutile phase transformation, with the temperature at which phase transformation occurs decreasing as the Ag concentration increases (Ningthoukhongjam and Nair, 2019).The doping increases the concentration of oxygen vacancies at the surface of the anatase grain increases, which favours the ionic rearrangement and structure recognization for rutile phase. El-Katoria et al. (2019) investigated on the different concentration of Ag (0, 1, 2, 5, 10 and 20 wt %) doped TiO$_2$ thin film coating with addition of chitosan as nano-assembling template for corrosion mitigation purpose. It was revealed that the anatase crystallize was observed by increasing silver contents up to 5 mol%. At this amount of addition, it was found the spreading of amorphous silver oxide layers is spreads through the titania crystallites. On the other hand, the addition of Ag content (10–20 mol %) favors crystallization of rutile titania and metallic silver particles which is accompanied by increased crystallite size.

Worked of Ag doped TiO$_2$ thin film deposited on glass slide substrate using sol gel and spin coating technique has been reported by Halin et al. (2018).The authors added two different amount of Ag content into TiO$_2$ sol which is 0.5 g and 1.0 g. The findings had obtained brookite phase for pure TiO$_2$ without addition of Ag, while samples doped with silver shows characteristics of only anatase peak with no significance peak of silver phase. Even for TiO$_2$-Ag 5%, XRD data doesn't show any peaks related to Ag species. This means that there are a lot of dopants spreading out in the TiO$_2$ samples (Lidiaine et al., 2015). The intensities of the diffraction peaks increase as the calcination temperature rises, while peak width at half-height of the individual peak decreases, indicating that the grain size of the

41

TiO$_2$ particles in the prepared films grows larger and the crystallinity improves (Ju, 2019). The synthesis of Ag-TiO$_2$ nanocomposite studied by Nagaraj et al. (2023) using 0.005, 0.01 and 0.015 M Ag coated titanium dioxide nanoparticles exhibited anatase phase and no shift in the diffraction position peaks. The authors also stated that there was no new peak of diffraction related to Ag because low amount of Ag content use and Ag amorphous state.

In a different studied by Aazam (2014), the Ag-TiO$_2$/multi-walled carbon nanotubes nanocomposites shows only TiO$_2$ phase even the amount of Ag range was 1 to 4 wt. %. This assumed that Ag is completely united with TiO$_2$ matrix since there is no Ag peak observed in the XRD pattern. Even so, the entire nanotube surface appeared with uniformly covered of Ag-doped TiO$_2$ nanoparticles although the XRD pattern of the Ag in MWCNT is unable to be identified. In a different study by Noberi et al. (2016) on nickel based metallic filter with Ag-TiO$_2$ coating by using electrophoretic deposition revealed the presence of anatase, rutile, AgO, Ag$_2$O and metallic Ag phases in the composite at high percent of Ag concentration (10 wt % and 15 wt %). While, at low Ag concentration (5 wt %) exhibited anatase, rutile and metallic Ag. The doping of Ag-TiO$_2$ by 0.04 Ag/Ti molar ratio done by Lopez Ortiz et al. (2015) revealed that silver peak overlapping with anatase phase and confirming the presence of metallic silver in the cubic phase

Considerably, the increasing of initial silver nitrate concentration led to the increment in the degree of crystallinity of samples. Cruz et al. (2022) studied the synthesis of Ag/TiO$_2$ composites by combustion modified with varied Ag content at amount 0.05 mmol, 0.1 mmol, and 0.2 mmol and it was found that the degree of Ag crystallinity increased as increased Ag content. In addition, promotes the phase change from anatase to rutile transformation. This was supported by Vakhrushev et al. (2017) which stated that the of TiO$_2$ phase transformed into whether anatase or rutile were accompanying silver nitrate decomposition processes. The finding by Mogal Sajid et al. (2014) that synthesized Ag−TiO$_2$ by a single-step sol gel

method with 0.75−3.5 at % Ag contributed to anatase phase and the mixed anatase-rutile at 3.0 and 3.5 %. From the study, it emphasized that Ag peak growth is observed when high amount of Ag of 2.5 to 3.5 % used.

TiO$_2$ thin film with no heat treatment didn't developed any phases while with heat treated contributed to presence of peak representing anatase and even rutile phase. This has been written by Kamrosni et al. (2022) where TiO$_2$ deposited on indium tin oxide (ITO) glass developed growth of anatase phase at 500 °C annealed temperature. Below 500 °C, TiO$_2$ film exist as an amorphous phase because the temperature range was not sufficient enough for crystallization process to occur. In fact, the intensity of the peak getting stronger as temperature increased up to 600°C. Generally, the addition of Ag promoted anatase phase and present of Ag phase. In another study done by Avciata et al. (2016) on Ag doped nanoparticles and coating on ceramic pellets for photocatalytic identified that all the powders have structure of anatase TiO$_2$ and contain element of silver. The synthesized TiO$_2$ nanoparticles measured 60.86 nm crystal size and Ag crystal value was found to between 12 and 23 nm. Table 2.10 shows the different amount of Ag content applied and phase present in Ag-TiO$_2$ coating.

Table 2.10: Amount of Ag content used for Ag-TiO$_2$ synthesize

Type of surface	Ag content	Phase	Authors
ITO glass	0.1 ml of 0.1 M	Anatase	Kamrosni et al. (2022)
Polyethylene	Not stated	Amorphous	Meydanju et al. (2022)
Nanoparticles	0.75, 2.5 and 3.5 %	Anatase	Mogal Sajid et al. (2014)
Titanium disc	0.5 wt %	Anatase and rutile	Gyorgyey et al. (2016)

| Graphene sheet | 75 mg of AgNO$_3$ | Ag metal | Choi et al. (2018) |

2.8 Effect of Ag content on the microstructure of Ag-TiO$_2$ coating

Lidiaine et al. (2015) agreed that the crystallite size decreases as the Ag amount increases (2015). This behaviour is related to the presence of dopant-induced association defects, which cause crystalline structure distortions and smaller crystallites. This behavior is related to the occurrence of association defects due to the presence of the dopant, leading to distortions in the crystalline structure and smaller crystallites. Also reported by Sangchay et al. (2018), who's investigated on the Ag doped TiO$_2$ by microwave assisted sol gel method with addition of 0.5 and 1 mol % Ag proved that the anatase crystallite size decreases as increased Ag. However, Demircia et al. (2016) studied Ag doped TiO$_2$ thin film deposited on Si substrate yield no remarkable neither reduction nor increase in crystalline size observed as increased silver amount (0.1, 0.3, 0.5, 0.7 and 0.9 % Ag). The author explained that owing to the differences of ionic radii of Ag$^+$ (129 pm) and Ti^{4+} (74.5pm), the Ag$^+$ ion migrate to the surface of TiO$_2$ either precipitation or dispersion on the surface.

The increase of Ag content induces to more porous structure of the films which advantages the photocatalytic of TiO$_2$ due to its enhanced surface area. This finding revealed by Halin et al. (2018). The author worked on Ag/TiO$_2$ thin film deposited on glass substrate with the addition of 0.5 and 1.0 g AgNO$_3$ and the surface morphology obtained shown in Figure 2.6 respectively. It can be seen that as increased amount of Ag content inhibited more porous sponge like structure.
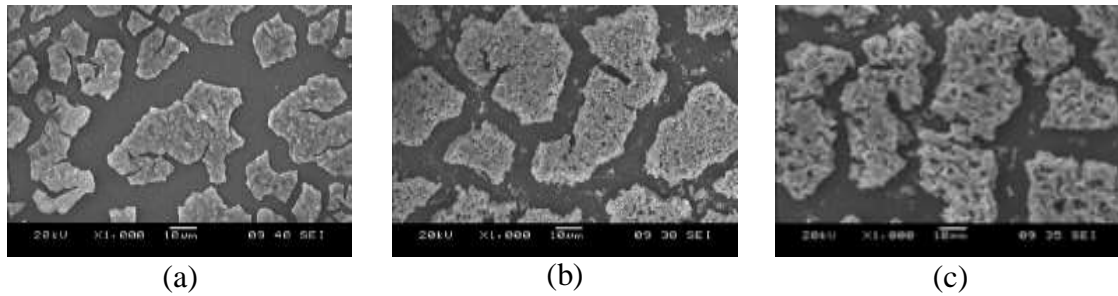
Figure 2.6 :SEM of Ag-TiO$_2$ film annealed at 450° (a) pure TiO$_2$, (b) doped TiO$_2$ 0.5 g Ag and (c) TiO$_2$ doped 1.0 g Ag (Halin et al., 2018)

The studied carried by Zheng et al. (2019) on Ag-TiO$_2$ composites found that Ag shaped is not really in regular cube with diameter around 20 nm. EDS and mapping analysis detected Ti, O and Ag peaks which proved the formation of Ag/TiO$_2$ composites. Generally, when Ag incorporated TiO$_2$, it expected that metallic Ag tend to appeared on the surface of the coating. Gyorgyey et al. (2016) found characteristic of rounded grains observed on the surfaces of the titanium discs that were coated with the silver photocatalyst containing copolymer film. Suwei et al. (2017) discovered that incorporation of 25 mol % Ag content incorporated Ag/BaTiO$_3$ composite film found that Ag nanoparticles were in spherical structure and uniformly dispersed in the BaTiO$_3$ amorphous matrix, apart from some aggregations and Ag cubic structure detected by TEM. While, Choi et al. (2018) formulated Ag-TiO$_2$/graphene oxide (GO) nanocomposites using 75mg Ag content and clarified that Ag-TiO$_2$ nanoparticles were thoroughly distributed in the graphene sheet. The particles were preferentially located at the edges rather than on the internal surface of the sheets. Nevertheless, Saraswati et al. (2019) innovation of Ag/TiO$_2$ nanocomposite coated on cotton fabric with 1, 3 and 5 wt % Ag content reported that it was difficult to distinguish between each catalyst constituent component.

The effect of Ag-TiO$_2$ coating with different TiO$_2$ content deposited on titanium substrate fabricated using electroless plating technique studied by Liua et al. (2018) identified that the TiO$_2$ nanoparticles incorporated well into Ag matrix and promoted Ag

45

ion release which superior the antibacterial activity of Ag-TiO₂ coatings. The author stated that Ag nanoparticles are homogenously distributed within the TiO_2 structure with Ag particles are spherical in shape while TiO_2 particles are in rectangular shape (Noberi et al., 2016).

According to Xinggang et al. (2015), Ag doped TiO_2 nanotubes fabricated by ion implantation and anodization suggested that Ag ions had improved the resistance of Ti foil to corrosion where after the implantation, a compact tubular structure of Ag doped nanolayer generated on the surface of Ti foil without Ag nanoparticles found on surface. The surface morphology of Ag-TiO₂ coating revealed homogenous, dense and cover the substrate completely with low amount of Ag used for doping TiO_2. These was discovered by Cotolan et al. (2016) using the ratio of 0.0037 Ag and Kaygusuz et al. (2016) uses 0.25, 0.5, 0.75, 1, 2 and 5 % of nano Ag-TiO₂ formed on leather samples. In another studied by Halin et al. (2018) on Ag-TiO₂ thin film deposited on glass substrate found that the surface morphology of the film porosity increased as increase Ag content (0.5-1.0 g Ag) and large flaky size and cracks throughout the coatings.

Besides Ag content, microstructure formation, Ag-TiO₂ grain size also affected by the heat treatment temperature. The full width with half maximum (FWHM) obtained from XRD data predicted the particle size of the film whether the size is smaller or getting bigger. FWHM values increased and narrowing indicating that the particle size increased. For example at different heat treatment temperature applied on Ag-TiO₂ thin film deposited on ITO done by Kamrosni et al. (2022) showed up that FWHM values decreased and narrowing meaning that the particle size increased. Besides, this finding supported by using scherer equation calculated which crystallite size of anatase increased from 40.4 nm at 500 °C annealed temperature to 46.0 nm when annealing at 600 °C. The increased annealing temperature to 600°C present stronger intensity of anatase peak with Ag₂O peak begins to

growth. It also revealed that film structure without annealing was porous and rough even though TiO_2 particles uniformly distributed. The TiO_2 structures started to form link at temperature above 300 °C and fully crystallize at 500 °C. Beyond that, exceeding temperature up to 600 °C, the film became porous and linkage of TiO_2 distance in Ag-TiO_2 thin film become wider with roughness surface 3.92 nm. Figure 2.7 illustrated film structure of Ag-TiO_2 coating layer annealed at different temperature presented by Kamrosni et al. (2022).
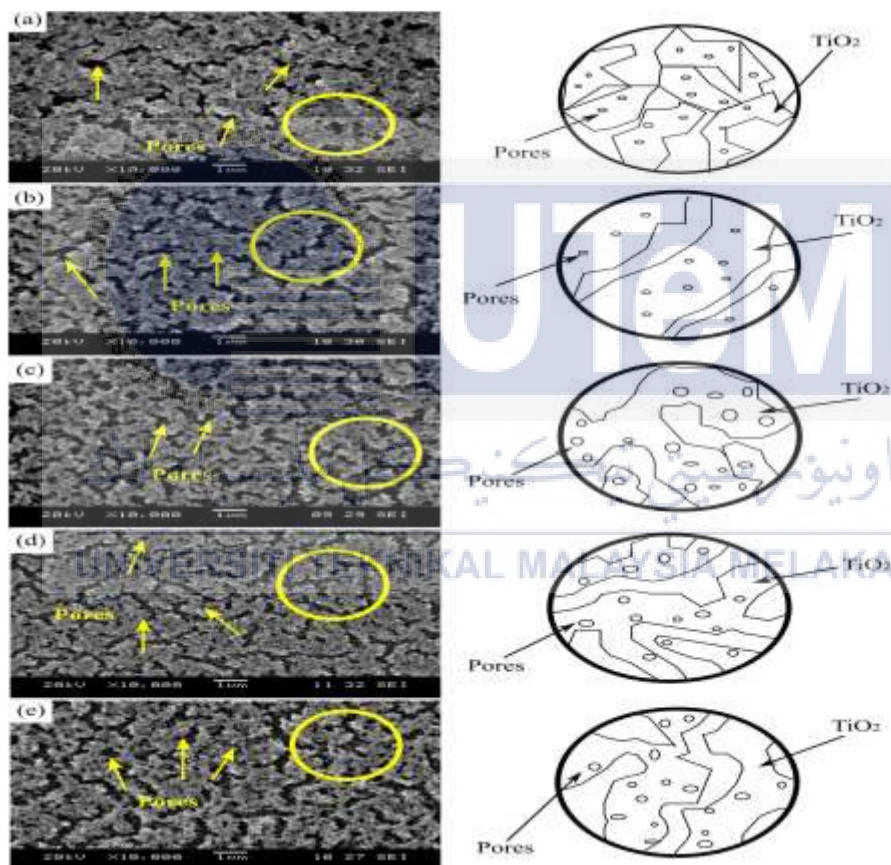
Figure 2.7: SEM micrograh and surface morphology of Ag-TiO_2 thin film with different annealing temperature, (a) non-annealing, (b) 300°C, (c) 400°C, (d) 500°C and (e) 600°C (Kamrosni et al., 2022)

2.9   Effect of Ag content on the photocatalytic performance of Ag-TiO_2 coating

The photocatalytic behaviors of Ag/TiO_2 composite were influenced by a number of factors, including the type of metal precursors, total metal loading, solvents, reducing agents,

47

pH, temperature, water/precursor molar ratio, and others (Abbad et al., 2020, Chakhtouna et al., 2021). Ag-doping were believed to give a significant effect on the inhibition of electron-hole recombination since the photoexcited electron possibly trapped by Ag particles, which acted as an electron storage sink on the TiO_2 surface (Cruz et al., 2022). Figure 2.8 shows an illustration of Ag doped TiO_2 coating particles on the effect of Ag concentration:
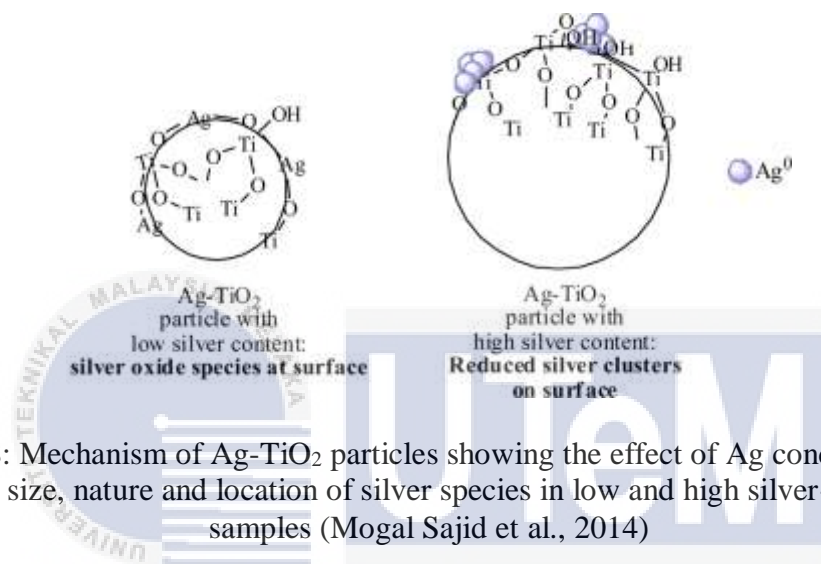
Figure 2.8: Mechanism of Ag-TiO_2 particles showing the effect of Ag concentration on particles size, nature and location of silver species in low and high silver-containing samples (Mogal Sajid et al., 2014)

According to work done by Zheng et al. (2019) this trapping effect is negligible for Ag content below 0.5 molar %. On the other hand, Ubonchonlakat et al. (2008) worked on Ag doped TiO_2 deposited on ceramic tile substrate at range 0.5 to 3 mol % Ag content revealed that the highest photocatalytic activity of film was obtained at 1 mol% Ag doped TiO_2 sintered at 500˚C.While Xin et al. (2005) investigated Ag-TiO_2 powder ranging from 0, 0.01, 0.03, 0.05, 0.1, 0.3,0.5, 1, 2, 3, 5, 7, and 10 mol % Ag content on the effects of the surface states, surface energy levels, and interfacial electron transfer for photocatalytic evaluation. It was found that at 5 mol % Ag content sintered at 400 ˚C for 4 hours was the highest degradation ratio of rhodamine B (RhB). Photocatalytic activity known to be the function of their surface properties; as surface area increase, the number of the active sites

also increases. High surface area gives better photocatalytic efficiency (Suwarnkar et al., 2013). The appropriate amount of Ag doped TiO_2 can effectively capture the photoinduced electron; photoinduced electron can be immediately transferred to oxygen adsorbed on the surface of TiO_2 and the amount of surface hydroxyl radical is increased led to the expanded response range of light to the visible region (Xin et al., 2005, Sobana et al., 2006).

The photocatalytic activity of TiO_2-Ag particles calcined at 500 ˚C was highest and decreased with increasing calcinations temperature up to 800 ˚C (Harikishore et al., 2014). Annealing at very high temperatures increases the particle size and decreases the surface area and favors the phase transformation from anatase to rutile. The photocatalytic properties of TiO_2 are enhanced by the addition of Ag dopant. Sangchay et al. (2018) works on TiO_2 doped 0.5 and 1 mol % Ag had degraded 68.30 % and 81.43 % Methylene blue under UV irradiation respectively. Nevertheless, Joao et al. (2019) highlighted that low amount of 0.1 wt % Ag is effective for the degradation mixture of five parabens (methyl, ethyl,propyl, benzylparaben and butylparaben) using low transferred ozone dose (TOD). Since the addition of Ag into TiO_2 create the trap levels between conduction bands and valence bands of TiO_2, the band gap of Ag-TiO_2 will definitely modified. The absorption spectra of Ag-TiO_2 nanocomposites broaden to the visible region and increase absorbance as increases Ag concentration whereby the optical band gap decreases. Hari et al. (2012) has observed the tuned of band gap Ag-TiO_2 using to 2.75 eV, 2 eV, 1.87 eV and 1.75 eV parallel with increasing Ag concentration from 0.015, 0.02, 0.05 and 0.1 wt. %.

The surface phenomenon of Ag-TiO_2 composite oxidizes/reduces or degrades the organic pollutants, biomolecules, micro-organisms into environment-friendly CO_2 and H_2O in presence of a photocatalyst (Prakash et al., 2022). Literally, the rules of photocatalytic of Ag-TiO_2 when exposed to light caused photogenerated/photoexcitation of electro-holes separation happened. The charge carrier of electron in valence band will excited to the

49

conduction band and react with oxygen molecules (•O$_2$). Meanwhile, the holes will then react with water molecules forming hydroxyl radical (•OH). These radical will then react with any foreign substances or organic pollutants by degradation into CO$_2$ and H$_2$O molecules. Equation 2.5 to 2.9 summarized the photocatalytic of Ag-TiO$_2$ reaction.

$$Ag/TiO_2 + hv \longrightarrow e_{CB}^- + h_{VB}^+ \qquad (2.5)$$

$$e_{CB}^- + O_2 \longrightarrow .O_2^- \qquad (2.6)$$

$$.O_2^- + H_2O \longrightarrow OH^- + H_2O. \qquad (2.7)$$

$$OH^- + h_{VB}^+ \longrightarrow .OH \qquad (2.8)$$

$$.OH + organic\ pollutants \longrightarrow Photodegradation\ products \qquad (2.9)$$
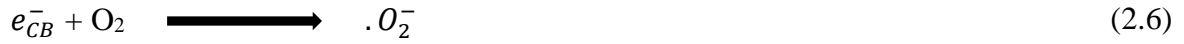
Saraswati et al. (2019) studied the antibacterial effect of nanocomposite Ag-TiO$_2$ coated cotton fabrics for footwear application , the optimum of Ag in disinfecting is 3% loading Ag as it is proven by the percentage of bacterial and fungal disinfection which reach 100% efficient, Ag-TiO$_2$ photocatalyst is an excellent and long-lasting antibacterial nanocomposite material (Akhavan, 2009). Moreover, addition of SiO$_2$ into Ag-TiO$_2$ coating also showed a high photocatalytic activity in hydrophilic and self-cleaning ability, superior to a TiO$_2$ or Ag-TiO$_2$ coating alone due to the high dispersion and the structural effects of the silica present.

The photocatalytic properties were certainly depends on the crystalline state and microstructure of Ag/TiO$_2$ composite. Hence, Kamrosni et al. (2022) worked on microstructure of Ag/TiO$_2$ thin film annealed at different temperature ranging from 300ºC to 600ºC. It was observed that Ag-TiO$_2$ thin film annealed at 500ºC displays highest cut-off wavelength which is 396 nm with lowest band gap energy, 3.13 eV. Table 2.11 shows band gap value of Ag/TiO$_2$ thin film with different annealing temperature defined by the studied:

Table 2.11: Band gap value of Ag-TiO$_2$ thin film with different annealing temperature
(Kamrosni et al., 2022)

Annealing temperature (°C)	Cut-off wavelength (nm)	Band gap (eV)
Non-annealed	379	3.27
300	382	3.45
400	388	3.19
500	396	3.13
600	390	3.18

2.9.1 Degradation under UV light irradiation

When exposed to UV light, there was an excitation of electron of TiO$_2$ from valance band (VB) to conduction band (CB). The photoinduced charge carrier of electron and holes will then reduce and oxidized in surrounding environment. The charge carriers on the surface interact with oxygen (O$_2$) and water molecules (H$_2$O). Holes oxidizes H$_2$O molecules into highly reactive hydroxyl radicals (•OH) and electrons reduces O$_2$ molecules to superoxide radical anion (•O$_2^-$), which is further reduced to •OH. These radical known as Reactive Oxygen Species (ROS) existed on TiO$_2$ surface which it react with harmful organic pollutants by degradation to CO$_2$ and H$_2$O (Prakash et al., 2022). Figure 2.9 proposed mechanism of Ag-TiO$_2$ coating exposed under UV-light irradiation.
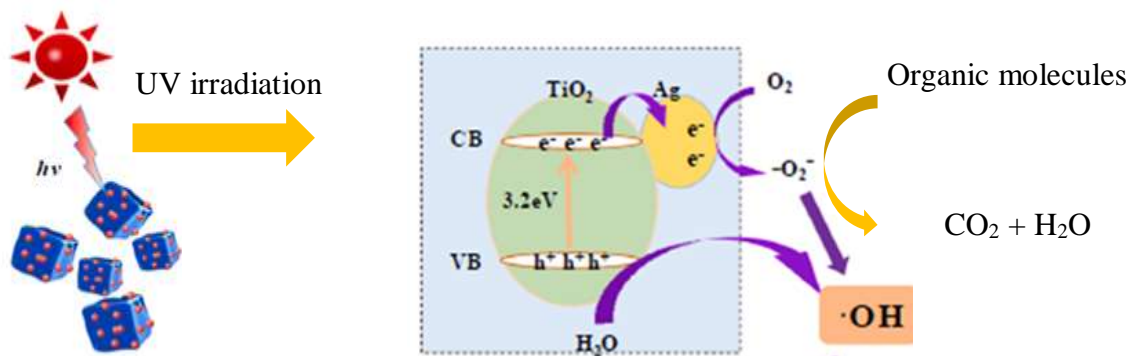

51

Figure 2.9: Photocatalytic mechanism of Ag-TiO$_2$ (Zheng et al., 2019)

The addition of Ag coupled TiO$_2$ when exposed to UV light, electron-hole separation will takes place. The electron in the valence bands agitated to conduction bands causing a vacancy in valence bands. These photogenerated electrons moved into metallic Ag and accumulated on its surface. Electrons then reacted with absorbed oxygen on Ag surface to form oxygen radicals (O$_2^-$) and further generated hydroxyl radicals ($^-$OH). The $^-$OH radical then reacts with H$^+$. Similarly, the holes in valence bands also will react with H$_2$O generating $^-$OH radical too. At the final stage, $^-$OH strong oxidation will oxidized the organic compound presence into H$_2$O and CO$_2$ (Zheng et al., 2019). Choi et al. (2018) reported on Ag-TiO$_2$/graphene oxide (GO) nanocomposites prepared by a simple one pot synthesis. It was found that when exposed to UV light, photocatalytic activity of Ag-TiO$_2$/GO nanocomposites degrade almost 80 % of methylene blue dye after 6 hour.

A thickness of 20 nm metallic Ag film were thermally evaporated onto crystalline TiO$_x$ film surface reported by Zhang et al. (2022a) and it was found that the decomposition efficiency of the MB solution under UV lamp irradiation improved. Ag doped TiO$_2$ thin film with Ag content 0.5 and 1 mol % coated onto glass slide via microwave-assisted sol gel route explored by Sangchay et al. (2018). The photocatalytic degradation of MB under UV irradiation was said greatly improved especially with incorporation of 1 mol % Ag having 81.43 % MB degradation. Nevertheless, Cruz et al. (2022) found that Ag-TiO$_2$ with Ag content at 0.05mmol exhibited the highest photocatalytic efficiency and the increase in the silver concentration did not improve the photocatalytic properties of the Ag-TiO$_2$ composites under UV light exposure. Parastar et al. (2013) discovered that 1 % was an optimal Ag content for doping TiO$_2$ nanoparticles by photodeposition method under UV light irradiation for nitrate removal.

2.9.2 Degradation under visible light irradiation

Generally visible light spectrum having light range, $\lambda \geq 400$ nm and at this condition photocatalytic of TiO_2 didn't activated. That is why the modification of TiO_2 studied continuously in order to improve the photocatalytic performance at the higher wavelength. Herein, Ag added into TiO_2 exposed to visible light causing photogenerated electron which produced by surface plasmon resonance (SPR) of metallic Ag transferred to the conduction band. The electrons will then react with absorbed O_2 molecules to generate O_2^- and finally react with H^+ to become ^-OH (Zheng et al., 2019). The Ag cation with an appropriate concentration aid to decrease in the recombination rate of photoreduced charges and beneficial for expanding the range of light absorption. Hence, Ag acted as h^+/e^- trapped by altering the h^+/e^- pair recombination rate whether it lowering or increasing depends on the concentration of Ag cation (Jiang et al., 2021). Figure 2.10 illustrates the photoreaction of Ag-TiO_2 coating under visible light irradiation.
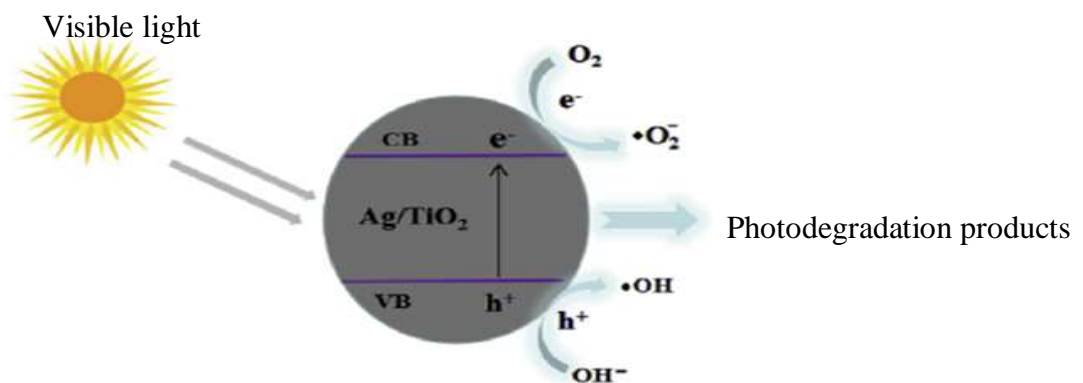
Figure 2.10: Schematic mechanism of Ag-TiO$_2$ photocatalyts under visible light irradiation (Mao et al., 2019)

Gyorgyey et al. (2016) studied silver coating on titanium disc for dental application and reported that the absorption spectrum between 400 and 550 nm with a maximum of 455 nm indicating the plasmonic effect of silver nanoparticles which enhances the photocatalytic efficiency of the coating under visible light region. Paper published by Suwei et al. (2017) on Ag nanoparticle-dispersed BaTiO$_3$ composite thin films revealed that Absorption peak in the wavelength region 450-600 nm results from SPR effect of Ag nanoparticles under visible light.

TiO$_2$-Ag with different Ag content of 0.5, 2.0 and 5.0 % m/m was prepared by Lidiaine et al. (2015) and photocatalytic properties of 5.0 mol % Ag content increase in the light scattering up to 800 nm. It explained that Ag° cluster present on TiO$_2$ surface contribute to the improvement of visible light region. Ag doped TiO$_2$ incorporated with clay at different amount investigated by Pohan et al. (2020) and evaluated the degradation of Orange II under visible irradiation. The authors reported that the removal efficiency of Orange II increased up to 62% with low amount of clay. Eventhough the incorporation of clay provided adsorption characteristics, increased clay content causing TiO$_2$ nanoparticles blocked them from exposure to the dye molecules.

2.10   Summary

Based on the reported works review, several considerations need to be taken into the design and development stage of a photocatalytic self-cleaning and antibacterial ceramic tile surfaces. In order to improve the characteristics and performances of TiO$_2$, many factors needs to be considered. The factors including the type of precursors use, synthesis method and technique, metal ions and substrate. All these will affect the microstructure such as phase crystallization, crystal size, elemental distribution, surface and cross section morphology of

TiO$_2$ that led to its performances. Most of the Ag-TiO$_2$ works were done on glass, metal and fabric surfaces instead of ceramic surface. Nevertheless, the need to explored Ag-TiO$_2$ potential on ceramic surface is necessary. This was due to the fact that ceramic surface are highly utilized in daily application such as indoor and outdoor area. Therefore, ceramic tile coated with Ag-TiO$_2$ coating was explored for the purpose of contributing a photocatalyst ceramic tile surfaces which can beneficial the ceramic tile industry in developing self-cleaning antibacterial surfaces. In accordance to the previous studies reported, it was found that less study utilized Degussa P25 into the sol gel of Ag-TiO$_2$ formulation. Most of the papers discussed the sol gel formulation of only using Ti precursor and Ag precursor without the incorporation of Degussa P25.

Hence, the fundamental on synthesizing Ag-TiO$_2$ coating deposited on unglazed and glazed ceramic tile coating with and without incorporation of Degussa P25 were conducted in this research. In addition, the amount of Ag that can control the particles size, surface area, thermal stability and band gap that contributes towards good photocatalytic performance of Ag-TiO$_2$ coating on ceramic substrate is limitedly explored. This study is also focussing to close this gap.

CHAPTER 3

METHODOLOGY

3.1   Introduction

In this chapter, the methodology of work carried out is explained related to achieve the aims of the study. Firstly, it starts with the design of the experimental research work and details of all the raw materials and chemicals employed. Next, this chapter describes the synthesis of Ag-TiO$_2$ coating with the aid of Degussa P25 and without Degussa P25 follows by the formulation of Ag-TiO$_2$ coating with different Ag content. During the synthesis process of Ag-TiO$_2$ sol it is important to ensure that the sol is properly prepared to avoid contamination issue and the clean workspace is always practice during material handling process.

This chapter also covers the characterization analyses and performance test of the derived Ag-TiO$_2$ coating such as crystalline phases, morphology and photocatalytic performances respectively. At the end of this work, the photocatalytic performances of the Ag-TiO$_2$ coating are evaluated related to its characteristics properties which lead to the understanding of its processing microstructure-performance relationship.

3.2   Experimental Design

The experiment work conducted in this research composes of five main stages that were; Preparation of materials and substrate, Preparation of Ag-TiO$_2$ sol coating with and without Degussa P25, deposition of Ag-TiO$_2$ coating on ceramic tiles, preparation of Ag-TiO$_2$ coating with various Ag content deposited on ceramic tiles, characterization and analyses of Ag-TiO$_2$ coating on ceramic tiles, and photocatalytic performance of Ag-TiO$_2$ coating. In the first stage, materials received are of analytical grades from different supplier

were secured accordingly. Substrates of unglazed and glazed ceramic tiles undergo cutting and cleaning process for the coating preparation.
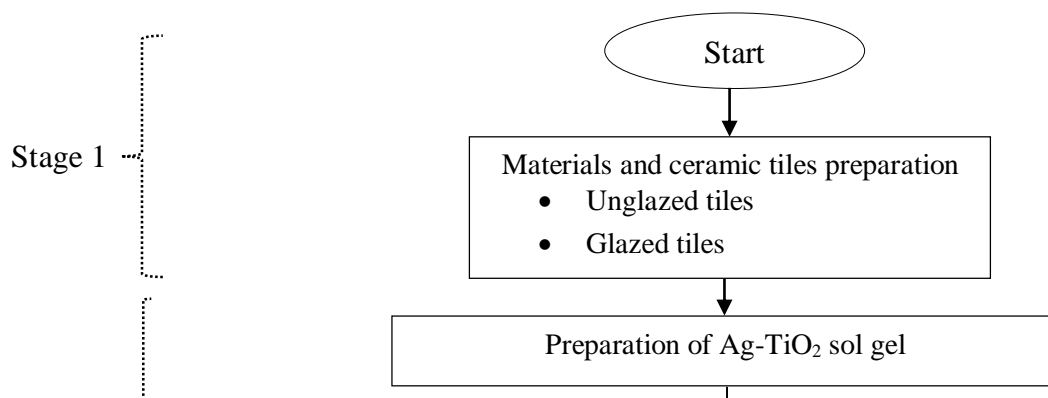
Stage two involved the preparation of Ag-TiO$_2$ sol with incorporation of Degussa P25 and without Degussa P25. Titanium tetraisopropoxide (TTiP) as the TiO$_2$ precursor together with Degussa P25 and without Degussa P25 were used during preparation of Ag-TiO$_2$ sol. The purposed of using Degussa P25 in TiO$_2$ are:

i.   for the surface to serve as the nucleation site and growth TiO$_2$ particle and prepare thicker TiO$_2$ coating with good adherability on substrate (Sreethawong et al., 2014).

ii.   Support the growth of particles size through crystal orientation and homogenous coating attached on the substrate. Therefore, better connection between TiO$_2$ structure and Degussa P25 which led to uniform distribution of titania (Musa et al., 2017a)

iii. Ag-TiO$_2$ coating added with Degussa P25 additive promoted more anatase and more homogenous microstructure that required for antimicrobial application (Nurhamizah et al., 2016a)

The incorporation of Degussa P25 is correlated to the study objective on the effect of Ag-TiO$_2$ coating with and without the presence of Degussa P25 on the characterization of Ag-TiO$_2$ deposited on unglazed and glazed ceramic tiles. In this stage, the amount of Ag-TiO$_2$ sol prepared with varied amount of Ag content that were 2.5. 5.0 and 7.5 mol % Ag.

Next, stage three was the deposition of Ag-TiO$_2$ coating with various Ag content on the ceramic tiles that is relevant to the second objective to of this research study that is to assess the effect of Ag content on the compositional, phase transition and microstructure of Ag-TiO$_2$ coating deposited on unglazed and glazed ceramic tiles. After the deposition of Ag-TiO$_2$ coating, stage four involve work where the coated Ag-TiO$_2$ ceramic tiles were characterized and analyzed using X-Ray diffraction analysis (XRD), Scanning electron

microscopy with energy dispersive X-ray spectroscopy (SEM/EDX) and Field Emission Scanning Electron Microscopy with Energy Dispersive X-Ray Spectroscopy (FESEM/EDX) for the crystal phases identification, surface and cross section morphology and elemental distribution mapping. At last, stages five assess the photocatalytic performance of Ag-TiO$_2$ coating by the degradation of methylene blue in ultraviolet (UV) and visible light irradiation. During the research, safety in handling the materials is a priority. The result obtained were examined carefully and reported in details. The experimental flowchart is shown in Figure 3.1.
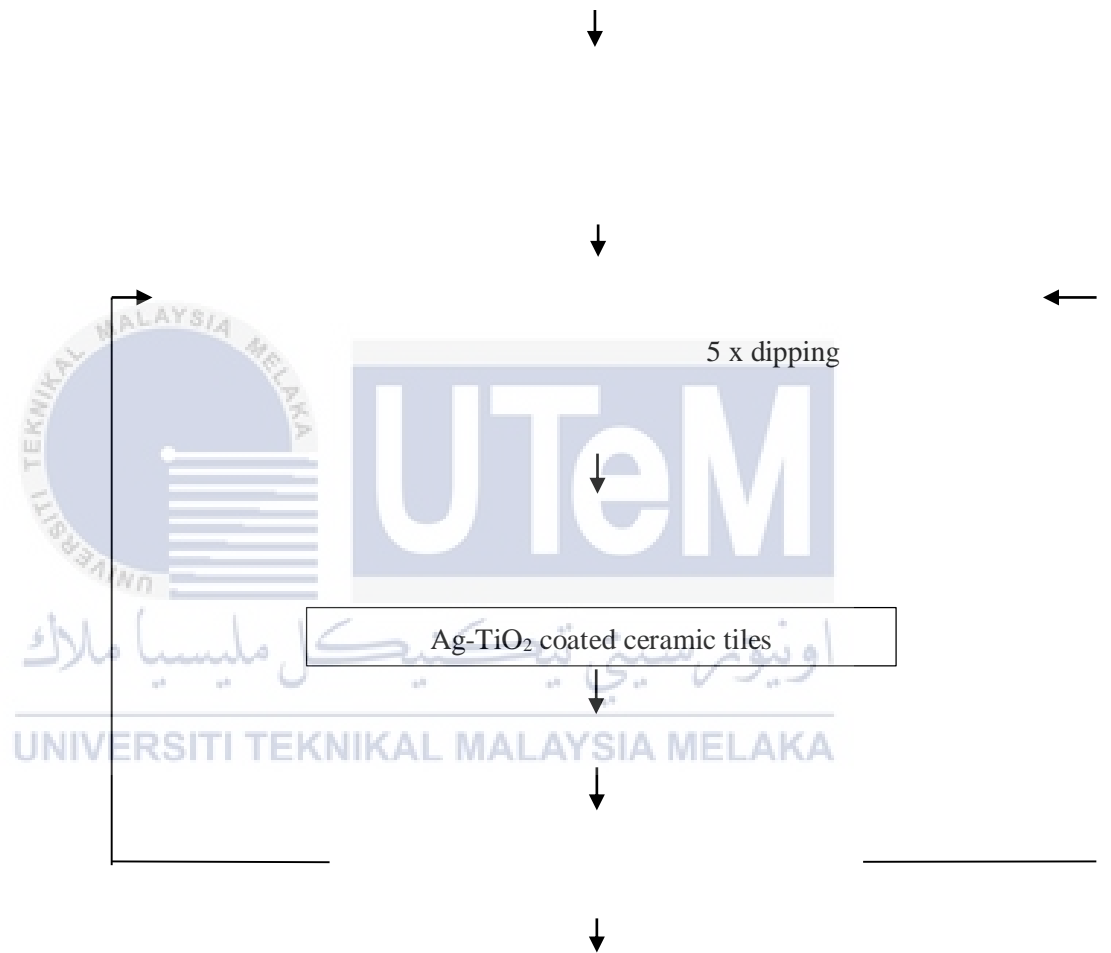
Start

Stage 1

Materials and ceramic tiles preparation
- Unglazed tiles
- Glazed tiles

Preparation of Ag-TiO$_2$ sol gel

5 x dipping

Ag-TiO$_2$ coated ceramic tiles

Figure 3.1: The experimental flowchart

3.3 Preparation of raw materials

Preparation of Ag-TiO$_2$ sol involved the use of , titanium tetraisopropoxide (TTiP) (Ti[OCH(CH$_3$)$_2$]$_4$) as titanium precursor because it is one of the suitable metal alkoxide precursor that produce non-toxic by-products during sol gel process (Collette et al., 2016). Meanwhile, ethanol and deionized used as solvent and hydrochloric acid acts as catalyst. The commercial TiO$_2$, Degussa P25 also as titanium precursor having anatase to rutile ratio of 4:1 and mean particle diameter of 22 nm was employed as an aid in preparing Ag-TiO$_2$ P25. Degussa P25 powder used directly as received where the XRD result analysis of that powder shown that pre-calcined Degussa P25 up to 500 ℃ gave no effect on the crystal structure of TiO$_2$ powder (Appendix A). Table 3.1 present the starting materials used in preparation of Ag-TiO$_2$ coating. All the chemicals must be free from contamination and still appropriate to use.

Table 3.1: The details of chemicals used for preparation of Ag-TiO$_2$ sol

Chemical/Raw material	Formula	Purity (%)	Commercial reference	Function
Degussa P25	TiO$_2$	99.5	Sigma Aldrich	TiO$_2$ enhancement
Titanium (IV) isopropoxide, TTIP	Ti(OC$_3$H$_7$)$_4$	97	Sigma Aldrich	TiO$_2$ precursor
Silver nitrate	AgNO$_3$	99.9	Merck	Ag precursor
Hydrochloric acid	HCl	37	Merck	Catalyst
Ethanol	EtOH	95	Polyscientific	Cleaning agent
Acetonitrile	CH$_3$CN	99.5	Merck	Reducing agent
Methylene blue, MB	C$_{16}$H$_{18}$N$_3$S		Comak	Pollutant
Deionized water, DI	H$_2$O		Polyscientific	Hydrolysis agent

The materials and chemicals must be handled with care because some of their properties such as brittleness of ceramic tiles, tendency of TTiP to oxidize and sensitivity of $AgNO_3$ that turn black in colour when exposed to high intensity of light. During the hydrolysis process of TTiP, the absorption occurred was substituted by its thermal degradation and the impurities due to the deterioration of TTiP affect the composition and crystallinity of the film, as well as its morphology (Kim et al., 2022). The $AgNO_3$ in the other hands started to hydrolyze when exposed to sunlight or any bright light. As it dissolves in water, it reduces into silver ions (Ag^+) and nitrate ions (NO_3^-). The incorporation of water produced hydrogen ions (H^+) from the dissociation of water molecules. These hydrogen ions can then reduce the silver ions to metallic silver (Ag^0), which appears as a black precipitate:

$$Ag^+ + e- \rightarrow Ag^0 \qquad (3.1)$$
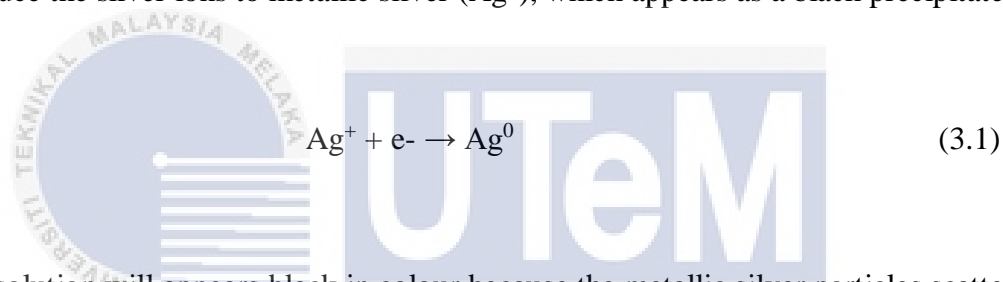
The solution will appears black in colour because the metallic silver particles scatter light, which happens when water acts as a reducing agent. This process involves donating electrons to silver ions, converting them into solid silver metal. Therefore, when handling $AgNO_3$, the environment condition needs to be in minimum amount of light.

3.4   Preparation of ceramic tile

Two different types of ceramic tiles were used in this work that was unglazed and glazed ceramic tiles. In order to prepare the small pieces of ceramic tiles, both ceramic tiles were cut by using tile cutter followed by precision cut off machine. The tiles in 10 mm x 20 mm (width and length) in size obtained by using low speed precision cut off machine model Micracut 151. The diamond wheel of 150 mm in size is set at 300 rpm/min with the presence of water during rotation. This is to reduce the heat generate during cutting process and

61

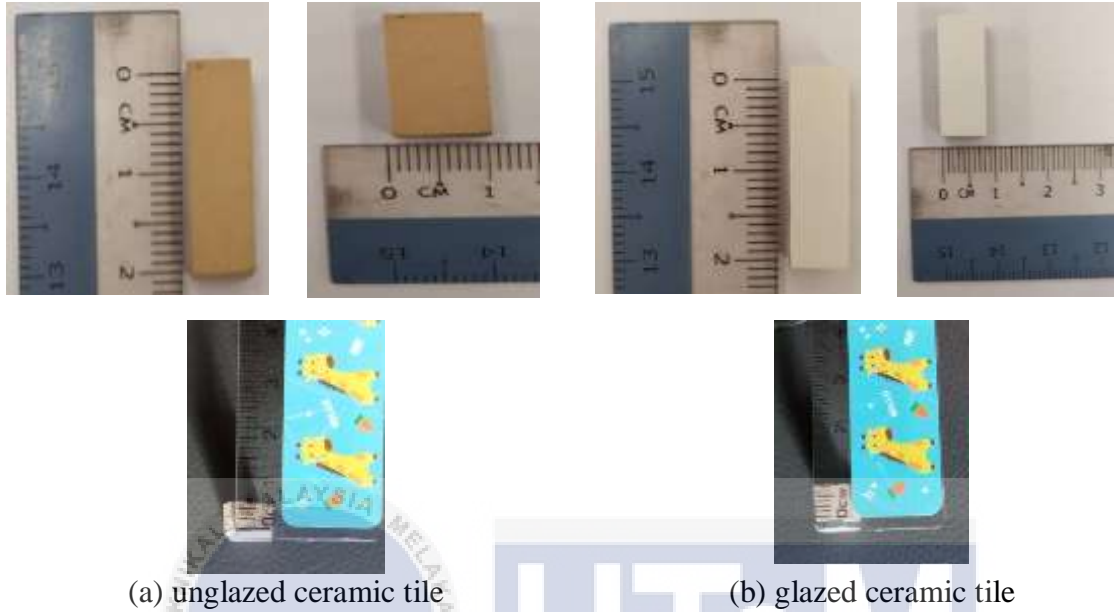residue from the tiles. Figure 3.2 illustrates the size dimension of unglazed and glazed ceramic tiles.

<center>(a) unglazed ceramic tile   (b) glazed ceramic tile</center>

Figure 3.2: Dimension measurement of (a) unglazed and (b) glazed ceramic tile

3.4.1 Ceramic tile cleaning

Before dipping, both unglazed and glazed ceramic tiles were cleaned from any dirt and any contaminant such as dust, oil and lint that stick on the tile surface. The cleaning part was necessary because it may affect the reaction bonding between the substrate and coating layer. The cubic shape of unglazed and glazed ceramic tiles prepared were cleaned by using acetone, ethanol and distilled water. Acetone was used as to remove any organic impurities on the unglazed and glazed ceramic tiles surfaces. While, ethanol used to remove the existed foreign particles on the unglazed and glazed ceramic tiles surfaces along with traces of acetone. Then, the unglazed and glazed ceramic tiles were put in a beaker soaking with deionized water (DI) and placed in ultrasonic bath which was a cleaner with a large transducer area and tanks that uses high power ultrasonic intensity to agitate a fluid throughout the entire oscillating tank for 10 minutes. After that, both unglazed and glazed

tiles were rinsed and soaked with deionized water (DI) approximately 10 minutes. At the end of the cleaning process, the unglazed and glazed ceramic tiles undergo drying process at 110 ºC for 2 hours to ensure that traces of water were completely removed. Figure 3.3 illustrates the process of cleaning unglazed and glazed ceramic tiles. While, the corresponding cleaning procedure is shown in Figure 3.4.

Ceramic tile

Figure 3.3: Cleaning process of unglazed and glazed ceramic tiles in ultrasonic bath
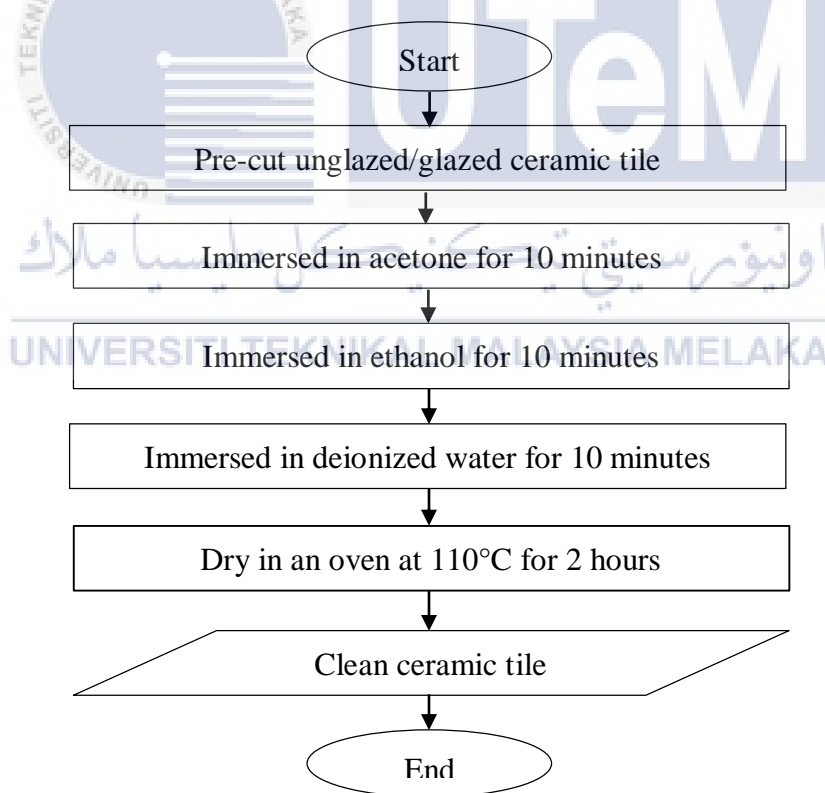

Figure 3.4: Preparation procedure for cleaned unglazed and glazed ceramic tiles

3.4.2 Surface Roughness (R_a) Measurement

The surface roughness of the clean unglazed and glazed ceramic tile was measured by the mean value of R_a (arithmetic mean of the absolute departures of the roughness profile) accordance to JIS 1994 standard. The purposed of measuring the surface roughness was to assess the adhesion between the coating layer and substrates. The measurement data collected by tracer method using portable surface roughness profilometer equipped with conical gauging point made of a diamond tip of 90° curvature and 2 μm tip roundness radius. The probe travelled along four non-intersect straight lines with specific length. The steps repeated on five different sample of unglazed and glazed ceramic tile to get the accurate results. The surface roughness of the unglazed and glazed ceramic tile obtained is 4.56 ± 0.02 μm and 0.05 ± 0.005μm respectively.

3.5   Preparation of Ag-TiO$_2$ sol gel

The preparation of Ag-TiO$_2$ was composed of three main stages that were:

  i. Ag-TiO$_2$ sol with incorporation of commercial Degussa P25

 ii. Ag-TiO$_2$ sol without incorporation of commercial Degussa P25

iii. Ag-TiO$_2$ sol formulation with various Ag content

During the preparation of Ag-TiO$_2$ sol, sol gel method was employed due to its convenience and suitability for the synthesis of Ag-TiO$_2$ (literature review section 2.5). The details of the preparation were discussed in the section 3.5.1 and 3.5.2.

3.5.1   Preparation of Ag-TiO$_2$ sol with incorporation of commercial Degussa P25

For the sol with Degussa P25, there were several steps need to be concerned during the sol preparation. The purpose was to ensure the compatibility and homogeneity of Degussa P25 in the prepared sol (Musa et al., 2017b). Hence, two different mixtures that are mixture X and mixture Y were formulated. Mixture X consists of 32 ml deionized water

(DI), 8 ml ethanol (etOH) and 0.4 ml HCL. Mixture Y composed of 2 ml TTiP and 8 ml etOH. Mixture X and Y mix together to form TiO_2 alkoxide sol and stirred for 3 hours. Then, 2.5 g Degussa P25 (50 g/L) was added into the sol and stirred for 1 hour forming TiO_2 sol. Then, the Ag content at 2.5, 5.0 and 7.5 mol % of silver nitrate ($AgNO_3$) were added into TiO_2 sol.

Next, the Ag-TiO_2 P25 sols were left for 48 hours aging at room temperature. The amount of Degussa P25 used was based on the previous studied by Chen and Dionysiou (2006) on depositing TiO_2-P25 coating on stainless steel substrate and heat treated at 600ºC. The author employed Degussa P25 content at 30 to 50 g/ L with only one dipping. The result found that 50 g/L content in TiO_2-P25 coating exhibited the finest film with good adhesion on stainless steel substrate and highest photocatalytic activity. Recent worked by Musa et al. (2018) on the effect of Degussa P25 content on TiO_2 coating using sol-gel dip-coating technique on the unglazed ceramic tiles also discovered that 50g/L content of Degussa P25 was the amount needed to achieved a good adherence coating on ceramic tiles. It is noted that the mixing process was performed in laboratory fume hood as the chemical used tends to be easily oxidized. During the preparation of Ag-TiO_2 P25 sol, the amber glass was used for the sol due to the sensitivity of Ag to the light exposure. The steps of preparation were shown in Figure 3.5.
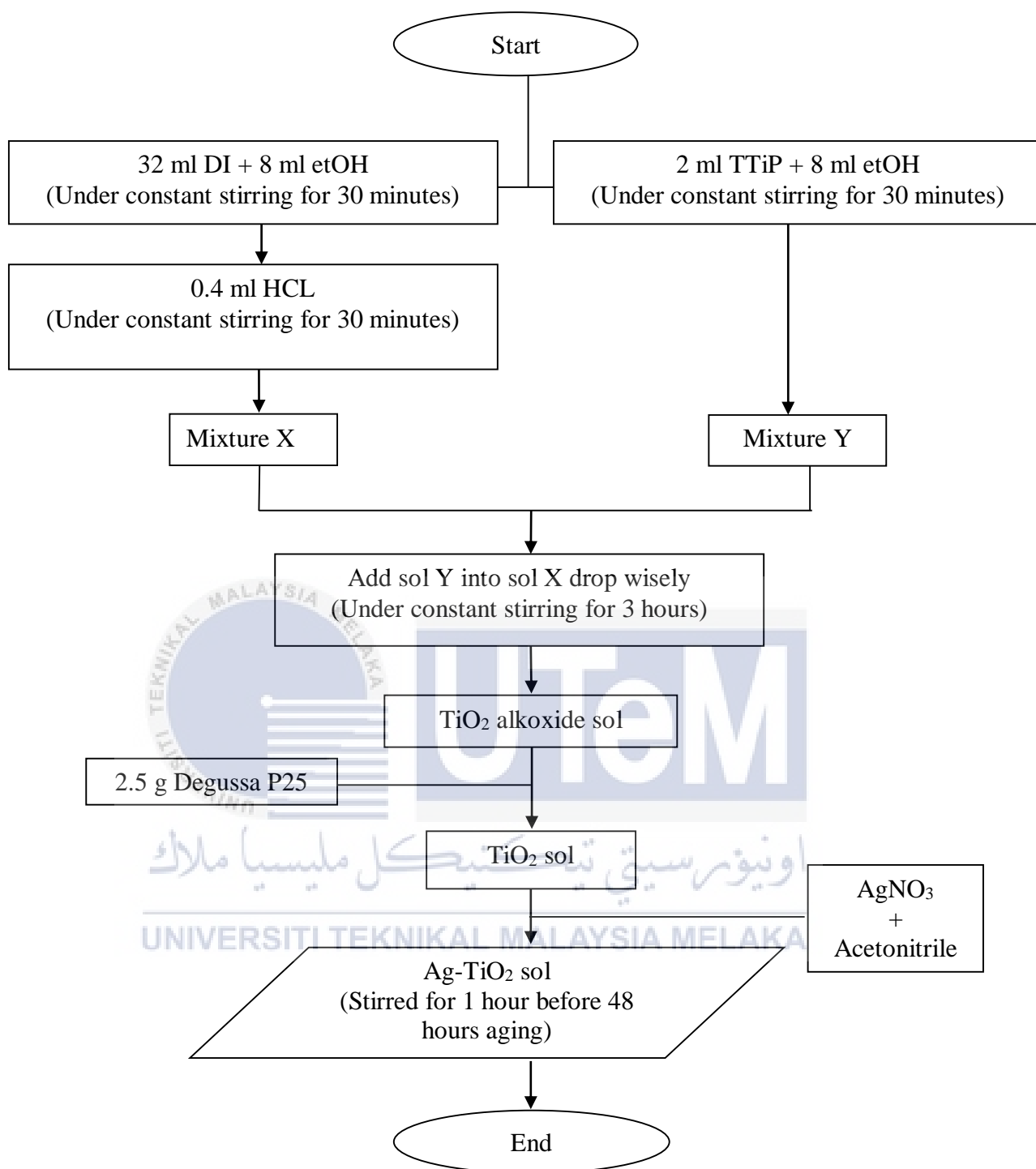
Figure 3.5: Preparation of Ag-TiO$_2$ sol with incorporation of Degussa P25

3.5.2 Preparation of Ag-TiO$_2$ sol without incorporation of commercial Degussa P25

In contrast, to prepare Ag-TiO$_2$ sol without incorporation of Degussa P25 a different

approach has been used. Preparation of Ag-TiO$_2$ sol without the incorporation of Degussa

P25 started with 4 ml of TTiP slowly dropped using glass dropper into 64ml deionized water (DI) water and the solution were constantly stirred for 30 minutes using magnetic stirrer at room temperature. The amount of TTiP and DI water used were doubled compare to amount of preparing Ag-TiO$_2$ P25 sols. This is to ensure enough precursor of TiO$_2$ in TTiP to growth the anatase phase of laboratory made Ag-TiO$_2$ sol coating (Yazid et al., 2019). Subsequently, 0.4 ml of concentrated hydrochloric acid (HCL) added dropwisely into the solution and continuously stirring for 3 hours. As previous, Ag content at 2.5, 5.0 and 7.5 mol % of silver nitrate (AgNO$_3$) were added into the sol and stirred for 1 hour. Then, the solution was left for 48 hours at room temperature for aging process before ready to use. The preparation of Ag-TiO$_2$ is shown as in Figure 3.6.
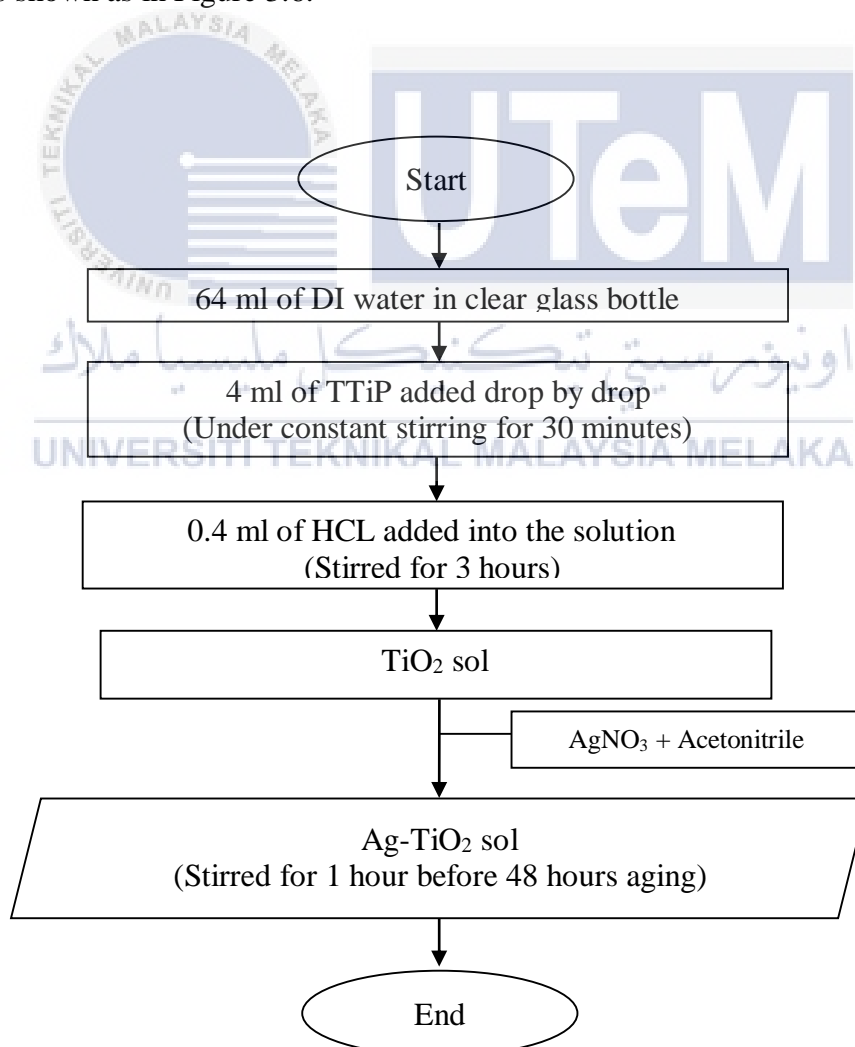

Figure 3.6: Preparation of Ag-TiO$_2$ sol

In previous section (3.5.1) the preparation of Ag-TiO$_2$ P25 had employed half amount of TTiP and deionized water for the sol preparation because the incorporation of Degussa P25 had already contributed to 70 % anatase and 30 % rutile phase. Literally, the Ag-TiO$_2$ P25 already contributed to the majority of the anatase phase in the coating. Therefore, the amount of chemical needed to prepare the Ag-TiO$_2$ P25 sol was half the amount needed to prepare Ag-TiO$_2$ sol without incorporation of Degussa P25.

3.6 Deposition of Ag-TiO$_2$ coating with varied Ag content on ceramic tile

Based on our aim of study that is to assess the effect of Ag content on the Ag-TiO$_2$ coating, three different formulation of Ag has been studied. In this study, 2.5, 5.0 and 7.5 mol % of Ag were introduced into the sols in order to have a better understanding on the effect of Ag content on coating deposition. Ag content of 2.5. 5.0 and 7.5 mol % were added before the aging process. The amount of Ag content ranging from 2.5 – 7.5 mol % has been studied due to the previous studied which reported various amount of Ag content in the Ag-TiO$_2$ coating deposited on various substrate had yield good coating indicating that the properties are influenced by the amount Ag content (Demircia et al., 2016, Kaygusuz et al., 2016, Halin et al., 2018, Saraswati et al., 2019, Liaqat et al., 2020). As been shown in Figure 3.5 and 3.6 previously, Ag was added at the last part after the TiO$_2$ sol preparation in order to produce Ag-TiO$_2$ sol. AgNO$_3$ was dissolved in acetonitrile which act as reducing agent before it is added into TiO$_2$ sol. The purpose was to break the chain of AgNO$_3$ and reduce to Ag ion. This was to ensure that formation of Ag particles during heat treatment of Ag-TiO$_2$ sol (Halaciuga et al., 2011).

The precaution that had to be taken care during the Ag-TiO$_2$ preparation is the usage of amber glass during the sol preparation due to the sensitivity of Ag to the light exposure. Therefore, Ag-TiO$_2$ coated on unglazed and glazed tile was done in a room with low intensity

of light. This is to prevent Ag ion from oxidize and coating layer turn dark color (Hou et al., 2013). These steps are important as to ensure the existence of Ag in coating layer. Figure 3.7 shows the unglazed and glazed ceramic tile coated with Ag-TiO$_2$ coating.
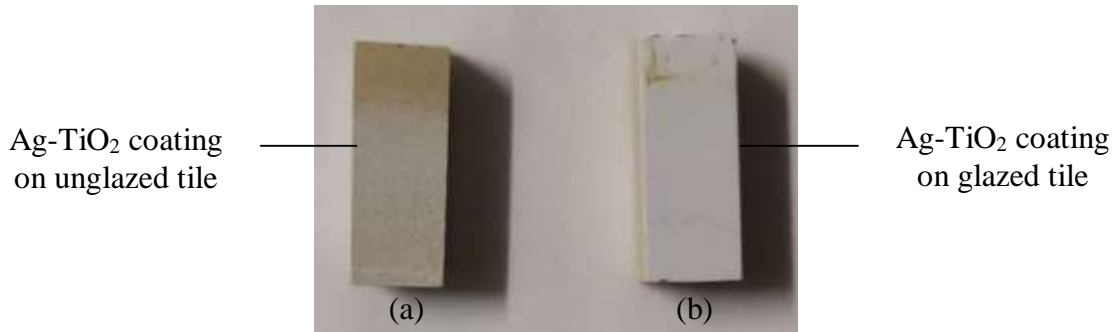
Ag-TiO$_2$ coating on unglazed tile

Ag-TiO$_2$ coating on glazed tile

(a) (b)

Figure 3.7: Ag-TiO$_2$ coating deposited on (a) unglazed and (b) glazed ceramic tiles

3.6.1 Deposition method and procedure

Ag-TiO$_2$ deposited on ceramic tile were carried out by dip coating technique using a precision dip coater machine model Tefini DP1000 as shown in Figure 3.8. The rate of withdrawal speed was set up for 30 mm/min with 5 s dwell time. The ceramic tile was clamped onto the dip coater arm and immersed in the solution. The coated ceramic tile then dried in room temperature for 3 hours followed by oven dried at 110 ˚C for 30 minutes. Based on Musa et al. (2018) study on the effect of Degussa P25 content on the deposition of TiO$_2$ coating on ceramic substrate, five dipping of TiO$_2$ sol was found appropriate to produce a uniform and continuous layer covering the tiles with average thickness of ~29μm . Thus, referring to the study, the steps were repeated for 5 times to obtained 5 layers coating on ceramic tiles (Musa et al., 2018).
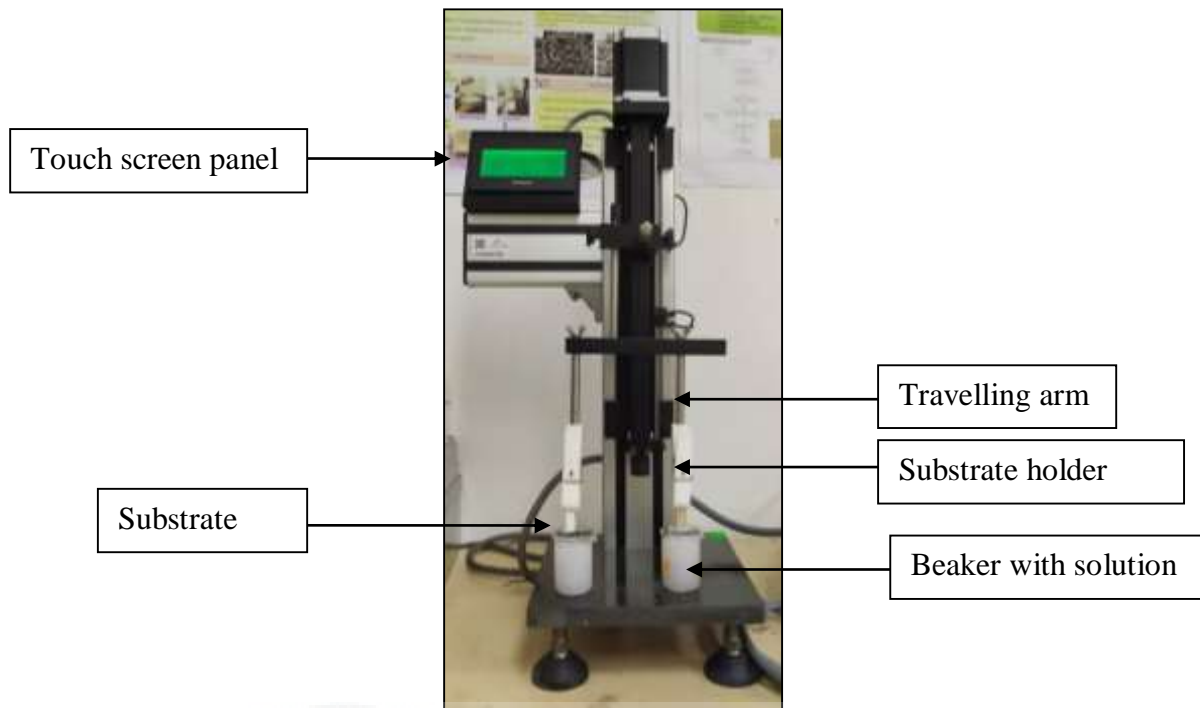
Figure 3.8: Dip coating machine

The parameter of Ag-TiO$_2$ deposited on unglazed and glazed ceramic tile coating prepared can be simplified as in Table 3.2:

Table 3.2: Summary for the samples prepared

Type of tile	Sol gel formulation	Ag content (mol %)	Deposition method
Unglazed	Ag-TiO$_2$ P25	2.5	
	&	5.0	Dip coating
Glazed	Ag-TiO$_2$	7.5	

3.6.2 Heat treatment

Ag-TiO$_2$ coated on both unglazed and glazed tile were heat treated using Nabertherm B180 furnace. Heat treatment is the final stage of sample preparation needed for the crystallization process of the Ag-TiO$_2$ coating prior to be analysed and subjected to any

70

testing. The ceramic tiles of Ag-TiO$_2$ coating on unglazed and glazed tiles were loaded on alumina plates and placed inside the furnace. The furnace was set up at 500°C for 1 hour soaking time with heating rate of 2 °C/min. The heat treatment temperature of 500 °C was chose based on the reported anatase phase transformation of TiO$_2$ which started at 500 °C. In fact, Ag-TiO$_2$ heat treated at 500 °C had exhibited the highest photocatalytic activity and decreased as increased in heat treatment temperature (Keyvanloo et al., 2016, Lee et al., 2005). Besides, Keyvanloo et al. (2016) reported that Ag-TiO$_2$ nanocomposite heat treated at 530 °C possed good degradation efficiency of Rhodamine B. The heat treated Ag-TiO$_2$ unglazed and glazed ceramic tiles then were kept in a clean, dark container and stored in drying cabinet before subjected to further testing. The heating profile process of Ag-TiO$_2$ coating was presented in Figure 3.9:
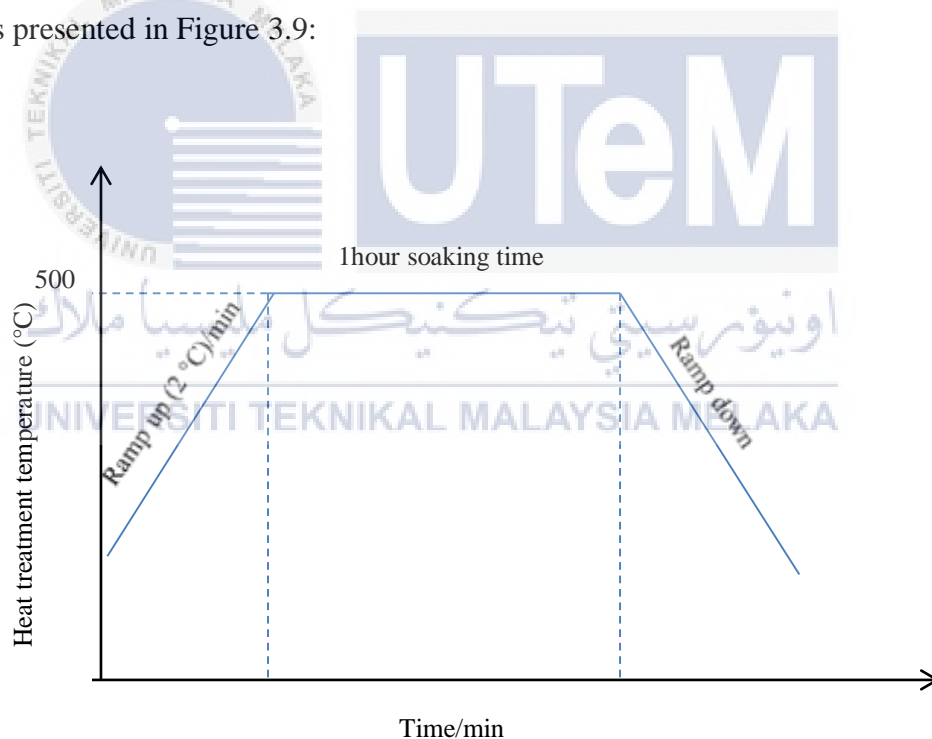

Figure 3.9: Heating profile of Ag-TiO$_2$ coating

3.7 Characterization and analysis of Ag-TiO$_2$ coating on ceramic tiles

The characterization and analysis of Ag-TiO$_2$ coated on unglazed and glazed tiles were carried out for the crystallinity and phase transformation using GAXRD, surface and

71

cross-sectional analysis using SEM/EDX and FESEM/EDX respectively. The samples were prepared according to the testing procedure.

3.7.1 Crystallographic analyses using GAXRD and XRD

The ceramic substrates phases of unglazed and glazed ceramic tiles were analyses by using X-ray Diffraction without implement any glancing angle. Meanwhile, the crystallinity of Ag-TIO$_2$ coating deposited on unglazed and glazed ceramic tiles were analyse by using Glancing Angle X-ray Diffraction PANalytical X'Pert PRO MPD Model PW 3060/60. The scanning was performed using Cu Kα radiation (λ = 1.54060A°) and scanning speed of 0.05°C/s.The detector position is recorded as the angle 2θ in a range of 10˚ - 80˚ at a 4˚ glancing angle that was the best glancing angle for ceramic substrate that was determined from previous studied by Nurhamizah et al. (2016b). The Cu Kα of 1.54060A° and generator settings at 30 mA and 40 kV. For this work, glancing angle was employed as to make GAXRD measurement more sensitive to the surface region of interest and at same time eliminate the contribution of the substrate on the diffraction response. Samples were placed in the sample holder and the X-ray tube will rotate for 30 minutes for the X-ray beam maintain focussed. After that, the quantitative and qualitative analysis of the GAXRD profiles were analyse using PANanalytical X'Pert Highscore Plus software. In order to calculate the crystallite size, the average crystallite size from XRD data was calculated using Scherrer's equation for the most intense diffraction peaks of anatase (101) at 25.3°, and rutile (110) at 27.5°, as shown in equation 3.2:

$$D = \frac{K\lambda}{\beta \cos\theta} \tag{3.2}$$

where D refers to the average size of the crystalline (unit in nm), K denoted to the constant, 0.94, λ represents the wavelength of X-rays, θ refers to the diffraction angle, β represents the full width at half maximum (FWHM). As preliminary study, the unglazed and glazed ceramic tiles without Ag-TiO$_2$ coating were also subjected to GAXRD analyses to examine the peak exist of ceramic material.

3.7.2   Surface morphology analysis and cross-section

The surface morphology of Ag-TiO$_2$ coated on unglazed and glazed ceramic tiles were examined by using SEM/EDX and the cross-sectional view by using FESEM/EDX. The thin layer of Ag-TiO$_2$ coating deposited on unglazed and glazed ceramic tile surface had limit the SEM/EDX on detecting the coating thickness. Thus, the FESEM/EDX was an alternative for the determination of coating layer thickness.

3.7.2.1 Surface morphological analysis using SEM

The scanning electron microscopy model Carl Zeiss-Evo 50 type was used to analyse the quality of surface microstructure of Ag-TiO$_2$ coating on unglazed and glazed ceramic tile surface. Before carrying the analyses, the surfaces of Ag-TiO$_2$ samples were mounted on aluminium stubs and sputter coated with a thin layer (1.5-3.0 mm) of palladium-gold inside a "sputter coater" machine in order to make the tile coating surface conductive enough as to avoid electrostatic charging and poor image resolution during examination prior to scanning surface morphology procedure. The SEM imaging in this study uses secondary electrons detector to examine the Ag-TiO$_2$ coating on ceramic tiles surface.

3.7.2.2 Elemental mapping and composition using EDX

Energy Dispersive X-ray spectroscopy (EDX) analysis model JEOL6010PLUS/LV was used to determine the elemental analysis and element distribution on the coating surface. X-ray spectrum emitted by a solid sample bombarded with focused beam of electrons to obtain a localized chemical analysis. Data of element distribution or maps and atomic number present in the coating will be shown by the computer screen. Then, the element analyses and distribution of Ag-TiO$_2$ coating on the unglazed and glazed ceramic tile of coating surface were distinguished according to the colour produced.

3.7.2.3 Cross-sectional analysis using FESEM

In this experiment, samples were observed under Field Emission Scanning Electron Microscopy (FESEM) model HITACHI SU5000. The unglazed and glazed ceramic tiles without coating and coated Ag-TiO$_2$ were study to examine the effect of Ag incorporation within the coating layer. In this research, to obtain the cross-sectional view, the pure uncoated unglazed and glazed ceramic tiles as well as Ag-TiO$_2$ coating on unglazed and glazed ceramic tile were fractured along the pre-created notch. The purposed of this step was to make sure that minimal damage on the Ag-TiO$_2$ coating as it will affect the analysis result. Then, the samples need to be current conductive by coating with a thin layer around 1.5 – 3.0 nm of gold-palladium. The coating thickness of at least five different parts along the coating cross-section images, t_{ave} was measured and averaged out.

3.8   Photocatalytic Performance of Ag-TiO$_2$ coating

The photocatalytic test of Ag-TiO$_2$ coating on unglazed and glazed ceramic tiles were performed to have an overview on the self-cleaning property. The degradation of aqueous methylene blue (MB) under UV light was measured according to the standard procedures of ISO 10678:2010 (Mills et al., 2012). Methylene blue was one of the industrial dyes that is

toxic, carcinogenic and non-biodegradable and at worst a severe threat to human and environmental safety. It has been applied in textile, pharmaceutical, medicine, food industries, dyeing, paper, paint and printing (Khan et al., 2022). Therefore, methylene blue was chosen in this study as a model of pollutant to conduct the photocatalytic test. In addition, methylene blue was suitable for the degradation under UV and visible light due to its ability to absorb light in visible range (600 – 700 nm) and partly in UV ($\leq$ 400 nm).

The undiluted MB solution (1 wt %, 500 ml) needs to dilute with distilled water in order to obtain 10 ppm concentration calculated by dilution formula as equation 3.3 (Chang and Goldsby, 2016) :

$$M_1 V_1 = M_2 V_2 \tag{3.3}$$

Where M_1 refer to the undiluted MB solution (ppm), V_1 is the volume of the undiluted MB needed (ml), M_2 is the concentration of MB solution (ppm). In this experiment, the concentration of MB use is 10 ppm and V_2 is the total volume of the diluted MB needed to conduct the experiment.

Photocatalytic activity of Ag-TiO$_2$ coating surfaces in this research were done by immersing the samples in aqueous medium of MB. Degradation of methylene blue (MB) under both UV and visible light irradiation were then calculated. Every single coated tile must undergo pre-irradiated by exposing under UV light for 24 hours. The purpose of pre-irradiated is to decompose any contaminants and this known as photocatalytic oxidation process (Thiruvenkatachari et al., 2008). Due to the nature of ceramic tiles that tend to absorb the dye molecules, the clean coated tiles must be immersed in 25 ml MB solution for 24 hours. After that, the tiles were placed in a new 25 ml MB solution and exposed them to the UV and visible light for 5 hours. Figure 3.10 illustrated the photocatalytic test conducted for degradation of MB in a photocatalytic reaction box.
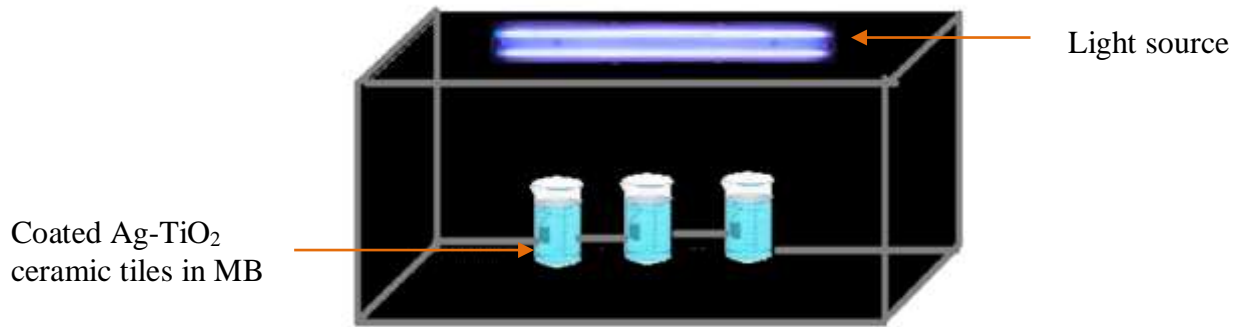
75

Figure 3.10: Schematic diagram of photocatalytic test for MB degradation

The degradation of MB was determined by UV-Vis spectrometer at adsorption spectrum of 664 nm wavelength. As for the references sample, the coated tiles were kept in the dark and its absorption spectrum were measured.

$$Degradation\ of\ MB\ (\%) = \left(\frac{A_o - A_t}{A_o}\right) \times 100\ \% \tag{3.4}$$

where A_o is the absorbance of MB solution before exposed to UV light illumination and A_t is the absorbance of the MB solution at UV light illumination of time t. The specific degradation rate, R

$$R = \frac{\Delta A_\lambda \times V}{\Delta t \times \varepsilon \times d \times A} \tag{3.5}$$

where, ΔA_λ is the absorption difference from one measurement to another (every 20min), V is the volume of MB solution (25 ml), ε is the MB molar extinction coefficient at 664 nm (7402.8 m^2/mol), d is the measuring cell length used at the spectrophotometer (10 mm), and A is the contact area of MB solution and Ag-TiO$_2$ coatings.

The degradation rate of irradiated, R_{irr} and dark samples, R_{dark} will make it possible to calculate specific photocatalytic activity, P_{MB} by using equation 3.5 and photonic efficiency, ζ_{MB} calculated as the equation 3.6 (ISO 10678:2010).

$$P_{MB} = R_{irr} - R_{dark} \tag{3.6}$$

$$\zeta_{MB} = \frac{P_{MB}}{E_P} \times 100 \tag{3.7}$$

where, E_P is the UV light radiation intensity.

The UV light intensity, E_p (W/m^2) is calculated by using equation 3.7 (Sharma et al., 2012):

$$UV\ light\ intensity, E_p = \frac{W}{4\pi D^2} \tag{3.8}$$

where W is the total wattage of the UV light source (W) and D is the distance between the lamp and the coating surface. The distance (D) measured in for the ceramic tiles in this studied was 16.00 cm.

3.9 Summary

At the beginning, two different sols were prepared that were Ag-TiO$_2$ P25 and Ag-TiO$_2$ sol. The preparation of these two different sols was very important in determining the best sol for ceramic tiles coating. After that, the preparation of Ag-TiO$_2$ sol coated on ceramic tiles was discussed by considering the amount of Ag in the best range based on the literature review. Ceramic tiles of unglazed and glazed has been used as substrate and coated with Ag-TiO$_2$ P25 and Ag-TiO$_2$ for 5 layer dipping times. The amount of 2.5, 5.0 and 7.5 mol % of Ag were used to determine the effect of different Ag content incorporated on

unglazed and glazed ceramic tiles and the influenced of Ag were studied. The crystallization of Ag-TiO$_2$ coating with and without Degussa P25 was compared to propose the appropriate Ag-TiO$_2$ coating for deposition on ceramic tiles. Further, several testing were carried out to study the effect of Ag content on the characteristics and structural properties of Ag-TiO$_2$ coating via Glancing Angle X-ray Diffraction (GAXRD), Scanning Electron Microscopy with Energy-dispersive X-ray Spectroscopy (SEM/EDX) and Field Emission Scanning Electron Microscopy with Energy-dispersive X-ray Spectroscopy (FESEM/EDX). The photocatalytic performances of Ag-TiO$_2$ coating on ceramic tiles were then performed by degradation of methylene blue under UV and visible light irradiation. The photocatalytic performances of Ag-TiO$_2$ coating on ceramic tiles were discussed upon the characteristics and properties analysis of Ag-TiO$_2$ coating respectively. By having an appropriate amount of Ag needed for coating ceramic tiles will lead to a better performances of photocatalytic tiles and antimicrobial in the future application.
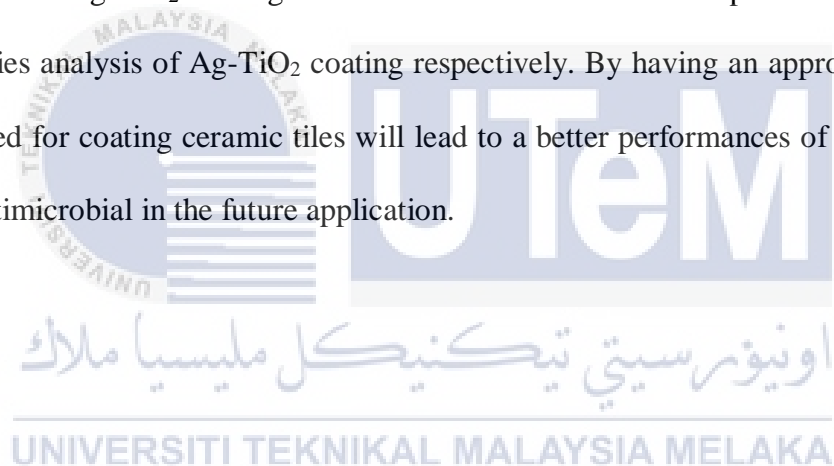
CHAPTER 4

RESULT AND DISCUSSION

4.1   Introduction

In this chapter, the characterization and microstructure of as received ceramic tiles without coating and ceramic tiles coated with Ag-TiO$_2$ coating are discussed in details. Firstly, the crystalline phase and surface morphology analyses of the ceramic tiles without coating is presented as reference. Then, the crystalline phase analyses of Ag-TiO$_2$ coating with Degussa P25 and without Degussa P25 on unglazed and glazed ceramic tiles is reported and discussed. The purpose of crystalline phase analysis of Ag-TiO$_2$ coating without Degussa P25 and with Degussa P25 on unglazed and glazed ceramic tiles were essential to confirm the presence of Ag phase in the coating layer before samples are subjected to photocatalytic test.

Next, the results works based on varied Ag content of Ag-TiO$_2$ coating deposited on ceramic tiles were presented. The effect of Ag content on the crystalline phase, surface morphology and cross section analyses, elemental distribution and photocatalytic performances of the Ag-TiO$_2$ coating exposed under UV and visible light irradiation were discussed. Later, the influence of Ag content on the crystalline formation, microstructure and its photocatalytic performance is evaluated and optimized Ag content for Ag-TiO$_2$ coating on ceramic tiles based on the scope of this work is suggested.

79

4.2   The ceramic tiles substrate

The as received ceramic tiles were studied for reference in this study. Both ceramic tiles of unglazed and glazed were examined for XRD analyses and surface morphology before being coated with Ag-TiO$_2$ sol.

4.2.1   Crystalline phase analyses

Figure 4.1 and 4.2 shows the crystalline phase of the unglazed and glazed tile respectively. Both unglazed and glazed tile shows presence of mixture crystalline phases that assigned to the ceramic components including cristobalite (JCPDS: 04-008-7642), quartz (JCPDS: 00-046-1045), mullite (JCPDS: 00-015-0776) and cordierite (JCPDS: 01-082-1884) that composed of silicon oxide (SiO$_2$), aluminium oxide (Al$_2$O$_3$), iron oxide (Fe$_2$O$_3$), calcium oxide (CaO), sodium oxide (Na$_2$O), potassium oxide (K$_2$O) and zirconia oxide (ZrO$_2$). This similar composition were reported in paper published by Ibrahim et al. (2017) where the ceramic waste powder consists of those chemical composition with different percentage. It can be deduced that both unglazed and glazed ceramic tile had similar peak but with different peak intensity. In comparison, unglazed tile illustrated lower peak intensity compare to glazed ceramic tile for example the Si phase at angle 2θ = 30.39° and 72.19° and Al phase at angle 2θ = 38.7°. These indicated that the crystal size of the crystalline phases exist in glazed tile was larger than the element crystal of unglazed tile. The XRD diffraction peak is related to the crystal structure and the size of the crystallites in the sample. The higher peak intensity indicates a higher number of atoms in the crystal, which could indicate a higher degree of crystallinity or larger crystal size (Terohid et al., 2018).
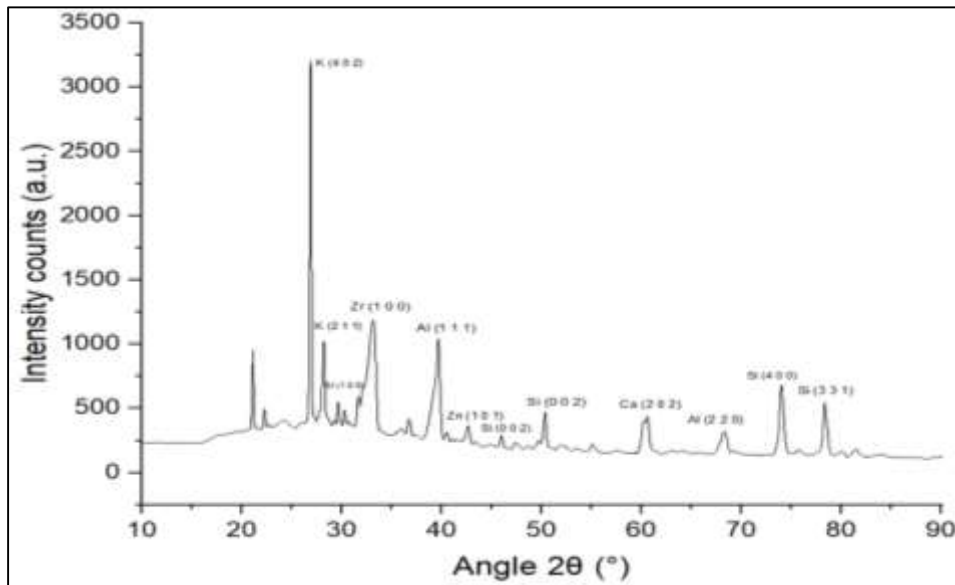
80

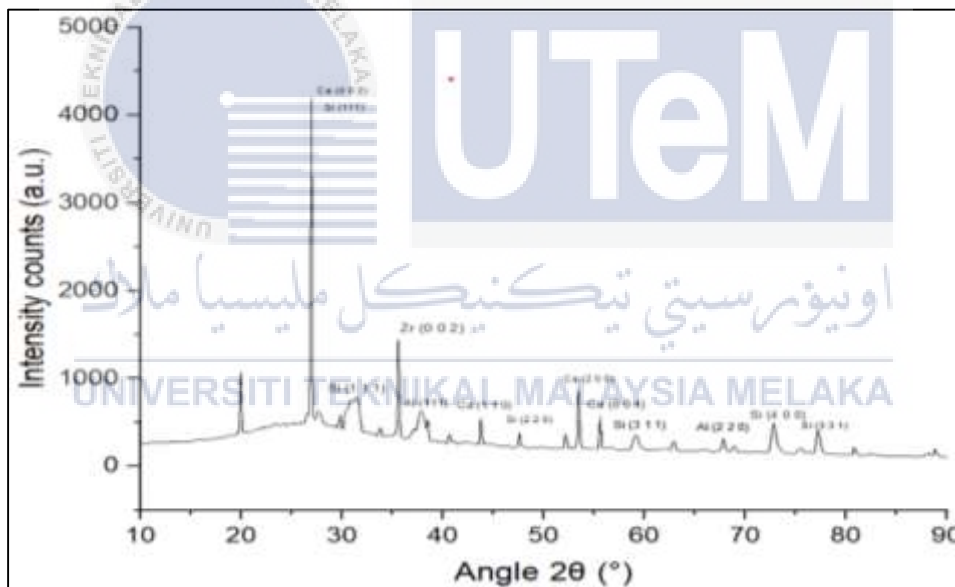Figure 4.1: XRD pattern of unglazed ceramic tile

Figure 4.2: XRD pattern of glazed ceramic tile

4.2.2 Surface morphology analyses

The surface morphology of unglazed ceramic tile in Figure 4.3 shows that the unglazed tile had a rough and wavy like surfaces correspond to the roughness measured that is 4.56 ± 0.02 µm as stated in section 3.4.2. It was observed that large holes are present on the surface. This large hole is related to the presence of pores in unglazed ceramic tiles. The

81

unglazed ceramic tiles consists of constituent element such as Oxygen (O), Magnesium (Mg), Aluminium (Al), Silicon (Si) , Clorine (Cl), Potassium (K) and Calcium (Ca) as similar element were identified by the XRD analyses reported in section 4.2.1. In addition, the presence of Aurum (Au) element was from the gold sputter coating applied that needs the samples to be conductive before subjected to SEM/EDX.

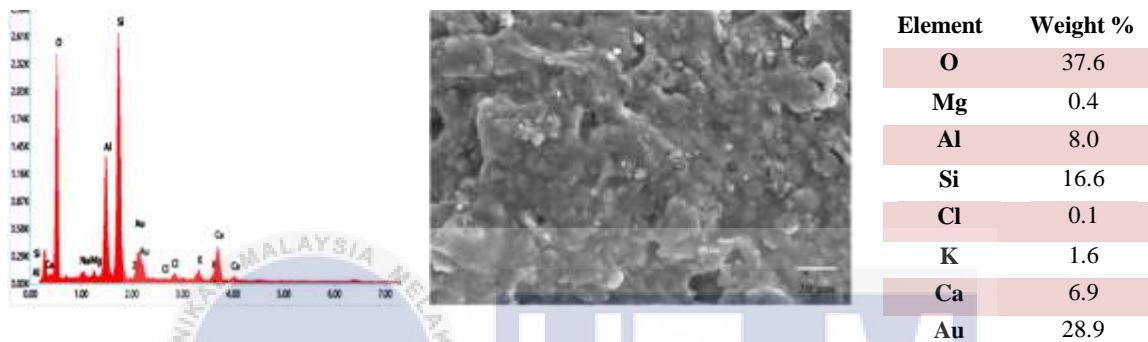| Element	Weight %
O	37.6
Mg	0.4
Al	8.0
Si	16.6
Cl	0.1
K	1.6
Ca	6.9
Au	28.9

Figure 4.3: The SEM/EDX of unglazed ceramic tile

In contrast, glazed ceramic tile SEM/EDX analyses shown in Figure 4.4 shows a smooth surfaces with small particles embedded on the surface which suggest belongs to the glazed microstructure. The smooth surface of the glazed tile correspond to the surface roughness measured $0.05 \pm 0.005\mu m$ stated in section 3.4.2. The glazed tiles consist of ceramic elements similar as the elements presence in unglazed tile. Nevertheless, the EDX analyses of glazed ceramic tile surface show the presence of small amount titanium which responsible for the smooth surface and resistant to external agents such as microorganisms (Reinosa et al., 2022). Titanium is known fluxes for the porcelain glazed and during firing this titanium formed opacity (Teixeira and Bernardin, 2009). The presence of zirconia (Zr) element for the wear resistance and strength that prevent the brittleness of ceramic material (Manicone et al., 2007).The element of Iron (Fe) meanwhile for the colouring mechanism that responsible for colour tones of the glaze tile (Gol et al., 2022).
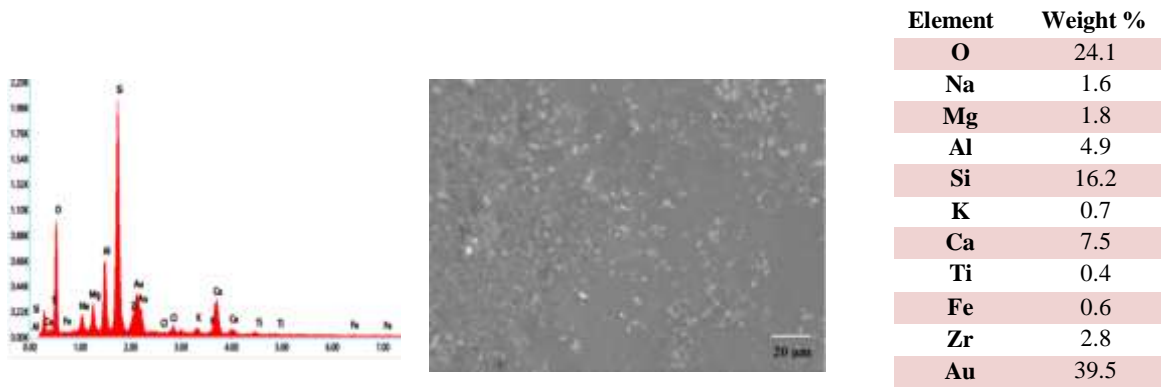
82

Element	Weight %
O	24.1
Na	1.6
Mg	1.8
Al	4.9
Si	16.2
K	0.7
Ca	7.5
Ti	0.4
Fe	0.6
Zr	2.8
Au	39.5

Figure 4.4: The SEM/EDX of glazed ceramic tile

4.3 Characterization of Ag-TiO$_2$ coating with Degussa P25 and without Degussa P25

In this section, the phase analyses of TiO$_2$ and Ag-TiO$_2$ coating on ceramic tiles with and without the presence of Degussa P25 were discussed. The effect of Degussa P25 addition into sol during preparation of Ag-TiO$_2$ coating were analysed to decide whether the Degussa P25 is beneficial to enhance the formation of Ag-TiO$_2$ coating on ceramic tiles. This is due to the earlier reported findings that suggests utilization of Degussa P25 as precursor for TiO$_2$ coating deposition help towards the formation of nanocomposite TiO$_2$ coating (Musa et al., 2017b).

4.3.1 Crystalline phase analyses

The GAXRD pattern of TiO$_2$ coating with the presence of Degussa P25 (TiO$_2$ P25) and without Degussa P25 (TiO$_2$) coating on unglazed tiles were shown in Figure 4.5 (a) and (b). It can be seen that TiO$_2$ P25 coating on the unglazed tile consists of anatase peak (JCPDS: 00-021-1272) at angle 2θ = 25.4 (101), 37.8 (004), 48.0 (200), 54.8 (105), 55.1 (211), and 75.1 (215) and rutile peak (JCPDS:00-021-1276) at angle 2θ = 27.4 (110) and 68.9 (301). While TiO$_2$ coating without Degussa P25 consists of majority rutile phase at angle 2θ = 26.4° (111), 27.9 (210), 39.5 (002), 50.07 (321), 54.8 (222), 68.03 (213) and 75.65 (521). Brookite phase (JCPDS: 00-029-1360) is identified by the angel 2θ = 36.4 (232)

83

and 41.3 (002). There is one peak of anatase phase (JCPDS: 00-021-1272) at angle 59.91 (208).
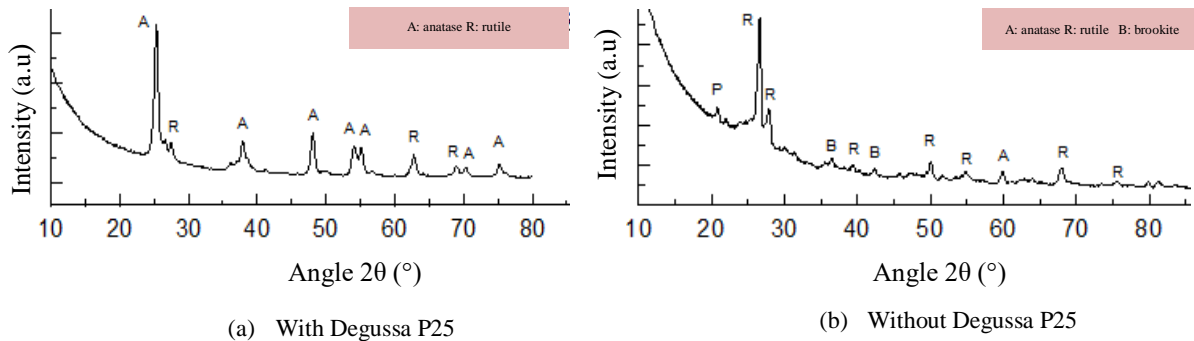

(a)   With Degussa P25

(b)   Without Degussa P25

Figure 4.5: GAXRD pattern of TiO$_2$ coating with Degussa P25 and without Degussa P25 deposited on unglazed ceramic tiles

The GAXRD peaks of TiO$_2$ coating on glazed tile in Figure 4.6 shows not much differ as the TiO$_2$ coating on unglazed tiles. It shows that the presence of Degussa P25, anatase and rutile peaks with high intensity of anatase peak (JCPDS: 00-021-1272) at angle 2θ = 25.4° (101), 37.8° (004), 48.0° (200), 54.8° (105), 55.1° (211), 68.7° and 75.1° (215) and rutile peak (JCPDS:00-021-1276) at angle 2θ = 27.4° (110) and 68.9° (301). No brookite phase is identified. For the coating without Degussa P25, the XRD peak shows presence of balance of mixed anatase, rutile and brookite. The anatase peaks were observed at angle 2θ = 25.4° (101), 63.7° (400) and 68.7° (228). Rutile peaks were observed at angle 2θ = 27.4° (110), 35.8° (220), 43.5° (112), 54.4° (222) and 57.6° (312). The presence of brookite phase (JCPDS: 00-029-1360) is also observed at angle 2θ = 39.8° (312), 40.8° (213), 47.6° (024), and 52.9° (044). Besides phases related to TiO$_2$, there is ceramic peak represent by Robinsonite (Pb$_4$S$_6$S$_{13}$) detected on the glazed tile surface of TiO$_2$ coating without Degussa P25 addition at angle 20.8°.This was due to the thin layer possessed by TiO$_2$ coating without Degussa P25 addition on ceramic tiles.
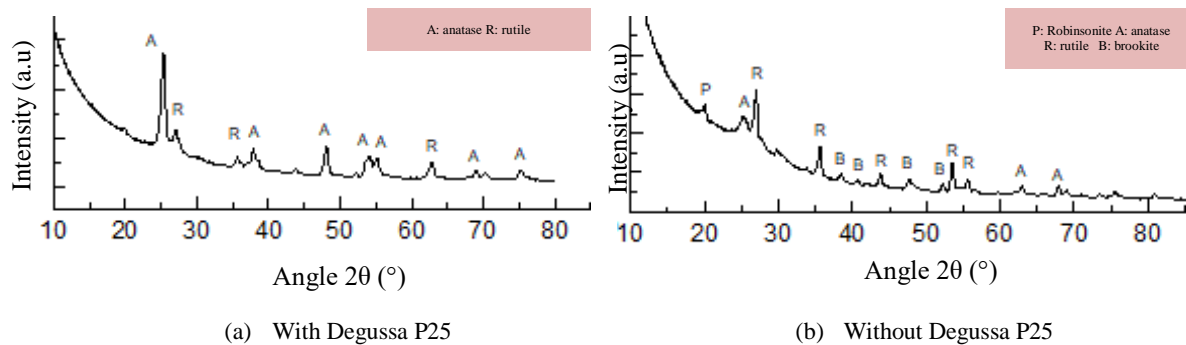
84

(a) With Degussa P25

(b) Without Degussa P25

Figure 4.6: GAXRD pattern of TiO$_2$ coating with Degussa P25 and without Degussa P25 incorporation deposited on glazed ceramic tiles

4.3.1.1 Effect of Degussa P25 addition on the crystalline phases of TiO$_2$ coating

Based on the observation, TiO$_2$ coating with Degussa P25 and without Degussa P25 shows the presence of anatase and rutile phases. While brookite phase observed only on TiO$_2$ without Degussa P25 addition. However, the deposition of TiO$_2$ coating with Degussa P25 shows more presence of peaks anatase compared to TiO$_2$ coating without Degussa P25. These can be relate to the composition of Degussa P25 that comprises of 70 % anatase and 30 % rutile phase that helps in the growth of anatase phase in the coating. As reported before, Degussa P25 plays an important role in promoting crystal structure of TiO$_2$. It provided a nucleation sites at which the particle growth happened on the surfaces of TiO$_2$ (Nurhamizah et al., 2016b, Sreethawong et al., 2014, Musa et al., 2017a). It was also realized that TiO$_2$ coating without Degussa P25 coated on glazed ceramic tiles shows more presence of brookite peaks compared to the TiO$_2$ coating with Degussa P25.

Moreover, the addition of Degussa P25 also contributed to bigger crystallite sizes of anatase for both TiO$_2$ coating deposited on unglazed and glazed ceramic tile. It can be deduced that the addition of Degussa P25 caused particles agglomeration that results in bigger grain size which will lead to the formation of bigger crystallite size (Musa et al., 2017b). Table 4.1 presents the crystallite size of TiO$_2$ with and without Degussa P25 coating on unglazed and glazed ceramic tile.

Table 4.1: Anatase crystallite size of TiO_2 with and without Degussa P25 coating on unglazed and glazed ceramic tile

Photocatalyst sample	Anatase crystallite size (nm)	
	Unglazed Tile	Glazed Tile
TiO_2 P25	17.2	19.2
TiO_2	8.6	8.6

4.3.1.2 Effect of Degussa P25 addition on the crystalline phases of Ag-TiO_2 coating

The effect of Degussa addition on the Ag-TiO_2 coating deposited on unglazed and glazed ceramic tiles is shown in Figure 4.7. The GAXRD pattern shows that the addition of Degussa P25 into the Ag-TiO_2 coating had suppress the presence of Ag phase at low Ag content on both substrates. More Ag phase related peaks are observed at 5 mol % Ag content. However, most of the peaks present with low intensity. At Ag content less than 5 mol %, no Ag related peaks are observed.
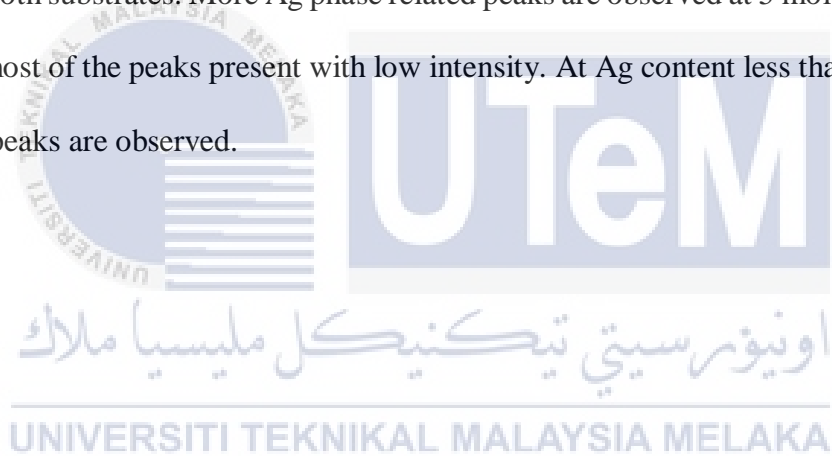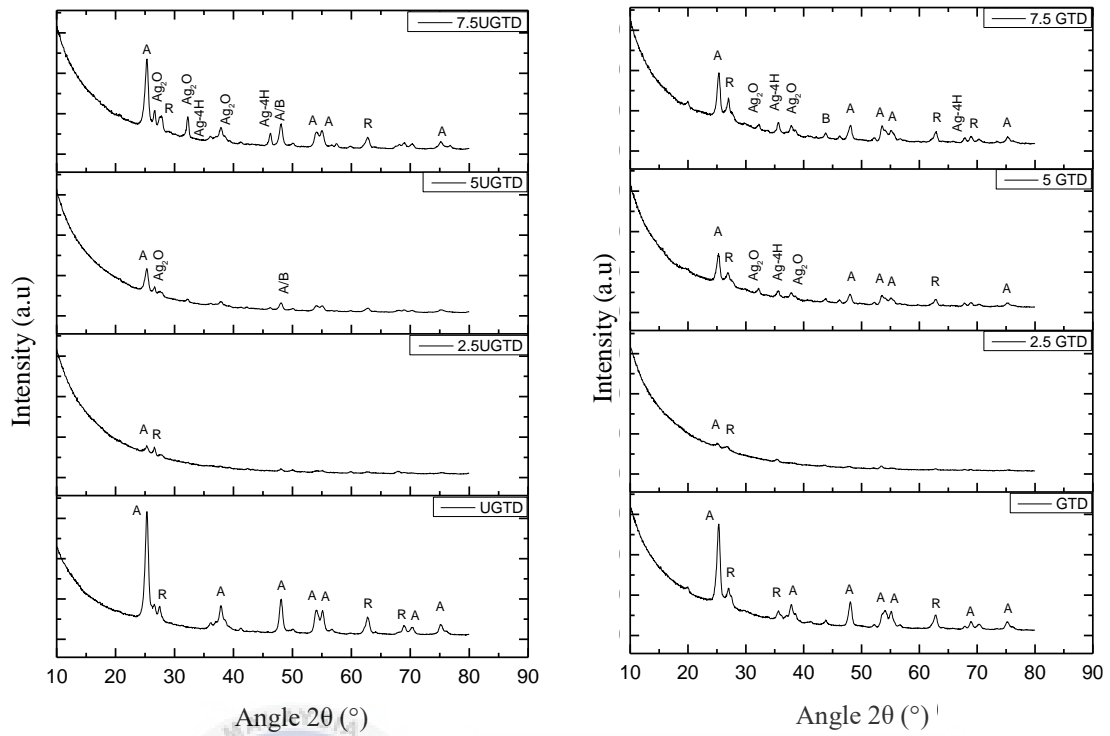
(a) Ag-TiO$_2$ P25 unglazed tile   (b) Ag-TiO$_2$ P25 glazed tile

Figure 4.7: GAXRD pattern of TiO$_2$ and Ag-TiO$_2$ coating with Degussa P25 addition deposited on ceramic tiles

Besides, the addition of Degussa P25 in Ag-TiO$_2$ coating seems to retard the formation of Ag phase of the Ag-TiO$_2$ coating. This is evidence as the crystalline peaks of Ag related phases are only identified at higher Ag content $\geq$ 5 mol %. The addition of Degussa P25 had interrupted the crystallization of Ag phase at low amount Ag content where Degussa P25 dominant anatase phase overlapped with Ag phase. Thus, formulation of sol-gel without the addition of Degussa P25 is more efficient for Ag-TiO$_2$ coating deposition on ceramic tile surface. The Ag-TiO$_2$ coating without Degussa P25 was the batch of samples that were subjected to the photocatalytic test based on the overall characterization analyses.

4.4   Characterization of Ag-TiO$_2$ coating with varied Ag content

87

The phase analyses of Ag-TiO$_2$ coating on ceramic tiles with varied Ag content (2.5, 5.0 and 7.5 mol % Ag) and the effect of Ag content on the crystalline phase formation of Ag-TiO$_2$ deposited on unglazed and glazed ceramic tiles were studied in particular. It should be noted that all the Ag-TiO$_2$ coating subjected to these analyses are deposited without the Degussa P25 formulation. This was because the incorporation of Degussa P25 in the sol formulation had restrained the growth of Ag peak and simultaneously formed bigger crystallite sizes which tend to cause agglomeration to occur.

4.4.1   Crystalline phase analyses

The GAXRD pattern of Ag-TiO$_2$ coating with varied Ag content deposited on unglazed tile is shown in Figure 4.8. It shows that Ag phases present   even at lower Ag content of 2.5 mol %. More peaks of Ag phases were observed as the Ag content increased up to 7.5 mol %. The presence of metallic Ag-4H peak are indicate by the presence of peaks at angle $2\theta = 32.29°$ (104), $50.59°$ (203) and $59.88°$ (001). The metallic Ag present in hexagonal structure. While Ag$_2$O presence is identified by crystalline peaks at angle $2\theta = 54.9°$ (331). Moreover, a peak of Ag$_2$O is observed with higher intensity at 7.5 mol % Ag content which it can be stated that the increase Ag content had promoted more Ag phase formation. As stated by Kien et al. (2022), the Ag$_2$O existence was due to the amount of silver that did not react completely but being oxidized under temperature to form Ag$_2$O. This Ag$_2$O peak will eventually disappear and the absence of oxidized forms in XRD pattern suggested that the Ag expected to exists in metallic state as suggested by Gong et al. (2012).
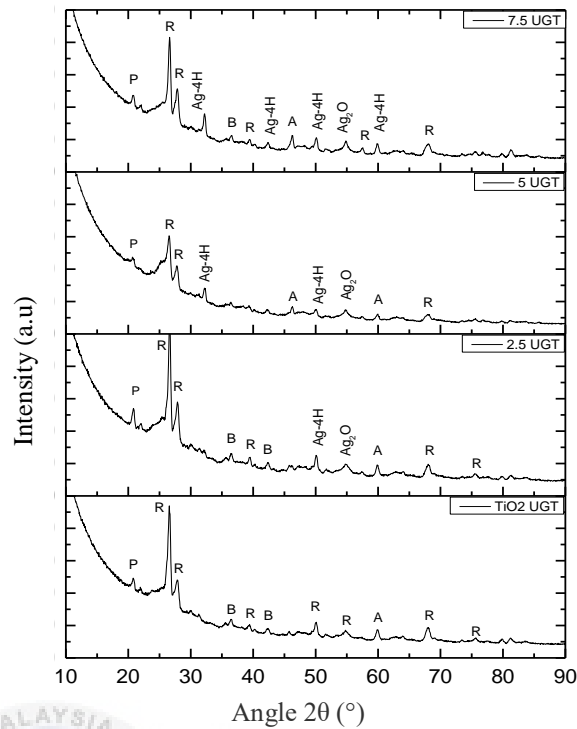
Figure 4.8: GAXRD pattern of TiO_2 and Ag-TiO_2 coating with varied Ag content deposited on unglazed ceramic tiles

The crystallite size of Ag-TiO_2 on unglazed tile is shown in Table 4.2. When Ag is incorporated into the TiO_2 coating, rutile phase shows no change in crystallite size even when increased Ag content. The anatase crystallite size of Ag-TiO_2 increased with increased Ag content. This was similar reported by Saraswati et al. (2019) work that found the crystal size of anatase TiO_2 P25 was 20 nm while the size was 39 nm for Ag-TiO_2 in her study of Ag-TiO_2 nanocomposites coated on cotton fabric with Ag content of 1, 3 and 5 wt % for bacterial and fungal disinfection. These explained that increased of Ag at certain amount will increased anatase crystallite size and fluctuate at the high amount of beyond Ag required. Ag will function as a trapper for electron if Ag was in an accurate position in the possible matrix to prevent recombination than its existence being a crystal (Saraswati et al., 2019). Nevertheless, increased crystallite size is also observed by Vakhrushev et al. (2017) where the average particle size of anatase, rutile and silver modified titanium (IV) oxide

89

increased with increasing of Ag up to 5.0×10^{-2} and further increased up to 7.5×10^{-2} had no effect on the crystallite size.

Table 4.2: Crystallite size of TiO_2 and Ag-TiO_2 coating on unglazed ceramic tiles

Photocatalyst sample	Crystallite size of Ag-TiO_2 coating on unglazed tile (nm)	
	Anatase	Rutile
TiO_2	8.6	24.8
2.5 mol % Ag-TiO_2	24.3	24.8
5 mol % Ag-TiO_2	26.2	24.8
7.5 mol % Ag-TiO_2	36.6	24.8

Besides, there is reported work that stated TiO_2 doped Ag produce smaller crystallite size than undoped samples. Research published by Aini et al. (2019) on silver doped TiO_2 photocatalyst synthesized by sonochemical method stated that the undoped TiO_2 having 18.97 nm crystallite size while the Ag doped TiO_2 in range of 8-11 nm only. In contrast, Saraswati et al. (2019) had observed that the anatase crystallite size of Ag/TiO_2 nanocomposite coated on fabric footwear was 34 nm while TiO_2 P25 was 20 nm. In our work, the porous surface nature of the unglazed ceramic tile which led the Ag-TiO_2 sol filling in the pores during coating. These could contribute to the bigger anatase crystallite size. In addition, the increase of anatase crystallite size of Ag-TiO_2 doped on unglazed tile indicated that a better crystallinity of the coating. This means that coating defects and dislocations were decreased with increased Ag content (Demircia et al., 2016).

The FWHM of the samples was influence by the strain, grain size and crystal imperfections. FWHM for the diffraction plane of (101) at angle $23° < θ < 27°$ calculated from the XRD data is shown in Figure 4.9 respectively. The value of FWHM of TiO_2 and Ag-TiO_2 coating on unglazed tile computed are 0.34, 0.29, 0.59 and 0.39. The value seems to increase as increase Ag content up to 5 mol % and decreased when reaching 7.5 mol % Ag.
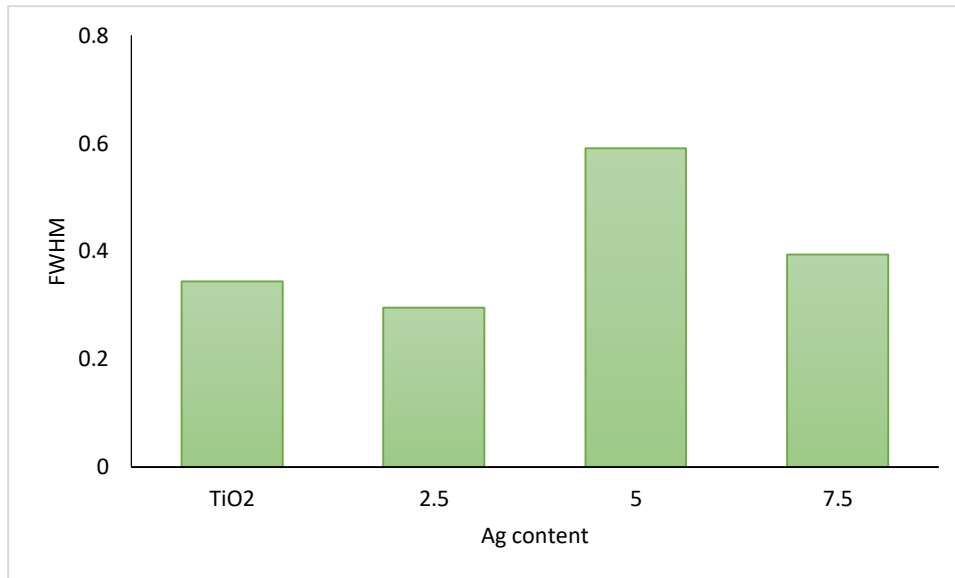
90

Figure 4.9: FWHM of TiO_2 and Ag-TiO_2 coated on unglazed tile

The GAXRD pattern of Ag-TiO_2 coating with varied Ag content deposited on glazed ceramic tiles is shown in Figure 4.10. The glazed ceramic tile in nature is having a smooth surface. The GAXRD pattern shows the presence of Ag peak even at low Ag content of 2.5 mol %. The anatase and rutile phase were presence at the same angle as reported in previous section (4.3.1). The anatase peaks are observed at angle $2\theta = 25.4°$ (101), 63.7° (400) and 68.7° (228). Rutile peaks are observed at angle $2\theta = 27.4°$ (110), 35.8° (220), 43.5° (112), 54.4° (222) and 57.6° (312). In addition, the presence of brookite phase (JCPDS: 00-029-1360) is also observed at angle $2\theta = 39.8°$ (312), 40.8° (213), 47.6° (024), and 52.9° (044). The metallic Ag-4H peaks observed at angle $2\theta = 42.8$ ° (104), 48.3° (203) and $= 54.9°$ (331). Based on the GAXRD patterns, the intensity of Ag related phase peaks for example the Ag-4H at angle $2\theta = 54.9°$ increased as the Ag content up to 5 mol % and decreased at 7.5 mol %. The studied by Cruz et al. (2022) on Ag/TiO_2 photocatalysts modified combustion method also revealed the same pattern where increased Ag content from 0.05 mmol to 0.2 mmol increased the intensity of Ag related peaks as well. While, Demircia et al. (2016) worked on Ag doped TiO_2 deposited on Si substrates with 0.1, 0.3, 0.5, 0.7 and 0.9 % Ag content stated that the intensities of film peaks decreased when increased Ag

91

content. This due to the presence of Ag ions that reduces its crystallinity and the angles of the diffraction peaks of Ag-TiO$_2$ remain unchanged indicated that Ag cannot enter the TiO$_2$ lattice (Wu et al., 2022).
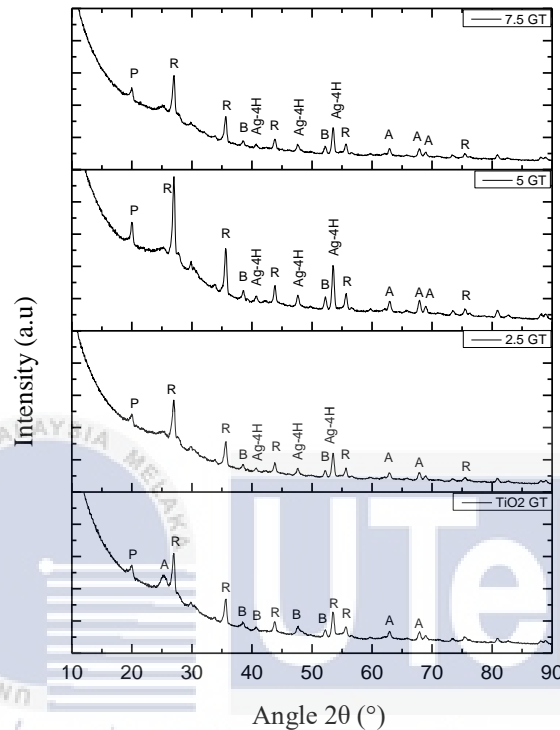

Figure 4.10: GAXRD pattern of TiO$_2$ and Ag-TiO$_2$ coating with varied Ag content deposited on glazed ceramic tiles

Table 4.3 presents anatase and rutile size of Ag-TiO$_2$ coating on glazed ceramic tiles dependant on Ag content. Rutile crystallite size of Ag-TiO$_2$ coating had no obvious effect changed with an increase of Ag content compared to anatase crystallite size. It can be seen that the size of anatase had a similar pattern as the anatase of Ag-TiO$_2$ coating on unglazed ceramic tile. Increased Ag content had increased the anatase crystal size then it decreased when Ag content was increased to 7.5 mol %. These indicated that the crystallinity of Ag increased as increased Ag at certain amount and tends to fluctuate when increased Ag more than required (Demircia et al., 2016).

Table 4.3: Crystallite size of TiO_2 and Ag-TiO_2 coating on glazed ceramic tiles

Photocatalyst sample	Crystallite size of Ag-TiO_2 coating on glazed tile (nm)	
	Anatase	Rutile
TiO_2	8.6	28.9
2.5 mol % Ag-TiO_2	10.8	21.7
5 mol % Ag-TiO_2	14.5	21.7
7.5 mol % Ag-TiO_2	10.8	24.7

A similar pattern of decreased FWHM observed in the Ag-TiO_2 coating on glazed tile is shown in Figure 4.11. The Ag-TiO_2 coating on glazed tile shows that the FWHM increased till 5 mol % Ag content and decreased with incorporation of 7.5 mol % Ag content. However, the FWHM values of Ag-TiO_2 coating on glazed tile were a bit higher compared to FWHM value of Ag-TiO_2 coating on unglazed tile. This indicates that, the Ag-TiO_2 coating on glazed tile having smaller anatase crystallite size compared to Ag-TiO_2 coating on unglazed tile. The bigger anatase crystal of Ag-TiO_2 coating on unglazed tile may due to the agglomeration of Ti sip into the unglazed tile and indicates that the type of surface also affect the anatase crystallite size. For the TiO_2 and Ag-TiO_2 coating on glazed tiles, the values of FWHM were 0.98, 0.78, 0.98 and 0.78. Here, the porous surfaces of unglazed tiles compared to the glazed tiles had caused the coating to fill in the pores instead of forming a coating layer. Hence, the coating sol tends to accumulate in the pores and caused particles aggregation.
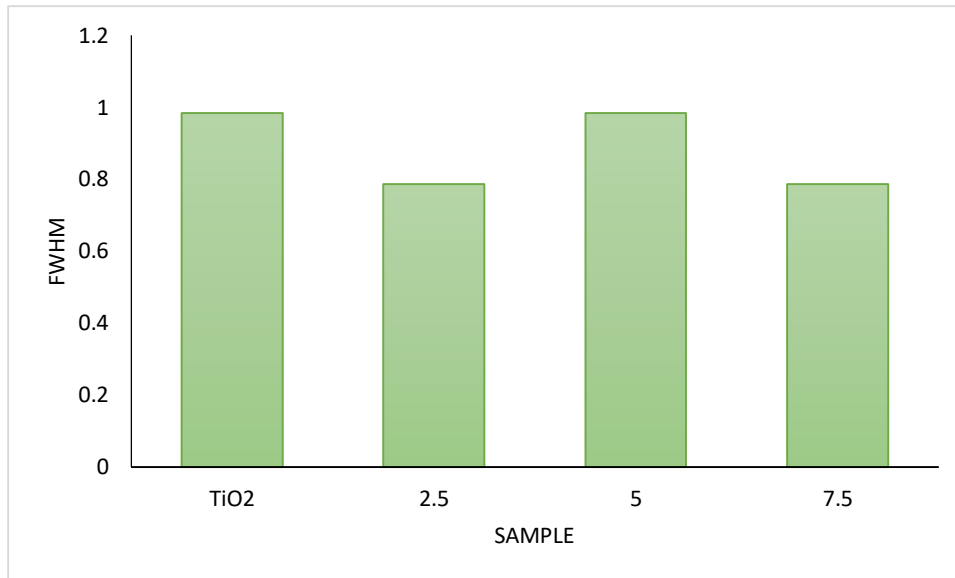
Figure 4.11: FWHM of TiO_2 and Ag-TiO_2 coating on glazed tile

4.4.1.1 Effect of Ag content on the crystalline phases

When Ag is added into Ag-TiO_2 P25 (section 4.3.1.2) and Ag-TiO_2, the presence of Ag is more obvious in Ag-TiO_2 sol compared to Ag-TiO_2 P25. Nevertheless, the radius of Ag^+ ions was ca. 126 pm and it is much larger than the radius of Ti^{4+} ions, ca. 68 pm (Ubonchonlakat et al., 2008, Kamrosni et al., 2019). Therefore, when Ag^+ ions were introduced using sol gel process, Ag^+ ions cannot enter into the lattice of TiO_2 anatase phase. During the heat treatment, the reduction of Ag^+ to $Ag°$ happened due to reduction of $AgNO_3$. These Ag^+ ions then migrate along with anatase grain boundaries to the surface of TiO_2 film. At the same time, anatase TiO_2 will grow and this caused Ag^+ ions exist on the surface of the anatase grains by forming Ag-O-Ti bonds (Kamrosni et al., 2019).

Furthermore, with the addition of Ag, brookite phase of TiO_2 coating is no longer presence and increased of Ag at 2.5 mol % to 7.5 mol % had shown presence of only anatase, rutile and Ag phase. This was also supported by El-Katoria et al. (2019) on the study of different Ag concentration doped TiO_2 film with addition of chitosan where anatase crystallize was discovered by raising silver contents up to 5 mol% that can confirm the

94

spreading of amorphous silver oxide layers through titania crystallite and improving Ag content (10–20 mol%) favors crystallization of rutile titania and metallic silver particles which is accompanied by increasing the crystallite size.

The relationship that can be drawn from the XRD data analysis is that increased the of silver content from 2.5 mol % to 7.5 mol % had led to an increase in the degree of crystallinity. This is expected to happened due to the transformation of TiO_2 phase is accompanied by the process of silver nitrate decomposition (Vakhrushev et al., 2017). In addition, Silver dopant has been reported to induce the phase transformation at high content dopant, high temperature, or may depend on the type of precursor and synthesis method (Aini et al., 2019). Raising silver contents up to 5 mol% had confirmed the spreading of amorphous silver oxide layers through titania crystallites. The presence of Ag particles on the titania surface prevents the growth of the crystallite size of titania compared to the pristine counterpart (Ramchiary et al., 2016). Moreover, anatase crystallite size grows during heat treatment to the critical size before transformations proceed to anatase-rutile phase (Zhang and Banfield, 1999, Zhang and Banfield, 2000).

### 4.4.2 Surface morphology and elemental mapping

SEM micrographs of TiO_2 and $Ag-TiO_2$ on unglazed ceramic tile are shown in Figure 4.12. The surface morphology shows that TiO_2 coating (Figure 4.12 (a)) consists of many visible mud crack shape layer on the entire surfaces. This finding was similar reported by Horkavcová et al. (2015), Demircia et al. (2016) and Musa et al. (2017b) where the cracks are due to the restructuring and relaxation during heat treatment process. This is because the heat treatment regime of the TiO_2 coating during deposition on a substrate is exposed to the thermal shock which could possible causing the cracks on the surfaces. The thermal shock

that lead to the non-uniform and cracked coating hence reduce the coating lucidity and transparency (Halin et al., 2018).

When Ag is incorporated into TiO_2 coating, 2.5 mol % Ag-TiO_2 coating (Figure 4.12 (b)) shows not much differ of TiO_2 coating surface. The pack of the cracks is seen similar and this indicated that the small amount of Ag content didn't contribute to the smooth surface of the coating. As increased amount of Ag content is added, 5 mol % Ag-TiO_2 coating shows uneven small pack of cracks over the surface. While, at 7.5 mol % Ag content, the surface shows less cracks with wavy look coating layer. Besides, it observed that features of holes believed as pores on the surfaces which might due to the coating peel off. The addition of Ag from 2.5 to 7.5 mol % showing small particles spread on the surfaces which were identified as Ag particles by SEM//EDX discussed later. Increasing ratio of Ag increased the formation of small particles on surfaces.
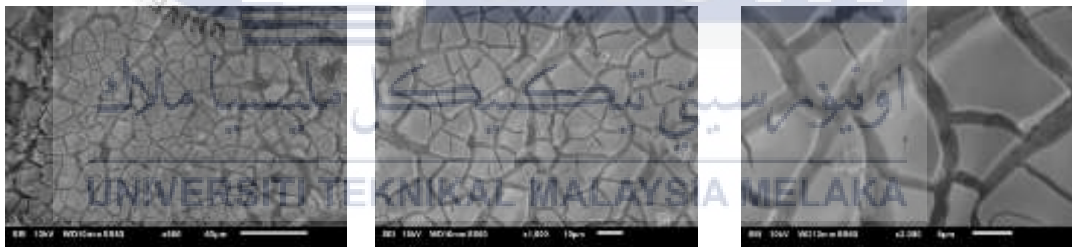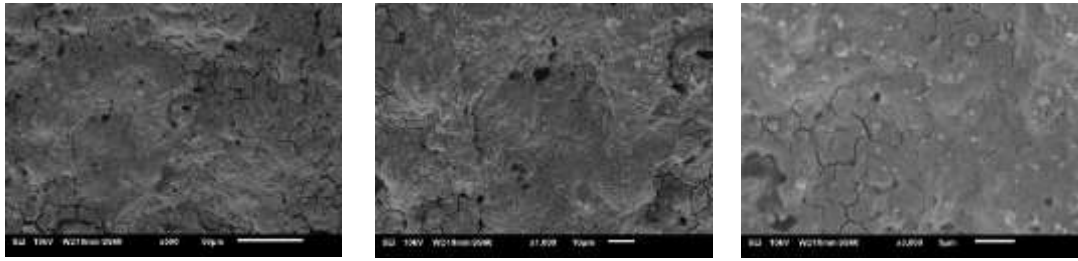

(a) TiO_2 coating on unglazed tile
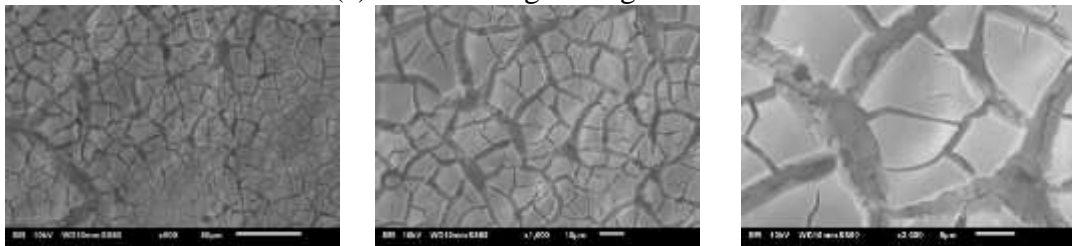
(b) 2.5 mol % Ag
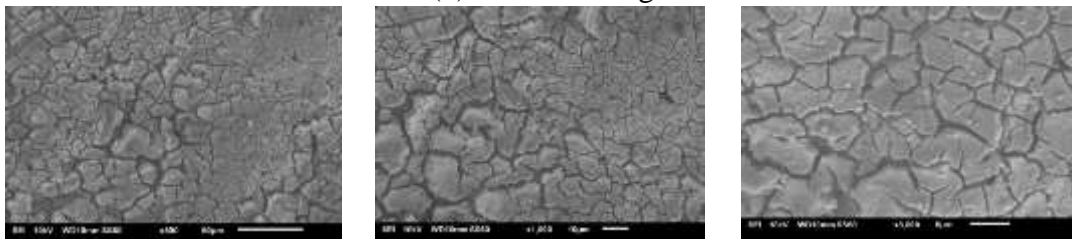
(c) 5 mol % Ag

(d) 7.5 mol % Ag

Figure 4.12: SEM of TiO_2 and Ag-TiO_2 coating on unglazed ceramic tile

Figure 4.13 depicts TiO_2 and Ag-TiO_2 coating on glazed ceramic tile. The TiO_2 coating shows a smooth surface with formation of crack island. As discussed before, the crack was due to the thermal shock during calcination process (Horkavcová et al., 2015, Demircia et al., 2016). In a meantime, there were no aggregation displaying on Ag-TiO_2 deposited on glazed ceramic tiles suggested that Ag were well dispersed in TiO_2 matrix. These was also deduced by SEM result of research done by Moongraksathuma and Chen (2018) where the smooth surface with no aggregation is observed proving that Ag nanoparticles well dispersed in TiO_2 matrix. When Ag is incorporated into TiO_2 coating, 2.5 mol % Ag-TiO_2 coating shows almost similar to TiO_2 coating surface but the cracks line illustrated were less obvious compared to TiO_2 coating surface. Addition of 2.5 mol % Ag appeared smooth surface and less crack with clear white dots distributed well on the coating surface. As Ag is added at 5 and 7.5 mol %, the coating surface exhibit clear cracks line with small white dots particles. The existence of Ag particles on the coating surface at higher ratio of Ag content also demonstrated by Demircia et al. (2016). Eventhough the Ag-TiO_2 coating formed crack for all samples, but they appeared to have smooth sandy like surface compare to Ag-TiO_2 coating on unglazed tile surfaces.
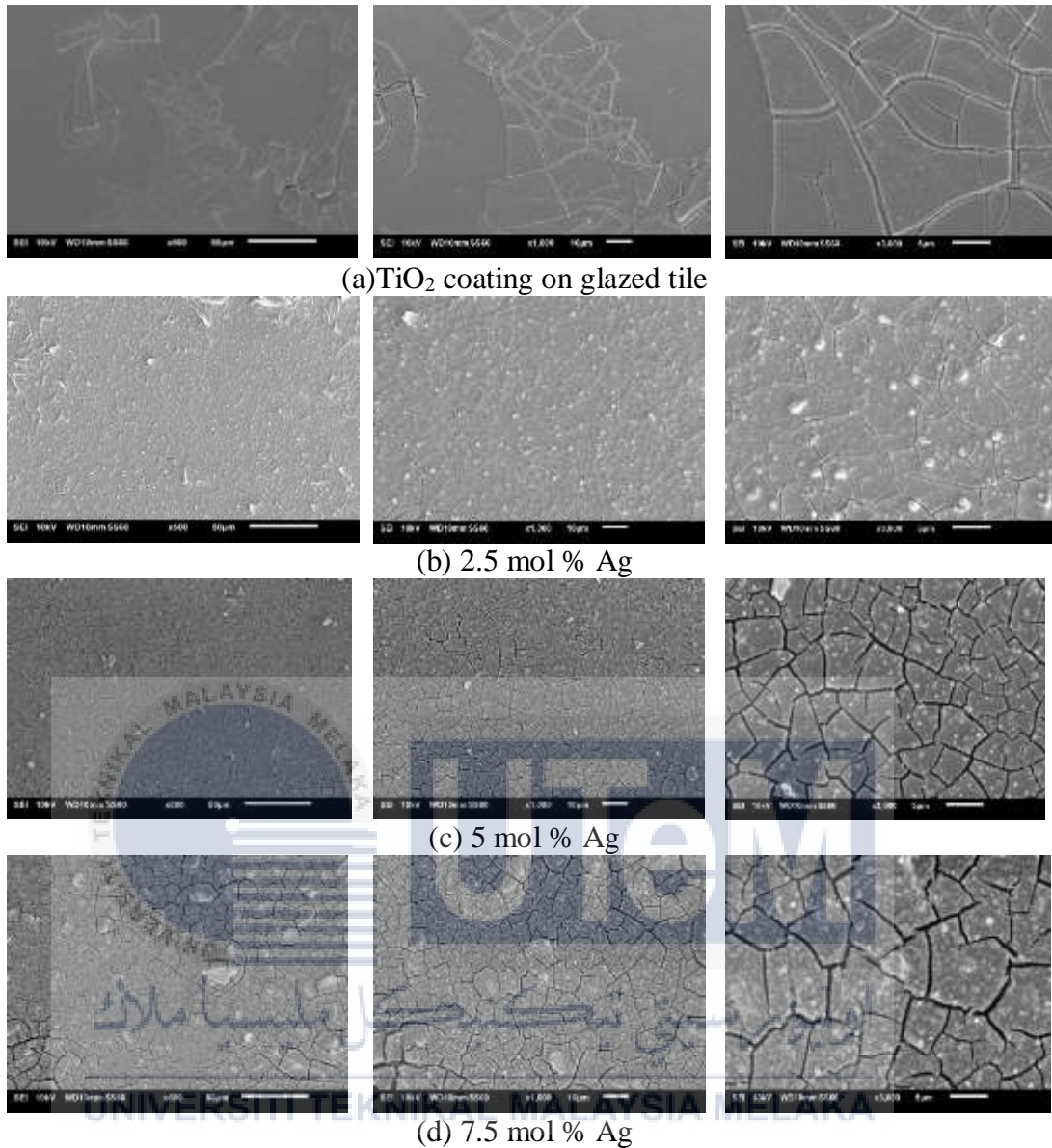
(a)TiO$_2$ coating on glazed tile

(b) 2.5 mol % Ag

(c) 5 mol % Ag

(d) 7.5 mol % Ag

Figure 4.13: SEM of TiO$_2$ and Ag-TiO$_2$ coating on glazed ceramic tiles

Based on the observation, it can be revealed that the surface structure of Ag-TiO$_2$ coating formed cracks over the entire surfaces. In contrast, the TiO$_2$ coating without silver deposited on unglazed and glazed ceramic tile shows mostly propagation of isolated cracks. Also, the surface morphology of Ag-TiO$_2$ coating on unglazed tiles are having a larger wide gap of cracks propagated along the surfaces compared to the surface morphology of Ag-TiO$_2$ coating on the glazed tile. These is because Zhang et al. (2022c) reported that Ag facilitated TiO$_2$ to form dense coating on glazed substrate surface. That small particles

distributed on the surfaces of Ag-TiO$_2$ coating on unglazed tiles were seen at high Ag content of 7.5 mol % (Figure 4.13 (d)). In contrast, the small particles spread on surface of Ag-TiO$_2$ coating of glazed tiles were clearly seen even at low amount of Ag content (Figure 4.13 (b)). These indicated that TiO$_2$ nanoparticles uniformly distributed on the surface. Behpour et al. (2010) study on the Ag-TiO2 nanoparticles deposited on Ti sheet for the water pollution degradation using electrochemical method reported that Ag gave no influence on the size of TiO$_2$ particles (< 200 nm) where similar particles size of TiO$_2$ observed on the Ag-TiO$_2$ coating surface.

Both Ag-TiO$_2$ coating on unglazed and glazed tiles demonstrated cracks propagated along the entire surfaces. However, Ag-TiO$_2$ coating with 7.5 mol % Ag (Figure 4.13 (d)) deposited on unglazed tile demonstrated small holes on the surface which can be identified as porous structure accompanying with crack on the surface. The presence of Ag at appropriate amount at TiO$_2$ interface improved the structural and textural properties of titania which gave a more mesoporous TiO$_2$ matrix that will then lead to create more active sites for photocatalysis (Cherif et al., 2023).
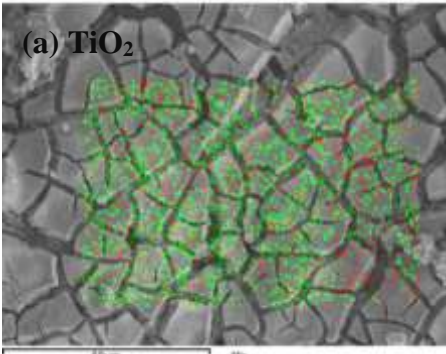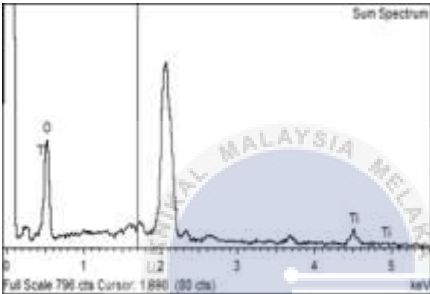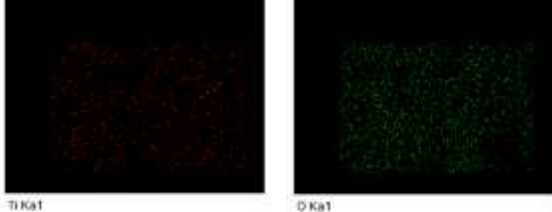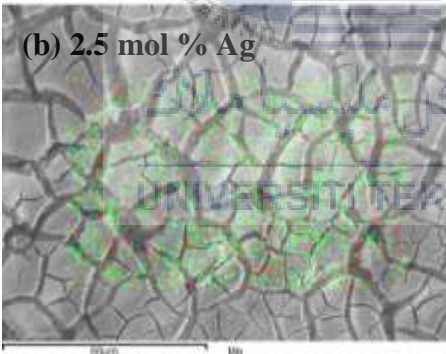
The elemental mapping of SEM/EDX analysis on the surface of Ag-TiO$_2$ coating on ceramic tiles were both done on the Ag-TiO$_2$ coating with varied Ag content deposited on unglazed and glazed ceramic tiles. Basically, when Ag is incorporated into TiO$_2$, it is expected that metallic Ag tend to present on the surface of the coating (Zheng et al., 2019). Therefore, EDX mapping analysis on both unglazed and glazed was aim to analyse the presence of Ti, O and Ag which is deducing the formation of Ag-TiO$_2$ composites of the coating layer.

The EDX mapping of Ag-TiO$_2$ coating with varied Ag content deposited on unglazed tile in Table 4.4 illustrated that the Ti, O and Ag particles were present on the surface, dispersed and distributed well on the entire coating. The spectrums in the figure have clear

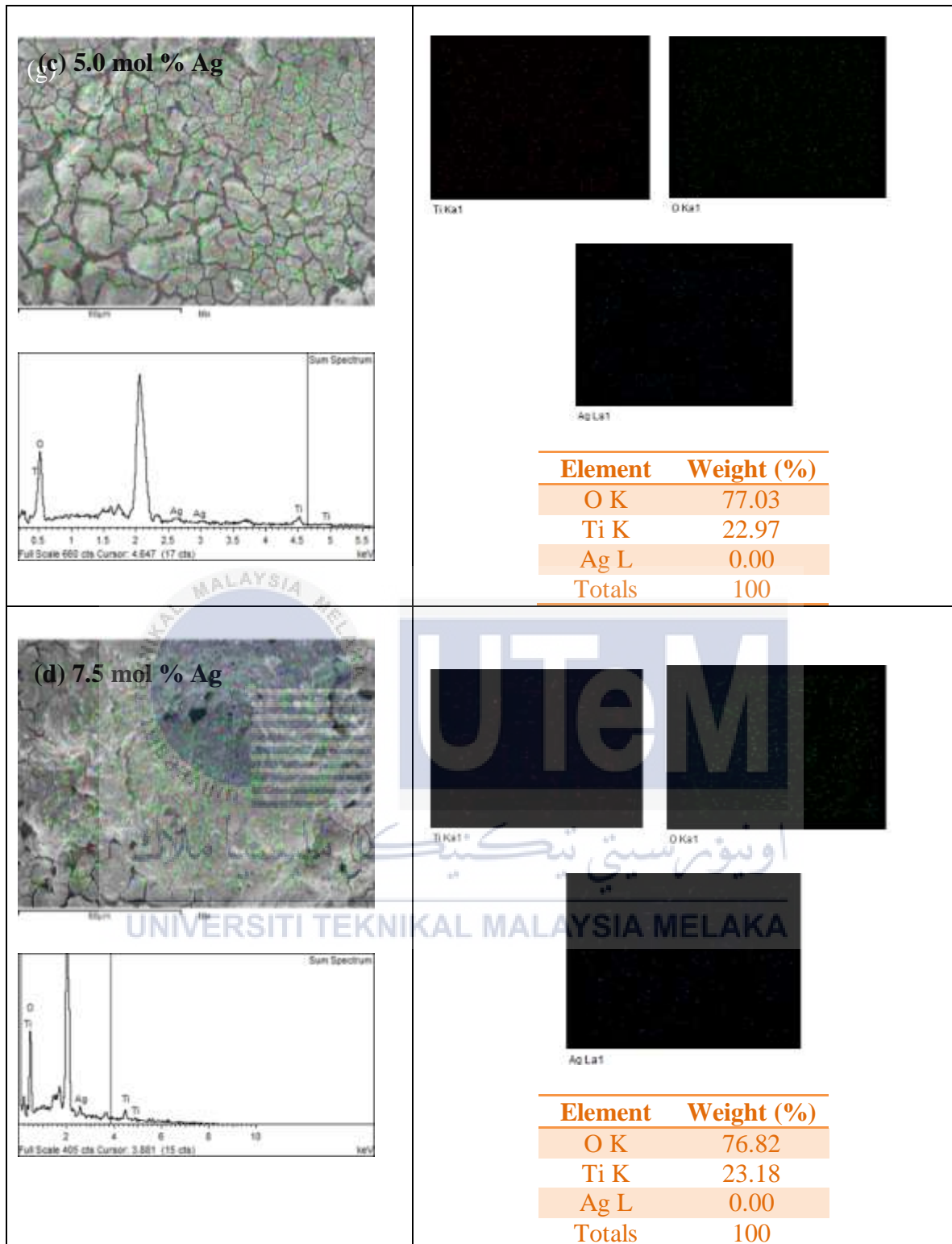peaks at 0.5 keV, 4.5 keV, and 4.9 keV that belongs to titanium element, and a peak at around 0.6 keV that designated to oxygen element. These peaks indicated the growth of TiO_2 nanoparticle in the coating layer (Al-Harbi et al., 2011). When varied Ag content is introduced into the Ag-TiO_2 coating on unglazed tiles, Ag peak is observed at 3 keV and 2.7 keV with low peak intensity. The spectrum also shows the strong peak of Au at 2 keV which it was from the sputter coater during sample preparation for analysis. The uniform distribution of Ag on TiO_2 surface has also been reported by Ling et al. (2019) that investigated upon the photocatalytic performance of Ag-TiO_2. In the report, the uniform Ag nanoparticles that uniformly distributed on TiO_2 surface had Ag nanoparticle was closely combined with TiO_2 with lattice fringes of spacing of anatase-type TiO_2 is 0.352 nm and Ag is 0.197 nm.

However, it was observed that Ag is not detected in the spectrum for all Ag-TiO_2 coating on unglazed tile. The porous surface of unglazed tile had caused the coating to sip through the porous surfaces and no continuous coating layer was observed. Hence, Ag percent is not revealed in the spectrum analysis accurately. Increased Ag content at 5.0 and 7.5 mol % shows more Ag particles presence on the surface where this was due to the Ag atoms become coordinated to the oxygen atoms on the anatase crystallites. As seen, the particles of Ag, Ti and O were surrounded by each other. The presence of Ag atoms always favors the adsorption places near the surface of oxygen atoms over binding with surface metal cations. In Ag-TiO_2 composite, the Ag_2 lies over one Ti(5c) atom parallel to the surface along the anatase (010) direction (Mazheika et al., 2011). Thus, phase transformation become highly favorable (Vakhrushev et al., 2017).

Table 4.4: SEM/EDX elemental mapping of TiO_2 and Ag-TiO_2 coating with varied Ag content deposited on unglazed tile

SEM/EDX Spectra	Mapping
(a) TiO₂	 Element / Weight (%): O K 73.72, Ti K 26.28, Totals 100
(b) 2.5 mol % Ag	 Element / Weight (%): O K 65.54, Ti K 34.46, Ag L 0.00, Totals 100

(a) TiO₂

Element	Weight (%)
O K	73.72
Ti K	26.28
Totals	100

(b) 2.5 mol % Ag

Element	Weight (%)
O K	65.54
Ti K	34.46
Ag L	0.00
Totals	100

(c) 5.0 mol % Ag

Element	Weight (%)
O K	77.03
Ti K	22.97
Ag L	0.00
Totals	100

(d) 7.5 mol % Ag

Element	Weight (%)
O K	76.82
Ti K	23.18
Ag L	0.00
Totals	100

EDX and mapping analysis of TiO_2 and Ag-TiO_2 coating with varied Ag content deposited on glazed ceramic tiles are shown in Table 4.5. The EDX spectrum shows that Ti, O and Ag particles were present on the surface of tiles coated with Ag-TiO_2. The peaks of

102

Ti, O and Ag were observed indicates the formation of Ag-TiO$_2$ composites on coating surfaces. The EDX spectrum shows peaks at 0.5 keV, 4.5 keV, and 4.9 keV that indicate the presence of titanium element and a peak of 0.6 keV belong to oxygen element. The spectrum of Ag-TiO$_2$ coating on glazed tiles also shows presence of weak peak of Ag element at 3 keV and 2.7 keV. The strong peak of Au at 2 keV also detected which it was from the gold coating in sputter coater during sample preparation for analysis.

The weight percent of Ag measured for 2.5, 5 and 7.5 mol % Ag- TiO$_2$ were 0 %, 5.26 % and 3.54 % respectively. The weight percent of Ag at low content is not able to be measured by the EDX analysis. As similar to Ag-TiO$_2$ coating on unglazed ceramic tile, the Ag particles of Ag-TiO$_2$ coati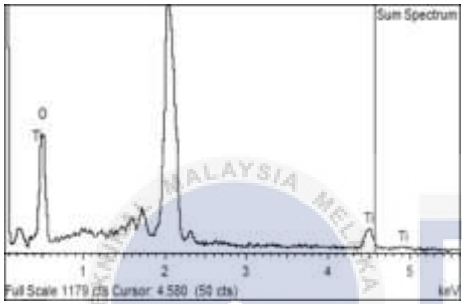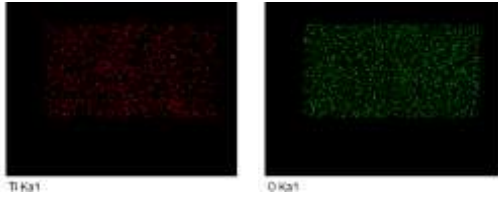ng on glazed tiles also uniformly distributed on the coating surfaces. Mazheika et al. (2011) study on the absorption of Ag clusters on the anatase TiO$_2$ (100) surface and revealed that Ag$_2$ overlapping with a Ti (5c) d orbital. Hence, this is correlated to our SEM/EDX mapping result where the particles of Ag, O and Ti particles were attached and even overlapped to each other.

Table 4.5: SEM/EDX elemental mapping of TiO_2 and Ag-TiO_2 coating on glazed tile

SEM/EDX spectra	Mapping
(a) TiO₂	Ti Ka1 O Ka1

Element	Weight (%)
O K	73.72
Ti K	26.28
Totals	100

| **(b) 2.5 mol % Ag** | Ti Ka1   O Ka1   Ag La1 |

Element	Weight (%)
O K	65.54
Ti K	34.46
Ag L	0.00
Totals	100

(c) 5.0 mol % Ag

Element	Weight (%)
O K	57.86
Ti K	36.88
Ag L	5.26
Totals	100

(d) 7.5 mol % Ag
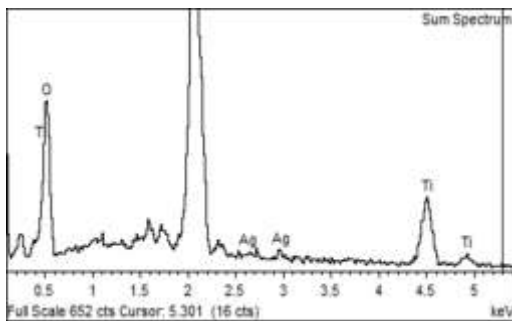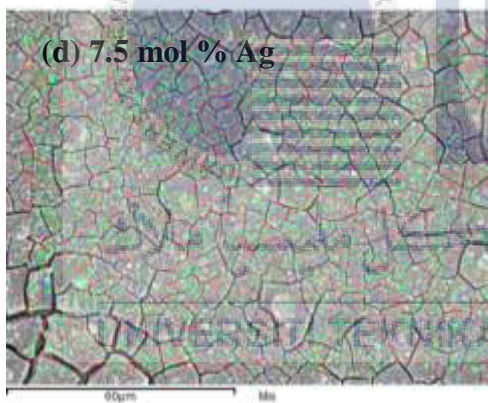
Element	Weight (%)
O K	53.17
Ti K	43.29
Ag L	3.54
Totals	100

4.4.2.1 Effect of Ag content on the surface morphology and elemental distribution

The elemental surface mapping for Ag-TiO$_2$ coating both on unglazed and glazed tiles were dispersed and distributed well on the surfaces. The EDX mapping on coating surface detected the compositional zonation of elements that confirmed the presence of Ti, O and Ag elements on the entire coating surfaces. In comparison, the amount of Ag in wt % of Ag-TiO$_2$ coating deposited glazed ceramic tiles were measured by the value of SEM/EDX spectra. For the Ag-TiO$_2$ coating on the unglazed, the SEM/EDX spectrum shows no wt. % of Ag measured. These can be due to the surface roughness of the substrates itself where unglazed tiles having higher surface roughness compared to glazed tile where the porous surface of unglazed tend to cause the Ag-TiO$_2$ coating to sip through the surfaces.

4.4.3 Cross sectional and elemental mapping

Literally, it has been known that the Ag will present on the surface of the coating because of the large radius of Ag atom which cannot enter the lattice Ti. The cross section of TiO$_2$ and Ag-TiO$_2$ coating deposited on unglazed and glazed ceramic tile is examined to study the thickness of the coating deposited and the incorporation of Ag within the coating layer.

The TiO$_2$ and Ag-TiO$_2$ coating on unglazed ceramic tile with varied Ag content cross section micrograph are shown in Figure 4.14. It was observed that TiO$_2$ and Ag-TiO$_2$ coating on unglazed tile has no distinguished layer of coating and the substrate for each of the samples. This could be due to the unglazed tile surface which having a roughness of 4.46 ± 0.02 µm and porous structure tends to absorb the sols causing the coating to fill in the pores of unglazed ceramic tile and cover up the surface. Therefore, the Ag-TiO$_2$ coating layer cannot be differentiated with the substrate. Hence, thickness of the Ag-TiO$_2$ coating layer deposited on the unglazed tiles was unidentified. The measurement of the coating thickness

was unable to determine. During the dip coating process, the Ag-TiO$_2$ sol sip through the unglazed ceramic tiles hence the presence of Ti, O and Ag element within the layer is expected. This is visible with the presence of Ag detected at 2.5, 5.0 and 7.5 mol % Ag. Apparently the high porosity of unglazed ceramic tile (34%) contributed to the diffusion of the sol into the substrate. The elements such as silicon (Si), calcium (Ca), aluminium (Al) and sodium (Na) also detected since those elements are parts of the unglazed ceramic tiles. Other elements such as gold (Au), palladium (Pd) and carbon (C) probably comes from the preparation sample for SEM/EDX testing. Since, the Ag-TiO$_2$ sol tend to sip into the substrate, the layer of Ag-TiO$_2$ coating of unglazed tiles were unable to be determine. Thus, the Ag-TiO$_2$ coating thickness for the unglazed tiles was unidentified.
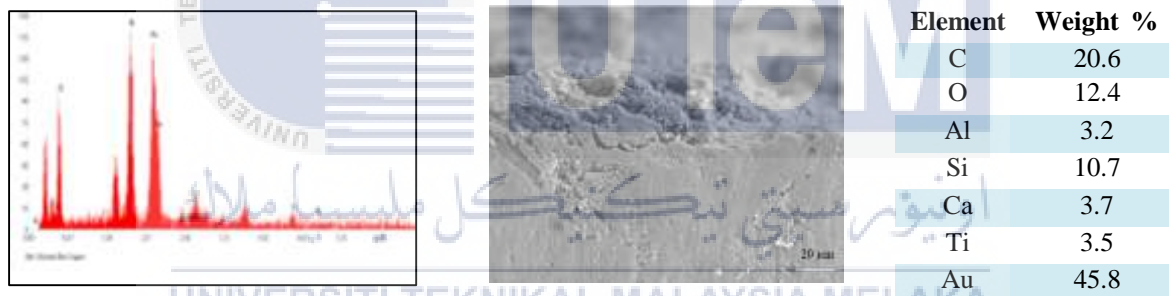
Element	Weight %
C	20.6
O	12.4
Al	3.2
Si	10.7
Ca	3.7
Ti	3.5
Au	45.8

(a) TiO$_2$ coating deposited on unglazed tile

Element	Weight %
O	18.2
Al	4.2
Si	21.5
Ca	7.1
Ti	6.9
Ag	5.0
Au	37.0

(b) Ag-TiO$_2$ coating with 2.5 mol % Ag content deposited on unglazed tile

Element	Weight %
C	17.0
O	11.3
Al	1.1
Si	15.3
Ti	6.5
Pd	6.9
Ag	1.0
Au	40.8
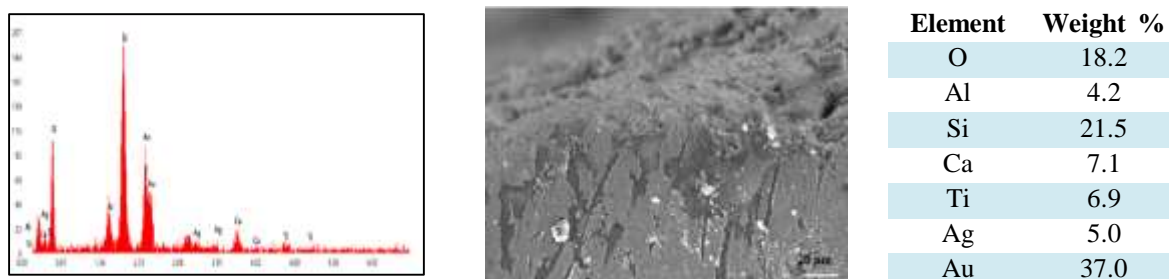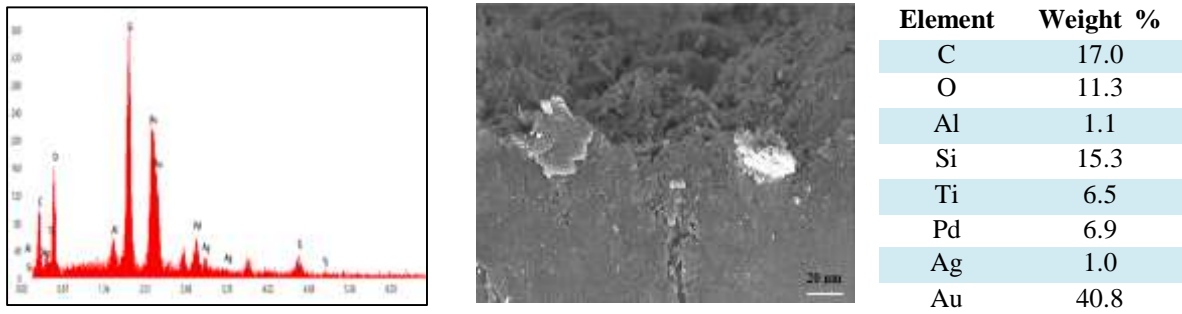
(c) Ag-TiO$_2$ coating with 5.0 mol % Ag content deposited on unglazed tile

Element	Weight %
O	15.6
Al	3.6
Si	16.2
Ca	3.9
Ti	4.0
Pd	10.2
Ag	0.0
Au	46.4

(d)) Ag-TiO$_2$ coating with 7.5 mol % Ag content deposited on unglazed tile

Figure 4.14: SEM/EDX on the cross-section of (a) TiO$_2$ and Ag-TiO$_2$ coating at (b) 2.5 mol % Ag, (c) 5.0 mol % Ag and (d) 7.5 mol % Ag content deposited on unglazed ceramic tile

On the other hand, the cross section of TiO$_2$ and Ag-TiO$_2$ coated glazed ceramic tiles in Figure 4.15 shows the presence of coating layer on top of the substrate. Here, sample of coated with only TiO$_2$ coating without incorporation of Ag (Figure 4.18 (a)) is having a thin layer with thickness around 1.07 ± 0.725 μm. The thickness of the coating increased when 2.5., 5.0 and 7.5 mol % of Ag incorporated into the Ag-TiO$_2$ coating. The Ag-TiO$_2$ coating thickness average measured 9.12 ± 3.04, 14.3 ± 1.2 and 5.26 ± 1.58 μm for 2.5, 5.0 and 7.5 mol % Ag content. Here, the thickness of Ag-TiO$_2$ coating layer increased up to 5 mol % Ag content and decreased when Ag content was 7.5 mol %. It was noticed that the sample of Ag-TiO$_2$ coating illustrated a fractured of cross section happened due the increased roughness of surface increased as increased Ag content reported by Liaqat et al. (2020)

108

where the increased of Ag doping increased the roughness and the aggregation of tiny particles at some points that contributed in the increase in the roughness parameters. In addition, during the grinding process at the end of the samples surface to eliminate the coating layer for the cross section view. It was also observed that the Ag-TiO$_2$ coating produced uneven layer because during the coating process each layer of coating must be dry first before proceed to the next coating layer until 5 dipping layer. Hence, it is normal that the cross section morphology illustrated uneven Ag-TiO$_2$ coating layer.

(a) TiO$_2$ coating

(b) 2.5 mol % Ag
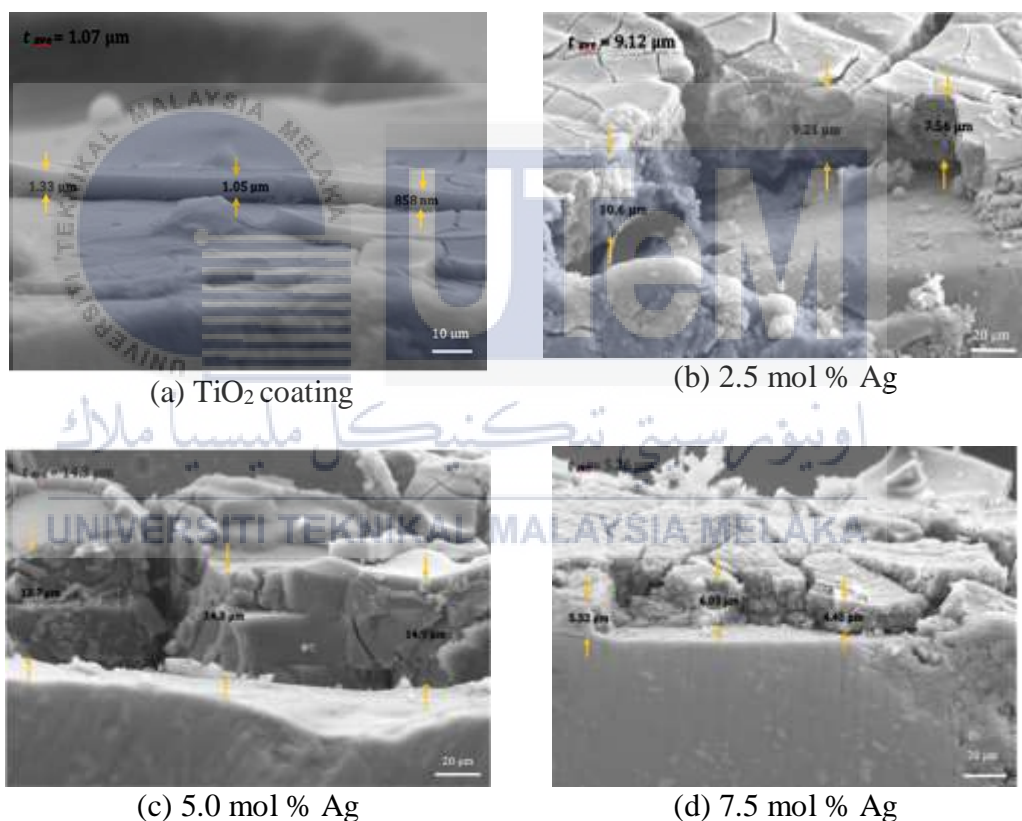
(c) 5.0 mol % Ag

(d) 7.5 mol % Ag

Figure 4.15 : Cross section morphology of (a) TiO$_2$ and Ag-TiO$_2$ coating at (b) 2.5 mol % Ag, (c) 5.0 mol % Ag and (d) 7.5 mol % Ag content deposited on glazed ceramic tile

As stated that, the element of ceramic tiles and sandpaper used for grinding during FESEM/EDX sample preparation were detected such as composed of silicon (Si), calcium (Ca), aluminium (Al) and sodium (Na), gold (Au), palladium (Pd), carbon (C) and oxygen

(O). Due to the nature of smooth surface glazed ceramic tiles, Ag-TiO$_2$ didn't get to sip into the substrate and Ti, O and Ag element were bonded within the layer. It observed that the incorporation of high amount of Ag content produced high amount of Ag wt % in the coating layer. It can be seen that the layer consists of small particles particularly Ti and Ag within the coating layer. Figure 4.16 demonstrated the cross section morphology and EDX layer of TiO$_2$ and Ag-TiO$_2$ coating deposited on glazed ceramic tile.

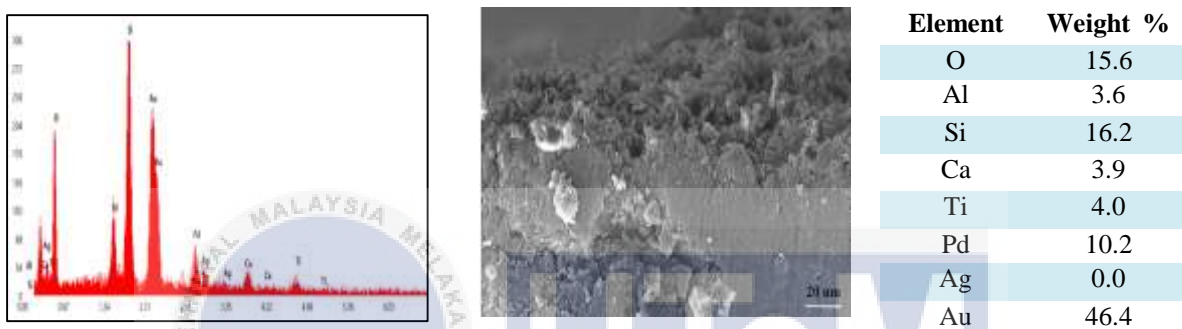(a) TiO$_2$ coating on glazed tile

(b) Ag-TiO$_2$ coating with 2.5 mol % Ag content deposited on glazed tile
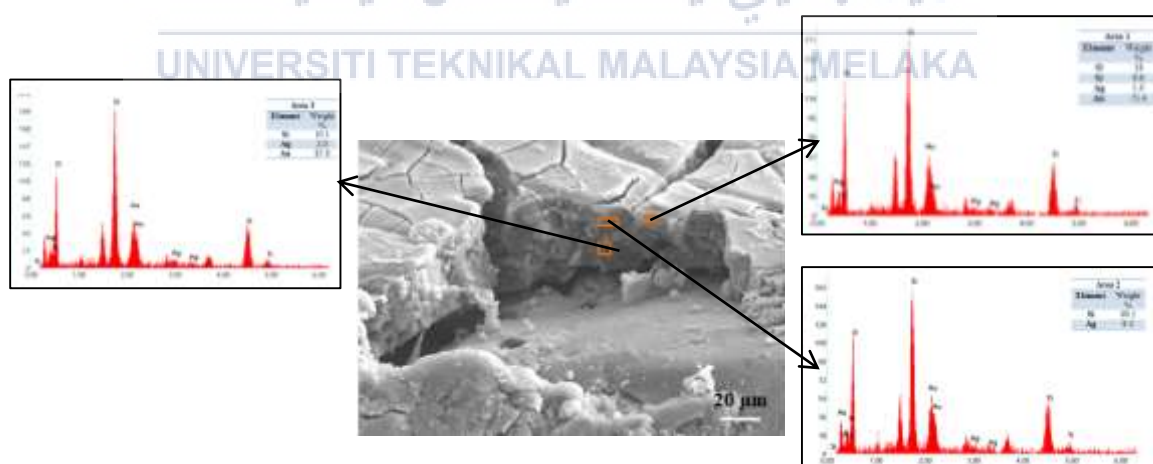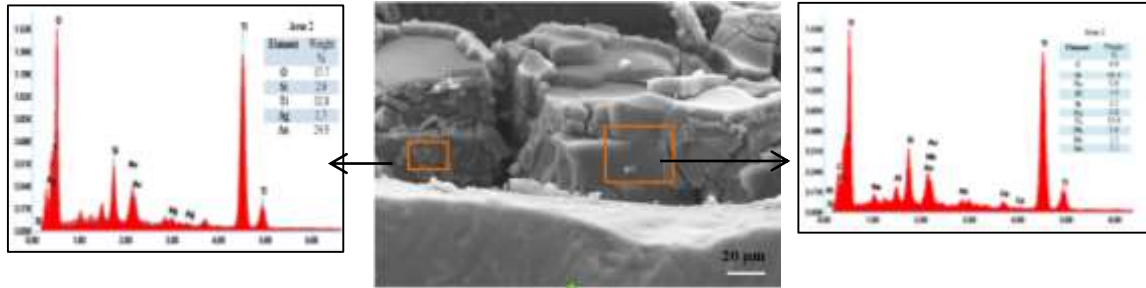
(c) Ag-TiO$_2$ coating with 5 mol % Ag content deposited on glazed tile
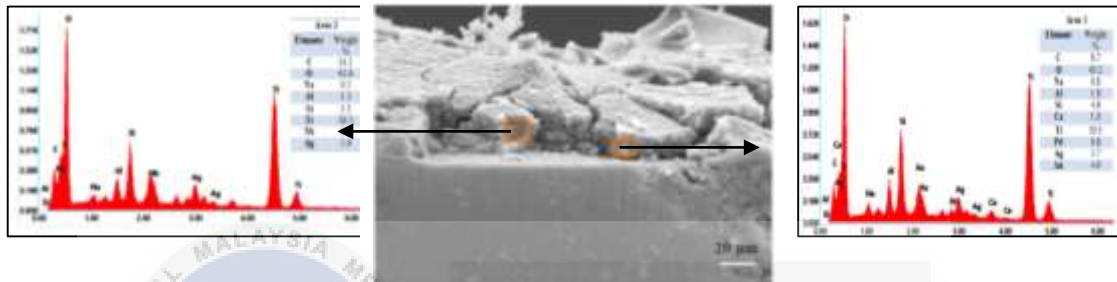
(d) Ag-TiO$_2$ coating with 7.5 mol % Ag content deposited on glazed tile

Figure 4.16: SEM/EDX on the cross-section of (a) TiO$_2$ and Ag-TiO$_2$ coating at (b) 2.5 mol % Ag, (c) 5.0 mol % Ag and (d) 7.5 mol % Ag content deposited on glazed ceramic tile

4.4.3.1 Effect of Ag content on the cross section microstructure

Since the Ag-TiO$_2$ coating on the unglazed ceramic tiles tends to sip into the substrate, the coating layer between substrate cause the thickness of Ag-TiO$_2$ coating on unglazed ceramic tiles cannot identified but it was detected the presence of Ti, O and Ag in the layer of coating substrate. While, the thickness of Ag-TiO$_2$ coating on the glazed ceramic tiles measured well and the thickness increased up to 5.0 mol % Ag content and fluctuate when increased Ag content to 7.5 mol %. Here, the surface gave major effect on determined the existence of coating layer and surface roughness contributed to the adhesion of the coating on the surface (Fattah et al., 2016). Therefore, it found that the Ag-TiO$_2$ coating with cracks on unglazed tile adhere well because it tends to diffuse into the substrate. The

111

Ag-TiO$_2$ coating on glazed ceramic tiles having thickness and can be peel off easily due to the nature of glazed ceramic tiles.

4.5 Effect of Ag content on the photocatalytic performances of Ag-TiO$_2$ coated on ceramic tiles

The photocatalytic activity measured using Methylene blue dye degradation as immersion solution of Ag-TiO$_2$ coating with varied Ag content were exposed under Ultra-violet (UV) and visible light spectrum. Generally, the photocatalytic initiate by exciting the ground state silver through the photon transition to the singlet excited state (Cruz et al., 2022).

4.5.1 Photocatalytic activity under UV light

The specific photocatalytic activity (P_{MB}) and photonic efficiency (ζ_{MB}) of unglazed ceramic tiles exposed under UV light radiation are displayed in Figure 4.17 and 4.18 respectively. The photocatalytic activity of TiO$_2$, 2.5, 5.0 and 7.5 mol % Ag-TiO$_2$ coating on unglazed tile under UV light irradiation was 4.53 x10^{-5}, 5.56 x 10^{-6}, 4.73 x 10^{-6} and 4.78 x 10^{-6} mol/m^{2}h respectively. While, the photonic efficiency measured was 3.64 X10^{-5}, 4.47 x10^{-6}, 3.8 x10^{-6}, and 3.84 x10^{-6} %. It is found that the photocatalytic performances decreased with increased Ag content from 2.5 to 7.5 mol %. The unglazed tiles coated TiO$_2$ without Ag addition present the highest photocatalytic activity when exposed under UV light. While, when adding Ag content, 2.5 mol % Ag shows the highest photocatalytic compared to 5.0 and 7.5 mol % Ag that is 5.56 x 10^{-6} mol/m^{2}h. The higher photocatalytic of Ag-TiO$_2$ coating with 2.5 mol % Ag content was due to the presence of brookite phase in the coating where stated by Freyria et al. (2020) the brookite mix phase of TiO$_2$ has been found to be responsible of a superior activity under solar light, especially when dye-sensitizing effects occur. The present findings revealed that the photocatalytic performances of Ag-TiO$_2$

112

coating on unglazed tile is lower compared to the performance of TiO_2 coating under UV light exposure. The photocatalytic activity of Ag-TiO_2 coated unglazed tile under UV light gave no significant effect with increasing Ag content.

Figure 4.17: Photocatalytic activity of Ag-TiO_2 coating on unglazed tile exposed under UV light irradiation
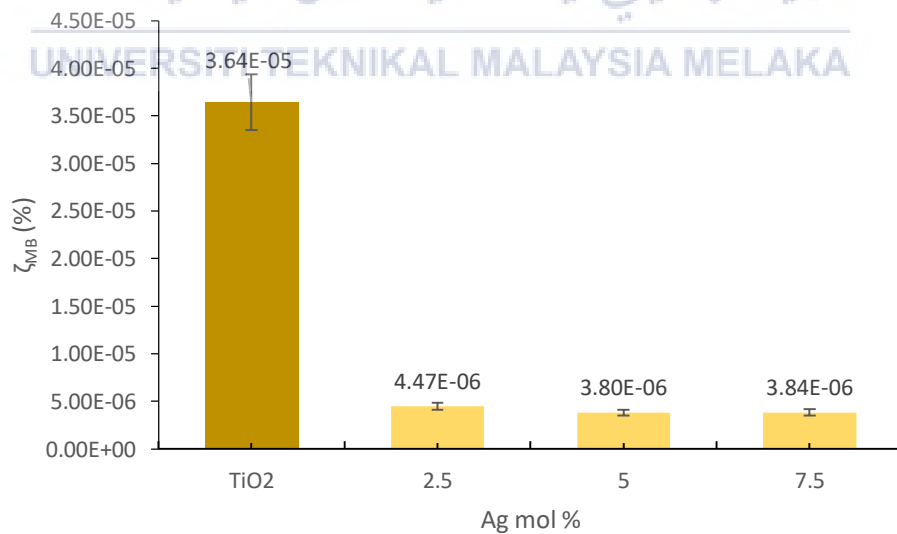
Figure 4.18: Photonic efficiency of Ag-TiO_2 coating on unglazed tile exposed under UV light irradiation

The graph bar in Figure 4.19 and 4.20 depict the photocatalytic activity and photonic efficiency of TiO_2 and $Ag-TiO_2$ coating on glazed ceramic tile under UV light irradiation respectively. Based on the graph, it is observed that the photocatalytic activity of $Ag-TiO_2$ coating on glazed tile at 2.5 mol % Ag content exhibited the lowest photocatalytic activity. This was due to the presence of less anatase crystalline phase shown before in Figure 4.10 (section 4.4.1). Anatase activated the photocatalytic reaction to occurred however, small amount of anatase phase gave no significant effect on photocatalytic activity. The TiO_2 coating on glazed tile however shows higher photocatalytic activity compared to $Ag-TiO_2$ coating with 2.5 mol % Ag content. The presence of more brookite phase aided the photocatalytic activity where the Žerjav et al. (2022) stated that the photogenerated electron in brookite was trapped at defects and led to decreased the number of free electron. Hence, it extended the lifetime of photogenerated electron and hole. The possibility of electron to encounter holes will then decrease. As increased more than 5.0 mol % Ag content, the photocatalytic activity decreased gradually. When exposed under UV irradiation, photocatalytic performances increased as increased Ag content till 5 mol % with the value of 4.19 x 10^{-6} mol/m^{2}h photocatalytic activity and 3.37 x10^{-6} % photonic efficiency. Increased Ag content up to 7.5 mol %, the photocatalytic activity measure decreased which is 3.86 x 10^{-6} mol/m^{2}h and photonic efficiency is 3.10 x 10^{-6} %. This was due to the high amount of Ag content caused agglomeration of Ag on TiO_2 surface that contributed to the less surface area of Ag exposed. The high amount of Ag covering the TiO_2 surface limits the amount of light. Hence, the electron-hole pairs tend to recombined and and photocatalytic activity decreased gradually (Razak et al., 2020).

114

Figure 4.19: Photocatalytic activity of Ag-TiO$_2$ coating on glazed tile exposed under UV light irradiation
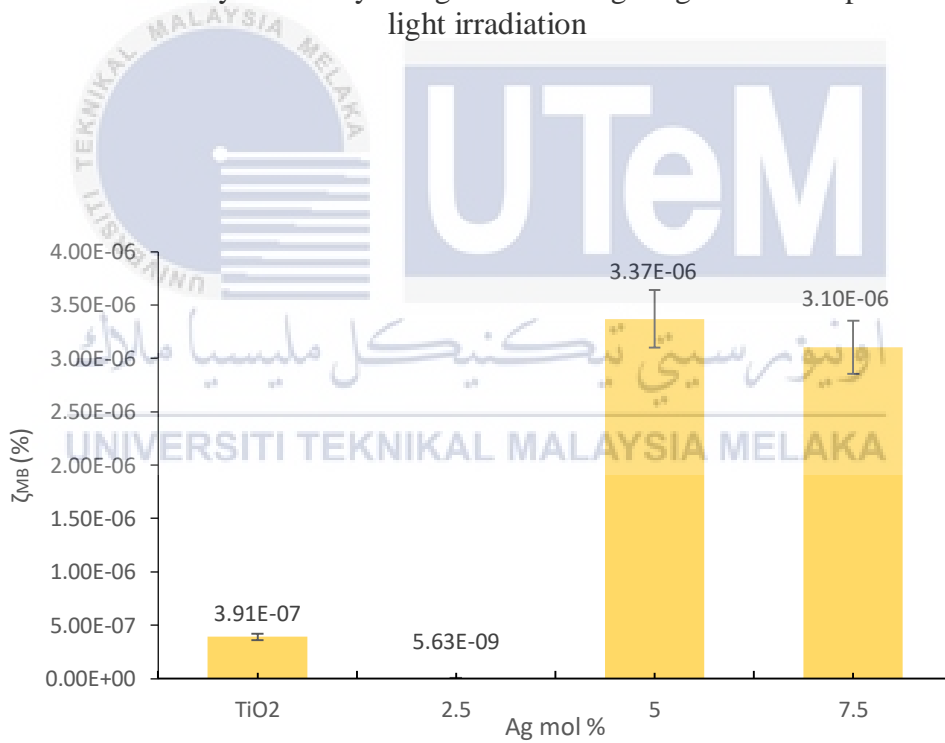
Figure 4.20: Photonic efficiency of Ag-TiO$_2$ coating on glazed tile exposed under UV light irradiation

Kien et al. (2022) explained that when Ag-TiO$_2$ exposed under UV light irradiation, the electrons beneath the Fermi level Ag will excited to the surface plasmon states and leaving behind the positive charge (h$^+$) below Fermi level energy, E$_f$. The electrons from Ag

on the surface of TiO_2 then excited to conduction band of TiO_2 as electron acceptor and forming superoxide anion radicals ($^{\bullet}O^{2-}$). The formation of superoxide radical ($^{\bullet}O^{2-}$) followed with protonation that yields to the formation of $^{\bullet}HO_2$ radicals which associated with trapped electrons producing H_2O_2 and at the end forming $^{\bullet}OH$ radicals.

4.5.2 Photocatalytic activity under visible light

Figure 4.21 and 4.22 show the photocatalytic activity and photonic efficiency of Ag-TiO_2 coating on unglazed tile exposed under visible light irradiation. It is found that the Ag-TiO_2 coating on unglazed tile exposed under visible light irradiation increased as increased Ag content from 2.5 mol % to 5 mol% and decrease when Ag content was 7.5 mol %. The photocatalytic activity of TiO_2 and Ag-TiO_2 coating on unglazed tile exposed under visible light were 5.05×10^{-6}, 4.49×10^{-7}, 8.06×10^{-6} and 5.44×10^{-6} mol/m^{2}h with photonic efficiency of 1.27×10^{-6}, 1.13×10^{-7}, and 2.03×10^{-6} and 1.37×10^{-6} % for 2.5, 5 and 7.5 mol %. Here, the photocatalytic activity increased .On contrary, the photocatalytic activity of Ag-TiO_2 coated on unglazed tile under visible light had a higher value at 5 mol %.
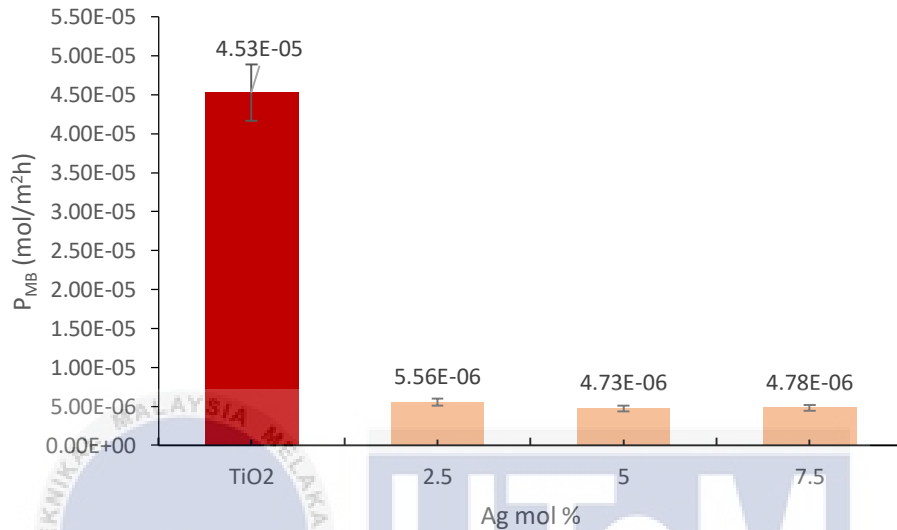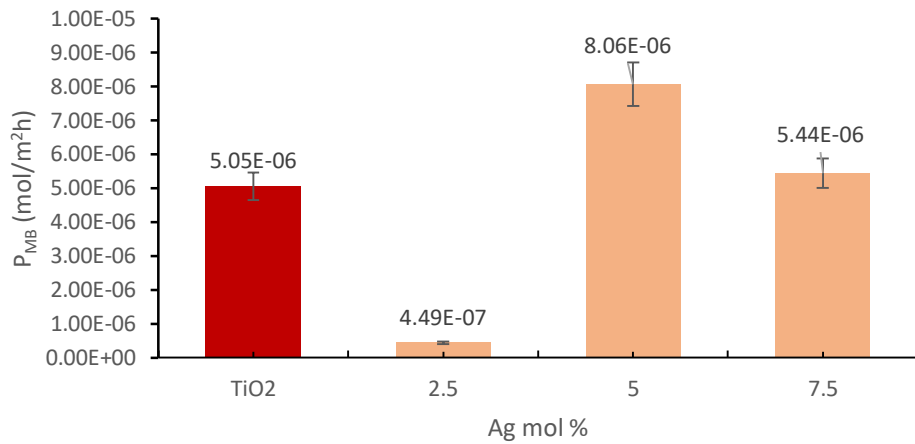
Figure 4.21: Photocatalytic activity of Ag-TiO$_2$ coating on unglazed tile exposed under visible light irradiation
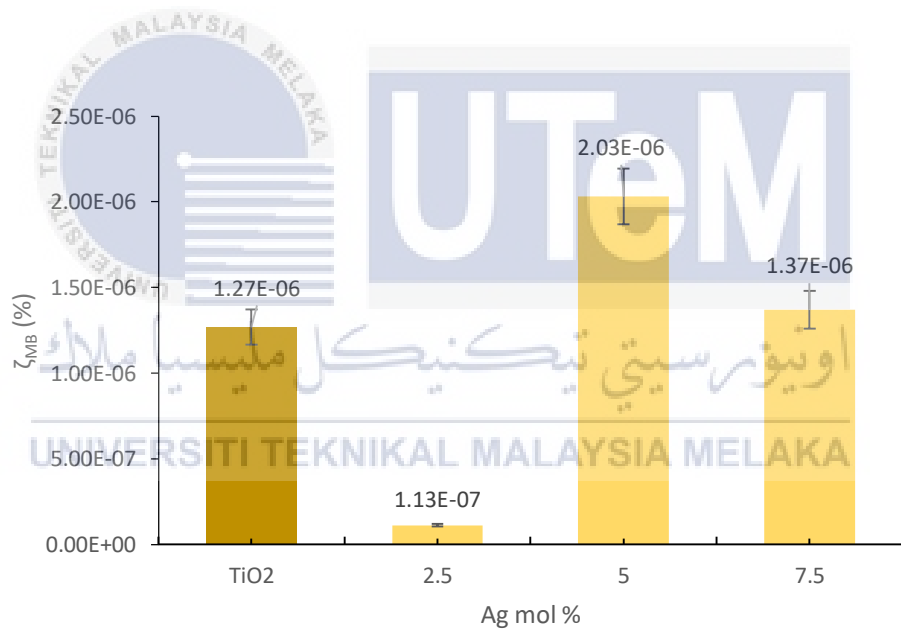
Figure 4.22: Photonic efficiency of Ag-TiO$_2$ coating on unglazed tile exposed under visible light irradiation

The photocatalytic activity and photonic efficiency of Ag-TiO$_2$ coating deposited on glazed tile exposed under visible light shown in Figure 4.23 and 4.24. When exposed under visible light irradiation, the photocatalytic increased up to 5 mol % and decreased when Ag content reach 7.5 mol %. The value of photocatalytic performance of 5 mol % Ag exposed under visible light was 3.14 x 10^{-6} mol/m^{2}h and 7.89 x 10^{-7} % photonic efficiency. The

photocatalytic activity of Ag-TiO$_2$ coating on glazed tiles decreased with increased Ag content more than 5 mol %. This was due to the presence of more peak of Ag-4H crystal which shown by XRD result before. Silver favourable in reducing the band gap by creating traps between the conduction and valence bands (Kien et al., 2022). However, excessive amount of silver used will reduce the photocatalytic performance as being studied by Komaraiah et al. (2020) that the degradation efficiencies increase with an increase in Ag$^+$ doping concentration reached a maximum at 5%Ag and then decreased at higher concentrations of Ag for the decomposition of dye under visible light illumination. Thus, when 7.5 mol % Ag content incorporated, the photocatalytic activity of Ag-TiO$_2$ tends to decrease.
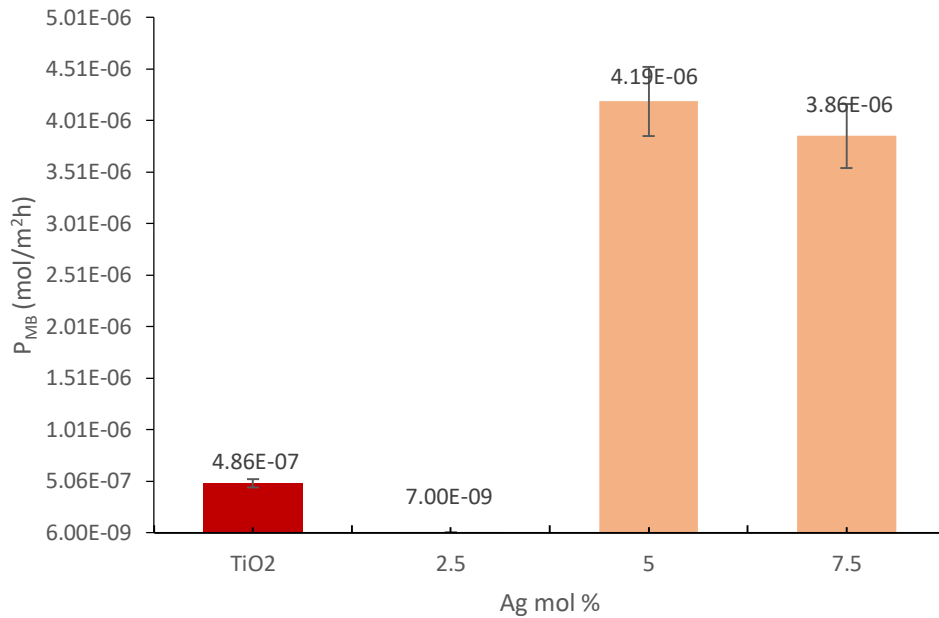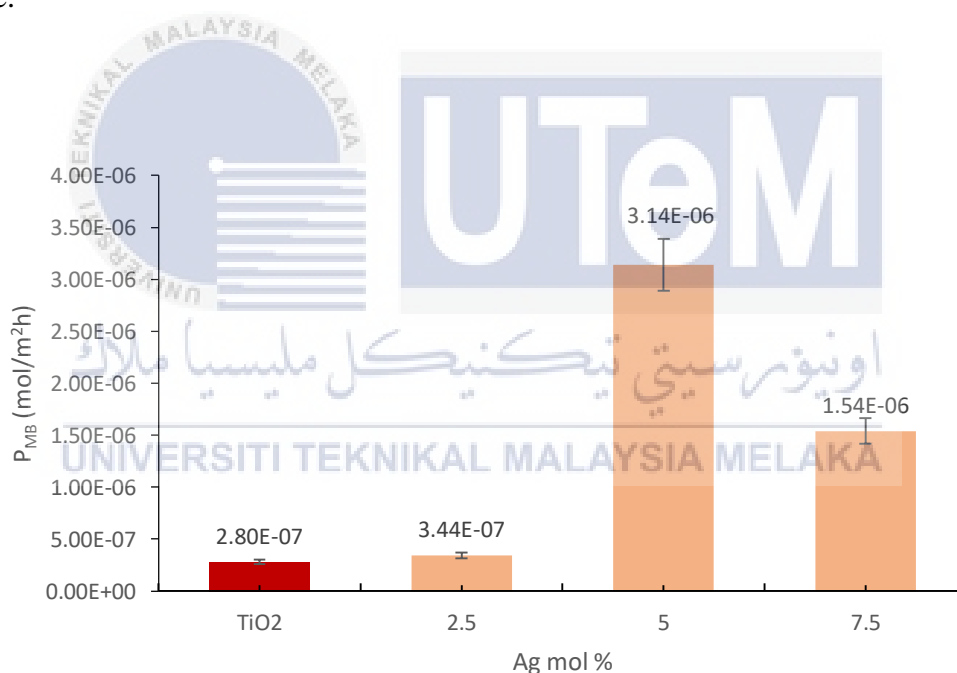

Figure 4.23: Photocatalytic activity of Ag-TiO$_2$ coating on glazed tile exposed under visible light irradiation
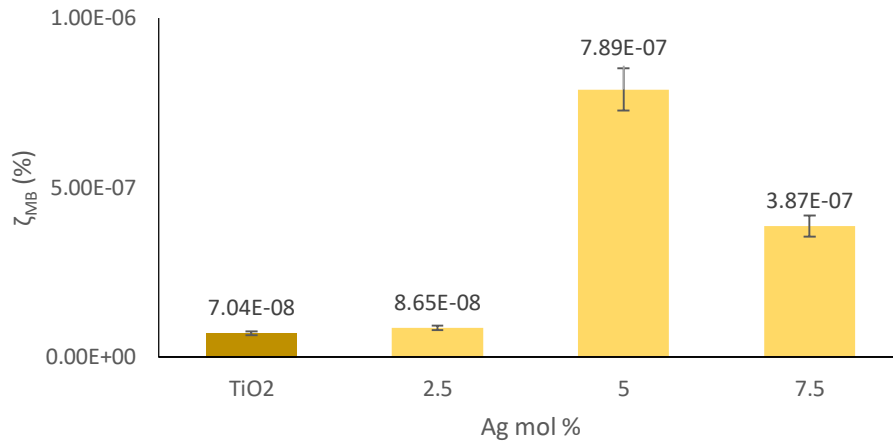
Figure 4.24: Photonic efficiency of Ag-TiO$_2$ coating on glazed tile exposed under visible light irradiation

4.5.3 The influence of Ag content on the photocatalytic performances of Ag-TiO$_2$ coated ceramic tiles

The photocatalytic performance generally depends on the surface properties; as surface area increase, the number of the active sites also increases. High surface area gives better photocatalytic efficiency (Suwarnkar et al., 2013). Table 4.6 shows the characteristics of the coating that give influenced to the photocatalytic performance of Ag-TiO$_2$ coating deposited on unglazed and glazed. The photocatalytic performances, Ag content, crystalline phase, crystalline size, surface morphology, cross section and elemental mapping obtained from the study is also summarized in Table 4.6.

Table 4.6: The characterization of Ag-TiO$_2$ coating on ceramic tiles that influences the photocatalytic performances

	Unglazed tile	**Glazed tile**
Performances (mol/m^{2}h)	2.5 mol % UV: 5.56 x 10^{-6} 5 mol % visible: 8.06 x 10^{-6}	UV: 4.19 x 10^{-6} Visible : 3.14 x 10^{-6}
Ag content (mol %)	2.5 mol % under UV light 5 mol % under visible light	5 mol % both under UV and visible light
Crystalline phase	2.5 mol %: anatase, rutile, brookite and Ag 5.0 mol %: anatase, rutile and Ag	Anatase, rutile, small brookite and Ag phase
Crystallite size (nm)	2.5 mol %: 24.3 5.0 mol %: 26.3	14.5
Surface morphology	 2.5 mol % 5.0 mol %	
Cross section	 2.5 mol % 5 mol %	
Elemental mapping	 2.5 mol % 5.0 mol %	
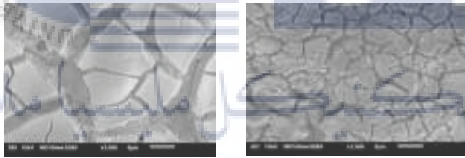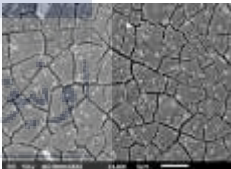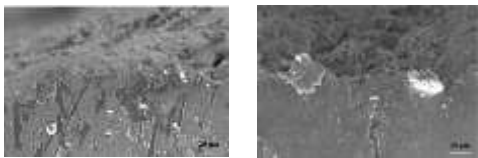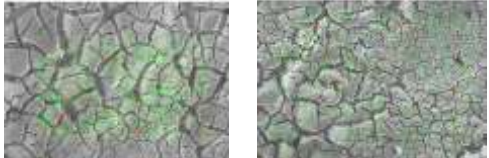
Ag-TiO$_2$ coating on unglazed ceramic tiles exposed under UV found that 2.5 mol % Ag content exhibited the highest photocatalytic while the photocatalytic of glazed tile under UV was highest at 5 mol % Ag content. These can be related to the anatase crystallite size of 2.5 mol % Ag content was 24.3 nm for Ag-TiO$_2$ coating on the unglazed tile ceramic. The size of the anatase belong to 2.5 mol % of unglazed ceramic tiles was the smallest compared to anatase crystallite size of 5 mol % and 7.5 mol % Ag. The Ag-TiO$_2$ coating on unglazed tile exposed to UV light (spectrum of light ≤340 nm) had highest photocatalytic activity at low amount of Ag can be explained by the small amount of Ag is enough for the Ag-TiO$_2$ coating on unglazed tile to degrade the pollutant. In addition, the presence of balance Ag$_2$O and Ag metallic for 2.5 mol % Ag was positively reacts on UV light exposure. As known that Ti generally active in UV light irradiation and in this case when increase amount of Ag content, the amount of Ti shown decreased. Hence, at 2.5 mol % Ag content, the amount of Ti measured by EDX cross section had high value and when exposed to UV light, the Ag-TiO$_2$ coating with 2.5 mol % Ag having high photocatalytic activity. The Ag ions within 2.5 mol % Ag-TiO$_2$ layer assisted in degrading the MB well as UV light nature in penetrating surface of the substrate. This can be explained by fewer cracks coating layer with pores display by SEM. The presence of pores on the surfaces also aid in better photocatalytic activity.

When exposed to visible light irradiation the Ag-TiO$_2$ coating on unglazed tile at 5 mol % Ag content tends to actively react compared to 2.5 and 7.5 mol % Ag content. The Ag presence in between the coating layer shown by the EDX cross section in form of Ag ion was around 1 wt % and it can be assumed that most of the Ag has been diffuse into the coating surface and actively response to visible light irradiation as visible light tends to penetrate into the coting layer of the substrate. Therefore, 5 mol % Ag-TiO$_2$ coating surface had the highest photocatalytic activity exposed under visible light exposure.

121

Nevertheless, the highest photocatalytic of Ag-TiO$_2$ coating on the glazed tiles was at 5 mol % Ag content. Even though the anatase crystallite size of 5 mol % Ag content was not the smallest one but the anatase crystallite size was not much differ compared to 2.5 mol % and 7.5 mol % Ag content and it has remarkably aiding in enhancing photocatalytic performances. The photocatalytic performances of Ag-TiO$_2$ coating on glazed tiles exposed both under UV and visible light increased as increased Ag up to 5 mol % then decrease when Ag was up to 7.5 mol %. As being stated from the crystallite size calculated using Scherer equation and FWHM result before, 5 mol % had 14.5 nm with highest FHWM value. The tendency of photocatalytic performances drops as increased Ag loading beyond 5 mol % could be attributed to the decrease concentration of photo-generated charge carriers such as holes and excited electrons. Higher loading of Ag may cover the TiO$_2$ surface which then limit the intensity of light irradiated and Ag may become recombination centers by reducing the amount of holes and excited electrons (Razak et al., 2020). In the other hand, the present of Ag° clusters on TiO$_2$ surface contributed to the improvement of visible light harvesting (Lidiaine et al., 2015). Cruz et al. (2022) mentioned that existence of Ag can retard the recombination reaction that happened after excitation of the semiconductor with UV light increasing the rate of reductive photo-processes. Instead, Ag on the surface TiO$_2$ has effect controversial upon the oxidation of organic compounds. This is because the photocatalyst surface itself can strongly modified by silver deposition and cause an intrinsic decrease in photocatalytic activity (Dozzi et al., 2009).

It can be observed that there was no linear relation of the photocatalyst ability with the content of Ag in TiO$_2$ similarly stated by Cruz et al. (2022) in the studied of Ag-TiO$_2$ composite in degradation of methylene blue. The present findings revealed that as for the unglazed tile, the photocatalytic performances of Ag addition in TiO$_2$ coating didn't improved under UV light but tend to improve a bit under visible irradiation. Yet the TiO$_2$

122

coating alone having highest photocatalytic performances under UV light exposure that is 4.53×10^{-5} mol/m^{2}h compare to coating with Ag addition that are 5.56×10^{-6}, 4.73×10^{-6} and 4.78×10^{-6} mol/m^{2}h for 2.5, 5.0 and 7.5 mol % Ag content. As for the unglazed surfaces, the porous surface structure supposed aiding photocatalytic performances. However, under UV light the addition of Ag tends to lower the photocatalytic performances. It defined that the photocatalytic activity of Ag-TiO$_2$ coated unglazed tile under UV light gave no significant effect with increasing Ag content. The case was supported by Ying et al. (2016) which stated that apparently the doped Ag into TiO$_2$ cannot increase the photocatalytic activity under UV light, instead it can increase the photocatalytic activity greatly under visible light irradiation because of effective electron-hole separation. This may due to the distribution of Ag and surface area exposed to the light illumination that influenced the different photocatalytic activity of the unglazed ceramic tile.

Furthermore, at 5 mol % Ag content of Ag-TiO$_2$ coating, the anatase crystallite size is the major contribute to the better photocatalytic activity by reduce the coating defects and dislocations surface. An excessive amount of metallic Ag may likely obstruct UV or visible light from interacting with TiO$_2$ where the fast recombination rate of electron-holes pair happened (Tijani et al., 2017). Enhanced photocatalytic activity may due to the addition of metallic Ag particles and slight increases in catalyst surface area after deposition of Ag particles. Reduction of photocatalytic activity with high increased Ag could be linked to the high coverage of TiO$_2$ surface with Ag as evident in SEM/EDX causing catalyst casing thus preventing light irradiation of the catalyst surface. Higher amount of Ag on the TiO$_2$ surface may constitute a barrier for the dye to contact the surface and act as recombination center for most photogenerated holes, thereby inhibiting the interaction between TiO$_2$ and MB. Excessive Ag often enlarges the diffusional distance which would affect the formation and interaction of hydroxyl radicals and subsequently decreases all photocatalytic activities.

123

Instead, the crack coarse sandy like surface accompany with pores and Ag particles dispersed on the coating surface ascribed that 5 mol % Ag addition having the better photocatalytic performances under visible light irradiation. Besides, the small anatase crystallite size of 5 mol % Ag-TiO$_2$ coating on unglazed tiles which is 26.2 nm supported by higher value of FHWM had contributed to the better photocatalytic performances under visible region. Instead of that, the better photocatalytic performances of 5 mol % Ag-TiO$_2$ coated on glazed tile can be related to its active crystallite that distribute well on the coating surface. Besides, the surface morphology and elemental mapping demonstrated that the crack with presence of small Ag particles dispersed well on the surface had contributed to the better photocatalytic performances. As mentioned before, beyond the required Ag content needed for Ag-TiO$_2$ coating on ceramic tiles, there were decrease concentration of photo generated charge carriers such as holes and excited electrons happened. Higher loading of Ag may cover the TiO$_2$ surface which then limit the intensity of light irradiated and Ag may become recombination centers by reducing the amount of holes and excited electrons (Razak et al., 2020). Exceeding Ag beyond the required amount needed can cause a fast rate of electron-hole pair recombination to happen.

The thickness of the coating also plays an important role to define the effectiveness of the photocatalytic performances where as seen that 5 mol % of Ag content for Ag-TiO$_2$ coating deposited on glazed tiles greatly enhanced photocatalytic performances. On the other hand, the value of photocatalytic activity measured for the unglazed was higher compared to the photocatalytic activity of the glazed tiles. This was supported by Zhang et al. (2022c) that the rough surfaces attributed to the greater available surface which helps in increases the photocatalytic reaction rate.

Based on the evaluation on the performance of Ag-TiO$_2$ coating at varied content on unglazed and glazed ceramic tile, it is deduced that by adding Ag incorporated into TiO$_2$ sol,

the Ag-TiO$_2$ nanocomposite coating form TiO$_2$ crystallite with Ag presence on the TiO$_2$ surface. The Ti, O and Ag are bind together within the nanocomposite coating. As been mentioned, the radius of Ag is greater than the lattice of Ti which it cannot enter the lattice TiO$_2$. Hence, most of the Ag existed on the TiO$_2$ surface. Figure 4.25 shows the schematic diagram of Ag-TiO$_2$ coating deposited on unglazed ceramic tile. The Ag-TiO$_2$ coating on unglazed tiles sip into the unglazed surfaces due to the porous nature of unglazed tile surfaces and some of the Ag embedded in the pore. Thus, the thickness of the Ag-TiO$_2$ coating layer was unidenfified. While, Figure 4.26 shows the schematic diagram of Ag-TiO$_2$ coating deposited on glazed ceramic tile. The Ag-TiO$_2$ coating on glazed tile contributed to a certain layer of coating thickness since the glazed tiles having smooth surface without pores. Most of the Ag has been successfully presence on the surface of TiO$_2$ which effective for photocatalytic properties.

| (a) 2.5 mol % Ag | (b) 5.0 mol % Ag | (c) 7.5 mol % Ag |
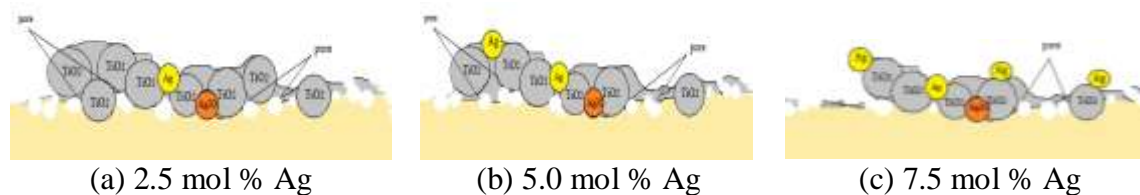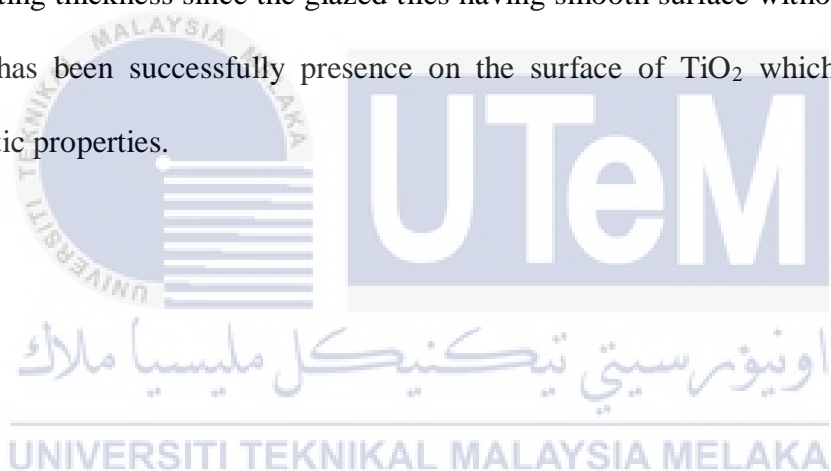
Figure 4.25: Schematic diagram of Ag-TiO$_2$ coating deposited on unglazed ceramic tile

125

(a) 2.5 mol % Ag (b) 5.0 mol % Ag (c) 7.5 mol % Ag
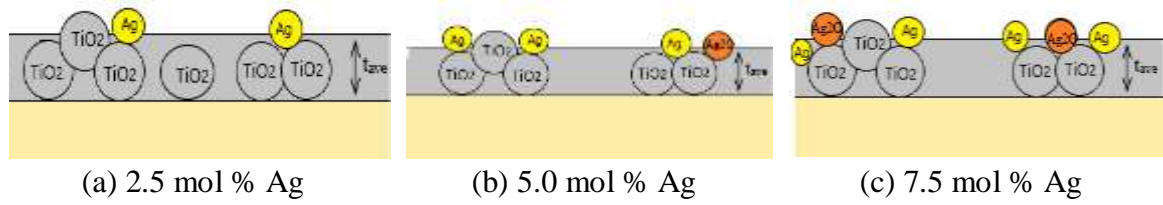
Figure 4.26: Schematic diagram of Ag-TiO₂ coating deposited on glazed ceramic tile

CHAPTER 5

CONCLUSION AND RECOMMENDATIONS

5.1 Conclusions

Thus, from all the findings and discussion of Ag-TiO$_2$ coating on ceramic tiles, the conclusion can be drawn as follows;

1. Ag-TiO$_2$ incorporated Degussa P25 had interrupted crystallization of the coating and Degussa P25 prevents the growth of Ag peak that actually overlapped with anatase phase. Since Degussa P25 made up of almost 70 % anatase hence detection of anatase was very strong instead of Ag phase. Due to this, more anatase phase presence in Ag-TiO$_2$ P25 compared to Ag-TiO$_2$ coating. Therefore, Ag-TiO$_2$ P25 retards the growth of Ag peak and Degussa P25 form of bigger anatase crystallite size. In contrast, Ag-TiO$_2$ coated without Degussa on unglazed and glazed tiles shows presence of anatase, rutile, brookite, Ag$_2$O and Ag metallic respectively. The coating inhibited a better crystallinity. The unglazed tile that has porous structure causes Ag-TiO$_2$ to sip by filling in the pores of the unglazed tile surface. Therefore, the peak intensity of Ag-TiO$_2$ coating on unglazed tile was lower than Ag-TiO$_2$ coated on glazed tiles. Incorporation of Ag increased anatase crystallite size with increasing Ag content. At a point, the anatase size decrease at 7.5 mol % Ag content. These supported by FWHM data where the highest value belongs to 5 mol % Ag and drop drastically at 7.5 mol % Ag content. Ag-TiO$_2$ coating on glazed tile had smaller anatase size compared to Ag-TiO$_2$ coating on unglazed tile which calculated by Scherer equation and supported by FWHM correspondingly.

127

2. The surface morphology of Ag-TiO$_2$ coating on unglazed tiles consisted of many visible mud crack shape layer on the entire surfaces. Meanwhile, as for the Ag-TiO$_2$ coating on glazed tile, there is crack exist, however no aggregation displayed. Both Ag-TiO$_2$ coating on unglazed and glazed tile showing small particles spread on the surfaces which were identified as Ag particles and spread evenly revealed by EDX mapping analysis. The element of Ti, O and Ag were well observed by EDX mapping analysis which distributed on the coating surface.

3. The photocatalytic performance of Ag-TiO$_2$ coating on unglazed tile under UV light irradiation decreased as increased Ag content from 2.5 to 7.5 mol %. But when exposed under visible light irradiation the photocatalytic performances increased up to 5 mol % Ag and drop when reaching 7.5 mol % Ag. For the unglazed tile, the photocatalytic performances of Ag-TiO$_2$ coating didn't improved under UV light but tend to improve a bit under visible irradiation. It can be deduces that for the unglazed tile, the existence of pores and Ti particle were already enough to degrade the pollutant under UV light irradiation. The Ag addition is needed if it involved visible light irradiation. Photocatalytic performances of Ag-TiO$_2$ coating on the glazed tile whereby improved at both UV and visible light irradiation mostly at 5 mol % Ag content.

In conclusion, Ag addition into TiO$_2$ coating deposited on ceramic substrate is to be conducted without the use of Degussa P25 addition. Moreover, the deposition is influenced by the type of the ceramic surface and the amount of Ag addition is dependent on the type of photocatalythic reaction needed either in the UV region or at visible region. For a common unglazed and glazed ceramic substrate, the Addition of 5 mol %Ag had shown improved performance of photocatalythic reaction for visible light application.

5.2 Recommendations

Based on the finding drawn from this current study, it is necessary to make some essential improvement for the fabrication of future ceramic tiles that can provide photocatalytic properties which importance to generate self-cleaning antimicrobial ceramic tile. Therefore, some of the suggestion includes:

i. The purpose of Ag-TiO$_2$ coating in this study was to produce good photocatalytic properties ceramic tiles that led to antimicrobial tiles. Hence, for that more test should be done such as such as water contact angle for the wettability performances to determine the hydrophilicity of the coating surface and standard antimicrobial for qualitative and quantitave study.

ii. Since the ceramic is use in variety of indoor and outdoor areas, the weathering test should be in consideration to ensure the coating can stand for such various weather conditions.

iii. Use of TEM to characterize the crystal formation with high resolution, BET for the determination of surface area, and XPS to analyze the sample surface, composition and binding state is also recommended.

Since ceramic tiles were used in multipurpose application including inside and outside use application whether in big or small industrial area, the works on Ag-TiO$_2$ need to be explore and expand alongside with the nowadays situation where the important self-cleaning surface is essential due to the spread of contagious virus recently such as Covid-19 viruses among people. Ceramic material needs researcher attention and focus since it used mostly for household utensil and highly potential to the breeding of bacterial. Instead of coating for the purpose of beautiful decoration, a future design need to concern about a creative development of surface coating with a healthy and safe besides an attractive value.

Thus, clear and thorough works in detail for application purposes need to be study to ensure a healthy future.

REFERENCES

Aazam, E. S., 2014. Visible Light Photocatalytic Degradation of Thiophene Using Ag–TiO$_2$/Multi-walled Carbon Nanotubes Nanocomposite. *Ceramics International,* 40, pp.6705-6711.

Abbad, S., Guergouri, K., Gazaout, S., Djebabra, S., Zertal, A., Barille, R. and Zaabat, M., 2020. Effect of Silver Doping on the Photocatalytic Activity of TiO$_2$ Nanopowders Synthesized by the Sol-Gel Route. *Journal of Environmental Chemical Engineering,* 8, pp.103718.

Abd Samat, S. F. and Mohd Saad, P. S., 2016. Effect of Different Dip Cycle on Optical Properties of Dip-coated TiO$_2$ Thin Films. *In:* XPLORE, I. (ed.) *IEEE Student Conference on Research and Development (SCOReD).* Kuala Lumpur, Malaysia.

Abdellah, M. H., Nosier, S. A., El-Shazly, A. H. and Mubarak, A. A., 2018. Photocatalytic Decolorization of Methylene Blue Using TiO$_2$/UV System Enhanced by air Sparging. *Alexandria Eng J.,* 57, pp.3727-3735.

Aini, N., Rachman, S., Maunatin, A. and Syarifah, A., Synthesis, Characterization and Antibacterial Activity of Silver Doped TiO$_2$ Photocatalyst. International Conference on Biology and Applied Science (ICOBAS), 2019. AIP Publishing.

Akhavan, O., 2009. Lasting Antibacterial Activities of Ag–TiO$_2$/Ag/a-TiO$_2$ Nanocomposite Thin Film Photocatalysts Under Solar Light Irradiation. *Journal of Colloid and Interface Science,* 336, pp.117-124.

Al-Harbi, L. M., El-Mossalamy, E. H., Arafa, H. M., Al-Owais, A. and Shah, M. A., 2011. TiO$_2$ Nanoparticles with Tetra-Pad Shape Prepared by An Economical and Safe Route at Very Low Temperature. *Modern Applied Science,* 5, pp.130-135.

Albert, E., Albouy, P. A., Ayral, A., Basa, P., Csík, G., Nagy, N., Roualdès, S., Rouessac, V., Sáfrán, G., Suhajda, A., Zolnaif, Z. and Hórvölgyi, Z., 2015. Antibacterial Properties of Ag–TiO$_2$ Composite Sol–Gel Coatings. *RSC Advances,* 5, pp.59070–59081.

Aliyu, S., Ambali, A. S., Oladejo, T. J., Mustapha, S., Egbosiuba, T. C. and Bada, S. O., 2023. Development of Ag-doped on Multi-Walled Carbon Nanotubes for the Treatment of Fish Pond Effluent. *Regional Studies in Marine Science,* 58, pp.1-25.

131

Ashraf, M. A., Liu Z., Peng, W. X., Jermsittiparsert, K., Hosseinzadeh, G. and Hosseinzadeh, R., 2019. Combination of Sonochemical and Freeze-Drying Methods for Synthesis of Graphene/Ag-Doped TiO$_2$ Nanocomposite: A Strategy to Boost the Photocatalytic Performance Via Well Distribution of Nanoparticles Between Graphene Sheets. *Ceramics Int.,* 46, pp.7446 - 7452.

Avciata, O., Benli, Y., Gorduk, S. and Koyun, O., 2016. Ag Doped TiO$_2$ Nanoparticles Prepared by Hydrothermal Method and Coating of the Nanoparticles on the Ceramic Pellets for Photocatalytic Study: Surface Properties and Photoactivity. *Journal of Engineering Technology and Applied Sciences,* 1, pp.34 -50.

Away, R. D. Y., Takai-Yamashita, C., Ban, T. and Ohya, Y., 2021. Photocatalytic Properties of TiO$_2$-SiO$_2$ Sandwich Multilayer Films Prepared by Sol-gel Dip-coating. *Thin Solid Films,* 720, pp.138522.

Bachhav, A. P., Shroff, M. R. and Shirkhedkar, A. A., 2020. Silver Nanoparticles: A Comprehensive Review on Mechanism, Synthesis and Biomedical Applications. *Asian J. Pharm. Res.,* 10, pp.202 - 212.

Bamsaoud, S. F., Basuliman, M. M., Bin-Hameed, E. A. B., Balakhm, S. M. and Alkalali, A. S., 2021. The Effect of Volume and Concentration of AgNO$_3$ Aqueous Solutions on Silver Nanoparticles Synthesized Using Ziziphus Spina–Christi Leaf Extract and Their Antibacterial Activity. *Journal of Physics: Conference Series,* 1900, pp.1-10.

Bao, S., Sun, S., Li, L. and Xu, L., 2023. Synthesis and Antibacterial Activities of Ag-TiO$_2$/ZIF-8. *Front. Bioeng. Biotechnol,* 11, pp.1-10.

Barrientos, L., Allende, P., Bercero, M. A. L., Pastrián, J., Becerrac, J. R. and Jensen, L. C., 2018. Controlled Ag-TiO$_2$ Heterojunction Obtained by Combining Physical Vapor Deposition and Bifunctional Surface Modifiers. *Journal of Physics and Chemistry of Solids,* 119, pp.147–156.

Barrow, D. A., Petroff, T. E. and Sayer, M., 1995. Thick Ceramic Coating Using a Sol Gel Based Ceramic-Ceramic 0-3 Composite. *Surface and Coatings Technology,* 76-77, pp.113-118.

Behpour, M., Ghoreishi, S. M. and Razavi, F. S., 2010. Photocatalytic Activity of TiO$_2$ /Ag Nanoparticle on Degradation of Water Pollutions. *Digest Journal of Nanomaterials and Biostructures,* 5, pp.467 – 475.

132

Bessergenev, V. G., Mateus, M. C., Rego, A. M. B. and Hantusch, M., 2015. An Improvement of Photocatalytic Activity of TiO$_2$ Degussa P25 Powder. *Applied Catalysis A: General,* 500, pp.40 - 50.

Bok, G. and Johansson, P., 2020. Microbial Growth Behind Tiles in Bathrooms. *E3S Web of Conferences,* 172, pp.1-4.

Bouanimba, N., Laid, N., Zouaghi, R. and Sehili, T., 2017. A Comparative Study of the Activity of TiO$_2$ Degussa P25 and Millennium PCs in the Photocatalytic Degradation of Bromothymol Blue. *International Journal of Chemical Reactor Engineering,* 16, pp.1- 19.

Braun, J. H., Baidins, A. and Marganski, R. E., 1992. TiO$_2$ Pigment Technology: A Review. *Progress in organic coatings,* 20, pp.105-138.

Brown, J. 2014. *Titanium Dioxide: Chemical Properties, Applications and Environmental Effects*, Nova Publishers.

Cai, R., Hashimoto K., Itoh, K., Kubota, Y. and Fujishima, A., 1991. Photokilling of Malignant Cells with Ultrafine TiO$_2$ Powder. *Bulletin of the Chemical Society of Japan,* 64, pp.1268-1273.

Canbaz, G. T., Çakmak, N. K., Eroğlu, A. and Açıkel, Ü., 2019. Removal of Acid Orange 74 from Wastewater with TiO$_2$ Nanoparticle. *Int Adv Res Eng,* 3, pp.75-80.

Chakhtouna, H., Benzeid, H., Zari, N., Qaiss, A. E. K. and Bouhfid, R., 2021. Recent Progress on Ag/TiO$_2$ Photocatalysts: Photocatalytic and Bactericidal Behaviors. *Environ Sci Pollut Res Int,* 28, pp.44638 - 44666.

Chang, R. and Goldsby, K. A. 2016. *Chemistry,* New York, MaGraw-Hill Education.

Chen, Y. and Dionysiou, D. D., 2006. TiO$_2$ Photocatalytic Films on Stainless Steel: The Role of Degussa P-25 in Modified Sol–Gel Methods. *Applied Catalysis B: Environmental,* 62, pp.255 - 264.

Cherif, Y., Azzi, H., Sridharan, K., Ji, S., Choi, H., Allan, M. G., Benaissa, S., Bendahou, K. S., Damptey, L., Silva Ribeiro, C. S., Krishnamurthy, S., Nagarajan, S., Mercedes, M. M. V., Kuehnel, M. F. and Pitchaimuthu, S., 2023. Facile Synthesis of Gram-Scale Mesoporous Ag/TiO$_2$ Photocatalysts for Pharmaceutical Water Pollutant Removal and Green Hydrogen Generation. *ACS Omega,* 8, pp.1249-1261.

Choi, B. K., Choi, W., K.,, Park, S. J. and Seo, M. K., 2018. One-Pot Synthesis of Ag-TiO$_2$/Nitrogen-Doped Graphene Oxide Nanocomposites and Its Photocatalytic Degradation of Methylene Blue. *Journal of Nanoscience and Nanotechnology,* 18, pp.6075-6080.

Collette, S., Hubert, J., Batan, A., Baert, K., Raes, M., Vandendael, I., Daniel, A., Archambeau, C., Terryn, H. and Reniers, F., 2016. Photocatalytic TiO$_2$ Thin Films Synthesized by the Post-Discharge of an RF Atmospheric Plasma Torch. *Surface and Coatings Technology,* 289, pp.172-178.

Cong, S. and Xu, Y., 2011. Explaining the High Photocalatytic Activity of a Mixed Phase TiO$_2$: A Combined Effect of O$_2$ and Crystallinity *Physical Chemistry Research,* 115, pp.21161-21168.

Coronado, D. R., Gattorno, G. R., Pesqueira, M. E. E., Cab, C., Coss, R. D. and Oskam, G., 2008. Phase-Pure TiO$_2$ Nanoparticles: Anatase, Brookite and Rutile. *Nanotechnology,* 19, pp.1-10.

Cotolan, N., Rak, M., Bele, M., Cör, A., Muresan, L. M. and Milošev, I., 2016. Sol-gel Synthesis, characterization and properties of TiO$_2$ and Ag-TiO$_2$ coatings on titanium substrate. *Surface and Coatings Technology,* 307, pp.790-799.

Cruz, D., Ortiz-Oliveros, H. B., Flores-Espinosa, R. M., Ávila Pérez, P., Ruiz-López, I. I. and Quiroz-Estrada, K. F., 2022. Synthesis of Ag/TiO$_2$ Composites by Combustion Modified and Subsequent Use in the Photocatalytic Degradation of Dyes. *Journal of King Saud University - Science,* 34, pp.1-8.

Das, A., Patra, M., Wary, R. R., Gupta, P. and Nair, R. G., 2018. Photocatalytic Performance Analysis of Degussa P25 Under Various Laboratory Conditions. *IOP Conf. Series: Materials Science and Engineering,* 377, pp.1 - 7.

Dash, T., Rani, S. T., Dash, B. and Biswal, S. K. 2023. 25 - Development of an advanced flexible ceramic material from graphene-incorporated alumina nanocomposite. *In:* GUPTA, R. K., BEHERA, A., FARHAD, S. and NGUYEN, T. A. (eds.) *Advanced Flexible Ceramics.* Elsevier.

Demircia, S., Dikici, T., Yurddaskal, M., Gultekin, S., Toparlic, M. and Celik, E., 2016. Synthesis and Characterization of Ag Doped TiO$_2$ Heterojunction Films and Their Photocatalytic Performances. *Applied Surface Science,* 390, pp.591-601.

Dondi, D., Albini, A. and Serpone, N., 2006. Interactions Between Different Solar UVB/UVA Filters Contained in Commercial Suncreams and Consequent Loss of UV Protection. *Photochemical & Photobiological Sciences,* 5, pp.835-843.

Dontsova, T. A., Yanushevska, O. I., Nahirniak, S. V., Kutuzova, A. S., Krymets, G. V. and Smertenko, P. S., 2021. Characterization of Commercial TiO_2 P90 Modified with ZnO by the Impregnation Method. *Journal of Chemistry,* 2021, pp.1-11.

Dozzi, M. V., Prati, L., Canton, P. and Selli, E., 2009. Effects of Gold Nanoparticles Deposition on the Photocatalytic Activity of Titanium Dioxide Under Visible Light. *Physical Chemistry Chemical Physics,* 11, pp. 7171–7180.

El-Katoria, E., Al Angarib, Y. M. and Abousalem, A. S., 2019. Corrosion Mitigation of Carbon Steel by Spin Coating with Ag–TiO_2 Gel Films in Acidic Solution: Fabrication, Characterization, Electrochemical and Quantum Chemical Approaches. *Surface and Coatings Technology,* 374, pp.852-867.

Evcin, A., Arli, E., Baz, Z., Esen, R. and Sever, E. G., 2017. Characterization of Ag-TiO_2 Powders Prepared by Sol-Gel Process. *Acta Physica Polonica A,* 132, pp.608-611.

Fakhouri, H., Arefi-Khonsari, F., Jaiswal, A. K. and Pulpytel, J. 2015. Effect of the Deposition Method on Silver Diffusion in Ag-TiO_2 Thin Coatings: Advantages and Inconvenienes for Photocatalytic Applications and Water Treatment. *22nd International Symposium on Plasma Chemistry.* Antwerp, Belgium.

Fattah, W. A., Gobara, M. M., El-Hotaby, W., Mostafa, S. F. M. and Ali, G. W., 2016. Coating Stainless Steel Plates with Ag/TiO_2 for Chlorpyrifos Decontamination. *Materials Research Express,* 3.

Freyria, F. S., Blangetti, N., Esposito, S., Nasi, R., Armandi, M., Annelio, V. and Bonelli, B., 2020. Effects of the Brookite Phase on the Properties of Different Nanostructured TiO_2 Phases Photocatalytically Active Towards the Degradation of N-Phenylurea. *ChemistryOpen,* 9, pp.903-912.

Fu, T., Shen, Y. G., Alamji, Z., Yang, S. Y., Sun, J. M. and Zhang, H. M., 2015. Sol–gel Preparation and Properties of Ag–TiO_2 Films on Surface Roughened Ti–6Al–4V Alloy. *Materials Science and Technology,* 31, pp.501-505.

Gol, F., Saritas, Z. G., Ture, C., Kacar, E., Yilmaz, A., Arslan, M. and Sen, F., 2022. Coloring effect of iron oxide content on ceramic glazes and their comparison with the similar waste containing materials. *Ceramics International,* 48, pp.2241-2249.

Golshan, V., Mirjalili, F. and Fakharpour, M., 2022. Self-Cleaning Surfaces with Superhydrophobicity of Ag–TiO$_2$ Nanofilms on the Floor Ceramic Tiles. *Glass Physics and Chemistry,* 48, pp.35 - 42.

Gong, D., Jeffrey, H. W. C., Tang, Y., Tay, Q., Lai, Y., Highfield, J. G. and Chen, Z., 2012. Silver Decorated Titanate/Titania Nanostructures for Efficient Solar Driven Photocatalysis. *Journal of Solid State Chemistry,* 189, pp.117-122.

Grabowska, E., Zaleska, A., Sorgues, S., Kunst, M., Etcheberry, A., Colbeau-Justin, C. and Remita, H., 2013. Modification of Titanium (IV) Dioxide with Small Silver Nanoparticles: Application in Photocatalysis. *J. Phys. Chem. C.,* 117, pp.1955 - 1962.

Greenwood, N. N. and Earnshaw, A. 1997. Titanium, Zirconium and Hafnium. *In:* GREENWOOD, N. N. and EARNSHAW, A. (eds.) *Chemistry of the Elements (Second Edition).* Oxford: Butterworth-Heinemann.

Guo, X., Rao, L., Wang, P., Wang, C., Ao, Y., Jiang, T. and Wang, W., 2018. Photocatalytic Properties of P25-Doped TiO$_2$ Composite Film Synthesized Via Sol–Gel Method on Cement Substrate. *Journal of Environmental Sciences,* 66, pp.71- 80.

Gyorgyey, A., Janovak, L., Adam, A., Kopniczky, J., Toth, K. L., Deak, A., Panayotov, I., Cuisinier, F., Dekany, I. and Turzo, K., 2016. Investigation of the In Vitro Photocatalytic Antibacterial Activity of Nanocrystalline TiO$_2$ and Coupled TiO$_2$/Ag Containing Copolymer on the Surface of Medical Grade Titanium. *Journal of Biomaterials Applications,* 31, pp.55-67.

Halaciuga, L., Laplante, S. and Goia, D. V., 2011. Precipitation of Dispersed Silver Particles Using Acetone as Reducing Agent. *Journal of Colloid and Interface Science,* 354, pp.620-623.

Halin, D. S. C., Abdullah, M. M. A., Mohd Salleh, M. a. A., Mahmed, N., Mohd Sakeri, A. N. and Abdul Razak, K., 2018. Synthesis and Characterization of Ag/TiO$_2$ Thin Film via Sol-Gel Method. *Solid State Phenomena,* 273, pp.140-145.

Halin, D. S. C., Razak, K. A., Mohd Salleh, M. a. A., Ramli, M. I. I., Abdullah, M. M. A., Azhari, A. W., Nogita, K., Yasuda, H., Nabialek, M. and Wyslocki, J. J., 2021. Microstructure Evolution of Ag/TiO$_2$ Thin Film. *Magnetochemistry,* 7, pp.2-10.

Haq, A. U., Saeed, M., Khan, S. G. and Ibrahim, M. 2022. Photocatalytic Applications of Titanium Dioxide (TiO$_2$). Titanium Dioxide. Advances and Applications. IntechOpen.

Hari, M., Joseph, S. A., Mathew, S., Radhakrishnan, P. and Nampoori, V. P. N., 2012. Band Gap Tuning and Nonlinear Optical Characterization of Ag:TiO₂ Nanocomposites. *Journal of Applied Physics,* 112, pp.1-8.

Harikishore, M., Sandhyarani, M., Venkateswarlu, K., Nellaippan, T. A. and Rameshbabu, N., 2014. Effect of Ag Doping on Antibacterial and Photocatalytic Activity of Nanocrystalline TiO₂. *Procedia Materials Science,* 6, pp.557-566.

Hasmaliza, M., Foo, H. S. and Mohd, K., 2016. Anatase as Antibacterial Material in Ceramic Tiles. *Procedia Chemistry,* 19, pp.828-834.

He, J., Du, Y. E., Bai, Y., An, J., Cai, X., Chen, Y., Wang, P., Yang, X. and Feng, Q., 2019. Facile Formation of Anatase/Rutile TiO₂ Nanocomposites with Enhanced Photocatalytic Activity. *Molecules,* 24, pp.1-14.

Hidayat, A., Taufiq, A., Supardi, Z. A. I., Jayadininggar, S. M., Sa'adah, U., Astarini, N. A., Suprayogi, T. and Diantoro, M., 2021. Synthesis and Characterization of TiO₂/ZnO-Ag@TiO₂ Nanocomposite and Their Performance as Photoanode of Organic Dye-Sensitized Solar Cell. *Materials Today: Proceedings,* 44, pp.3395-3399.

Horkavcová, D., Zmeškal, Z., Šanda, L., Zlámalová Cílová, Z., Jablonská, E. and Helebrant, A., 2015. Preparation of Titania Sol-Gel Coatings Containing Silver in Various Forms and Measuring of Their Bactericidal Effects Against E.Coli. *Ceramics – Silikáty,* 59, pp.238-243.

Hou, W. C., Stuart, B., Howes, R. and Zepp, R. G., 2013. Sunlight-Driven Reduction of Silver Ions by Natural Organic Matter: Formation and Transformation of Silver Nanoparticles. *Environmental Science & Technology,* 47, pp.7713 - 7721.

Hu, B., Yin, N., Yang, R., Liang, S., Liang, S. and Faiola, F., 2020. Silver Nanoparticles (AgNPs) and AgNO₃ Perturb the Specification of Human Hepatocyte-Like Cells and Cardiomyocytes. *Sci Total Environ,* 725, pp.1-10.

Ibrahim, A. B., Oladimeji, O. and Festus, O., 2017. Effect of Salt Water on the Comprehensive Strength of Ceramic Powder Concrete. *American Journal of Engineering Research (AJER),* 6, pp.158 - 163.

Irfan, F., Tanveer, M. U., Moiz, M. A., Husain, S. W. and Ramzan, M., 2022. TiO₂ as an Effective Photocatalyst Mechanisms, Applications, and Dopants: A Review. *The European Physical Journal B,* 95, pp.184.

Jiang, D., Otitoju, T. A., Ouyang, Y., Shoparwe, N. F., Wang, S., Zhang, A. and Li, S., 2021. A Review on Metal Ions Modified TiO_2 for Photocatalytic Degradation of Organic Pollutants. *Catalysts,* 11, pp.1-82.

Joao, F., Gomes, J. F., Lopes, A., Gmurek, M., Quinta-Ferreira, R. M. and Martins, R. C., 2019. Study of the Influence of the Matrix Characteristics Over the Photocatalytic Ozonation of Parabens using Ag-TiO_2. *Science of the Total Environment,* 646, pp.1468-1477.

Ju, C., 2019. Photocatalytic Degradation of TOC by Ag/TiO_2 Coated on Light Ceramic. *Procedia Manufacturing,* 37, pp.267-272.

Kamat, P. V., 2002. Photophysical, Photochemical and Photocatalytic Aspects of Metal Nanoparticles. *Journal of Physical Chemistry B,* 106, pp.7729 – 7744.

Kamrosni, A. R., Dewi Suryani, C. H., Azliza, A., Mohd. Mustafa, A. B. A., Mohd. Arif Anuar, M. S., Norsuria, M., Chobpattana, V., Kaczmarek, L., Jeż, B. and Nabiałek, M., 2022. Microstructural Studies of Ag/TiO_2 Thin Film; Effect of Annealing Temperature. *Arch. Metall. Mater,* 67, pp.241-245.

Kamrosni, A. R., Halin, D. S. C., Azliza, A., Mohd. Mustafa, A. B. A., Mohd. Arif Anuar, M. S., Norsuria, M., Ramli, M. M. and Sepeai, S., 2019. Mesoporous Structure of Doped and Undoped PEG on Ag/TiO_2 Thin Film. *IOP Conference Series: Materials Science and Engineering,* 551, pp.1-7.

Kay, A. and Grätzel, M., 1996. Low Cost Photovoltaic Modules Based on Dye Sensitized Nanocrystalline Titanium Dioxide and Carbon Powder. *Solar Energy Materials and Solar Cells,* 44, pp.99-117.

Kaygusuz, M. K., Lkhagvajav, N., Yaşa, I. and Çelik, E., 2016. Antimicrobial Nano-Ag-TiO_2 coating for Lining Leather. *Romanian Biotecnological Letters,* 21, pp.11866-11874.

Keyvanloo, T., Rad, R. Y. and Asadian, K., 2016. Effect of Formation of $Ag_2Ti_4O_9$ Phase on Photocatalytic Activity of Ag-TiO_2 Nanocomposite. *International Journal of Engineering (IJE), TRANSACTIONS B: Applications,* 29, pp.663-668.

Khan, I., Saeed, K., Zekker, I., Zhang, B., Hendi, A. H., Ahmad, A., Ahmad, S., Zada, N., Ahmad, H., Shah, L. A., Shah, T. and Ibrahim, K., 2022. Review on Methylene Blue: Its Properties, Uses, Toxicity and Photodegradation. *Water,* 14, pp.1-30.

Khojasteh, F., Mersagh, M. R. and Hashemipour, H., 2021. The Influences of Ni, Ag-Doped TiO_2 and SnO_2, Ag-doped SnO_2/TiO_2 Nanocomposites on Recombination Reduction in Dye Synthesized Solar Cells. *Journal of Alloys and Compounds,* 890, pp.1-13.

Kien, K. D. T., Minh, D. Q., Minh, H. N. and Nhi, N. V. U., 2023. Synthesis Of TiO_2–SiO_2 from Tetra-N-Butyl Orthotitanate and Tetraethyl Orthosilicate by the Sol-Gel Method Applied As a Coating on the Surface of Ceramics. *Ceramics-Silikáty,* 67, pp.58-63.

Kien, K. D. T., Nhi, N. V. U., Minh, H. N. and Minh, D. Q., 2022. Optical properties of the Bi_2O_3-B_2O_3-ZnO glass system combined with TiO_2 or Ag/TiO_2. *Journal of Ceramic Processing Research,* 23, pp.350 - 355.

Kim, H., An, J., Maeng, S., Shin, J. S., Choi, E. and Yun, J. Y., 2022. Decomposition Characteristics of the TTIP (Tetraisopropyl Orthotitanate) Precursor for Atomic Layer Deposition. *Materials (Basel),* 15.

Komaraiah, D., Radha, E., Sivakumar, J., Reddy, M. V. and Sayanna, R., 2020. Photoluminescence and Photocatalytic Activity of Spin Coated Ag^+ Doped Anatase TiO_2 Thin Films. *Optical Materials,* 108, pp.1-14.

Kulczyk-Malecka, J., Kelly, P. J., West, G., Clarke, G. C. B., Ridealgh, J. A., Almtoft, K. P., Greer, A. L. and Barber, Z. H., 2014. Investigation of Silver Diffusion in $TiO_2/Ag/TiO_2$ Coatings. *Acta Materialia,* 66, pp.396-404.

Lee, M. S., Hong, S. S. and Mohseni, M., 2005. Synthesis of Photocatalytic Nanosized TiO_2-Ag Particles with Sol-Gel Method Using Reducing Agent. *Journal of Molecular Catalysis A: Chemical,* 242, pp.135-140.

Leong, K. H., Gan, B. L., Ibrahim, S. and Saravanan, P., 2014. Synthesis of Surface Plasmon Resonance (SPR) Triggered Ag/TiO_2 Photocatalyst for Degradation of Endocrine Disturbing Compounds. *Applied Surface Science,* 319, pp.128-135.

Li, S., Li, D., Zhang, Q. Y. and Tang, X., 2016. Surface Enhanced Raman Scattering Substrate with High-Density Hotspots Fabricated by Depositing Ag Film on TiO_2-Catalyzed Ag Nanoparticles. *Journal of Alloys and Compounds,* 689, pp.439-445.

Li, X., Pustulka, S., Pedu, S., Close, T., Xue, Y., Richter, C. and Taboada-Serrano, P., 2018. Titanium dioxide Nanotubes as Model Systems for Electrosorption Studies. *Nanomaterials (Basel),* 8, pp.1-13.

Liaqat, M. A., Hussain, Z., Khan, Z., Akram, M. A. and Shuja, A., 2020. Effects of Ag Doping on Compact TiO_2 Thin Films Synthesized Via One-Step Sol–Gel Route and

Deposited by Spin Coating Technique. *Journal of Materials Science: Materials in Electronics,* 31, pp.1-10.

Lidiaine, M. S., Werick, A. M., Marcela, D. F., Karen, A. B., Roberto, M. P., Antonio, O. T. P. and Antonio, E. H. M., 2015. Structural Characterization of Ag-doped TiO_2 with Enhanced Photocatalytic. *RSC Advances,* 5, pp.103752-103759.

Linak, E. and Inoguchi, Y., 2005. Chemical Economics Handbook: Titanium Dioxide. *SRI Consulting, Menlo Park.*

Ling, L., Feng, Y., Li, H., Chen, Y., Wen, J., Zhu, J. and Bian, Z., 2019. Microwave Induced Surface Enhanced Pollutant Adsorption and Photocatalytic Degradation on Ag/TiO_2. *Applied Surface Science,* 483, pp.772-778.

Liua, C., Genga, L., Yua, Y., Zhanga, Y., Zhaob, B. and Zhaoc, Q., 2018. Mechanisms of the Enhanced Antibacterial Effect of $Ag-TiO_2$ Coatings. *Biofouling,* 34, pp.190-199.

Loffler, F., 2000. Functional Metal-Based Coatings on Ceramic Substrates. *Surface and Coatings Technology,* 132, pp.222-227.

Lopez Ortiz, A., Melendez Zaragoza, M., Salinaz Gutierrez, J., Marques Da Silva Paula, M. and Collins-Martinez, V., 2015. Silver Oxidation State Effect on the Photocatalytic Properties of Ag Doped TiO_2 for Hydrogen Production Under Visible Light. *International Journal of Hydrogen Energy,* 40, pp.17308-17315.

Lu, Z., Zhou, H. F., Liao, J. J., Yang, Y. Y., Wang, K., Che, L. M., He, N., Chen, X. D., Song, R., Cai, W. F., Liu, H. and Wu, X. E., 2019. A Facile Dopamine Assisted Method for the Preparation of Antibacterial Surfaces Based on Ag/TiO_2 Nanopartilces. *Appl Surf Sci,* 481, pp.1270–1276.

Luttrell, T., Halpegamage, S., Tao, J., Kramer, A., Sutter, E. and Batzill, M., 2014. Why is Anatase a Better Photocatalyst than Rutile? - Model Studies on Epitaxial TiO_2 Films. *Scientific Reports,* 4, pp.1-8.

Mahdieh, Z. M., Shekarriz, S. and Taromi, F. A., 2021. The Effect of Silver Concentration on $Ag-TiO_2$ Nanoparticles Coated Polyester/Cellulose Fabric by In situ and Ex situ Photo-reduction Method – A Comparative Study. *Fibers and Polymers,* 22, pp.87-96.

Malini, T. P., Ramesh, A., Selvi, J. A., Arthanareeswari, M. and Kamaraj, P., 2016. Kinetic Modeling of Photocatalytic Degradation of Alachlor Using TiO_2 (Degussa P25) in Aqueous Solution. *Orient J Chem,* 32, pp.3165 - 3173.

Manicone, P. F., Iommetti, P. R. and Raffaelli, L., 2007. An overview of zirconia ceramics: Basic properties and clinical applications *Journal of Dentistry,* 35, pp.819-826.

Mansoori, G. A., Mohazzabi, P., Mccormack, P. and Jabbari, S., 2007. Nanotechnology in Cancer Prevention, Detection and Treatment: Bright Future Lies Ahead. *World Review of Science, Technology and Sustainable Development,* 4, pp.226-257.

Mao, H., Fei, Z., Bian, C., Chen, S. and Y., Q., 2019. Facile Synthesis of High-Performance Photocatalysts Based on Ag/TiO$_2$ Composites. *Ceramics International,* 45, pp.12586-12589.

Markowska-Szczupak, A., Wei, Z. and Kowalska, E., 2020. The Influence of the Light Activated Titania P25 on Human Breast Cancer Cells. *Catalysts,* 10, pp.238.

Mazheika, A. S., Bredow, T., Matulis, V. E. and Ivashkevich, O. A., 2011. Theoretical Study of Adsorption of Ag Clusters on the Anatase TiO$_2$ (100) Surface. *The Journal of Physical Chemistry C,* 115, pp.17368-17377.

Mechiakh, R., Meriche, F., Kremer, R., Bensaha, R. and Boundine, B. A., 2007. TiO$_2$ Thin Films Prepared by Sol-Gel Method for Waveguiding Applications: Correlation Between The Structural and Optical Properties. *Optical Materials,* 30, pp.645-51.

Meydanju, N., Pirsa, S. and Farzi, J., 2022. Biodegradable Film Based on Lemon Peel Powder Containing Xanthum and TiO$_2$-Ag Nanoparticles: Investigation of Physicochemical and Antibacterial Properties. *Polymer testing,* 106, pp.1-12.

Michela D'alessandro, M., Lanterna, N., Scaiano, A. E. and Juan, C., 2016. Improving the Sunscreen Properties of TiO$_2$ Through an Understanding of Its Catalytic Properties. *Acs Omega,* 1, pp.464-469.

Mills, A., Hill, C. and Robertson, P. K. J., 2012. Overview of the Current ISO Tests for Photocatalytic Materials. *Journal of Photochemistry and Photobiology A: Chemistry,* 237, pp.7 - 23.

Milošević, I., Rtimi, S., Jayaprakash, A., Van Driel, B., Greenwood, B., Aimable, A., Senna, M. and Bowen, P., 2018. Synthesis and Characterization of Fluorinated Anatase Nanoparticles and Subsequent N-Doping for Efficient Visible Light Activated Photocatalysis. *Colloids Surf B: Biointerfaces,* 171, pp.445-450.

Mîndroiu, V. M., Stoian, A. B., Irodia, R., Trusca R. and Vasile, E., 2023. Titanium Dioxide Thin Films Produced on FTO Substrate Using the Sol–Gel Process: The Effect of the Dispersant on Optical, Surface and Electrochemical Features. *Materials,* 16, pp.1-18.

Mogal Sajid, I., Gandhi Vimal, G., Mishra, M., Tripathi, S., Shripathi, T., Joshi, P. A. and Shah, D. O., 2014. Single-Step Synthesis of Silver-Doped Titanium Dioxide: Influence of Silver on Structural, Textural, and Photocatalytic Properties. *Industrial & Engineering Chemistry Research,* 53, pp.5749-5758.

Moongraksathuma, B. and Chen, Y. W., 2018. Anatase TiO_2 Co-Doped with Silver and Ceria for Antibacterial Application. *Catalysis Today,* 310, pp.68-74.

Musa, M., Juoi, J. M., Rosli, Z. M. and Johari, N. D., 2017a. Characterization of TiO_2 Coating Deposited on Ceramic Substrate. *Solid State Phenomena,* 264, pp.38 - 41.

Musa, M., Juoi, J. M., Zulkifli, M. R. and Johari, N. D., 2017b. Effect of Degussa P25 on the Morphology, Thickness and Crystallinity of Sol-Gel TiO_2 Coating. *Solid State Phenomena,* 268, pp.224-228.

Musa, M. A., Juoi, J. M., Rosli, Z. M., Johari N.D and Moriga, T., 2018. Effect of Degussa P25 Content On The Deposition of TiO_2 Coating On Ceramic Substrate. *Journal of Advanced Manufacturing Technology,* pp.111-123.

Nagaraj, K., Thankamuniyandi, P., Kamalesu, S., Lokhandwala, S., Parekh, N. M., Sakthinathan, S., Chiu, T. W. and Karuppiah, C., 2023. Green Synthesis, Characterization and Efficient Photocatalytic Study of Hydrothermal-Assisted $Ag@TiO_2$ Nanocomposites. *Inorganic Chemistry Communications,* 148, pp.1 - 8.

Nguyen, H. H., Park, J., Kang, S. and Kim, M., 2015. Surface Plasmon Resonance: A Versatile Technique for Biosensor Applications. *Sensors,* 15, pp.10481-10510.

Nicoara, A. I., Ene, V. L., Voicu, B. B., Bucur, M. A., Neacsu, I. A., Vasile, B. S. and Iordache, F., 2020. Biocompatible Ag/Fe Enhanced TiO_2 Nanoparticles as an Effective Compound in Sunscreens. *Nanomaterials (Basel),* 10, pp.1-14.

Ningthoukhongjam, P. and Nair, R. G., Tuning the Photocatalytic Performance of Degussa P25 through Phase Ratio Optimization. Proceedings of the International Conference on Advanced Materials, 2019. pp.1-6.

Noberi, C., Kaya, F. and Kaya, C., 2016. Synthesis, Structure and Characterization of Hydrothermally Synthesized Ag-TiO$_2$ Nano-Structures onto Ni Filters Ni Filters Using Electrophoretic Deposition. *Ceramics International,* 42, pp.17202-17209.

Noreena, Z., Khalid, N. R., Abbasic, R., Javeda, S., Ahmadd, I. and Bokharia, H., 2019. Visible Light Sensitive Ag/TiO$_2$/Graphene Composite as a Potential Coating Material For Control of Campylobacter Jejuni. *Materials Science & Engineering C,* 98, pp.125-133.

Nour, B., Nassima, L., Razika, Z. and Tahar, S., 2017. A Comparative Study of the Activity of TiO$_2$ Degussa P25 and Millennium PCs in the Photocatalytic Degradation of Bromothymol Blue. *International Journal of Chemical Reactor Engineering,* 16, pp.1-19.

Nurhamizah, A. R., Zulkifli, M. R. and Juoi, J. M., 2016a. Effect of Additives on the Characteristic of Ag-TiO$_2$ Coating Deposited on Specially Made Unglazed Ceramic Tile. *Key Eng. Mater.,* 694, pp.160 - 164.

Nurhamizah, A. R., Zulkifli, M. R., Juoi, J. M. and Musa, M. A., 2016b. Effect of Dipping Numbers on the Crystalline Phase and Microstructure of Ag-TiO$_2$ Coating. *Key Engineering Materials,* 694, pp.133-137.

Nyankson, E., Awuzah, D., Tiburu, E. K., Efavi, J. K., Tuffoura, B. A. and Paemkac, L., 2022. Curcumin Loaded Ag–TiO$_2$-Halloysite Nanotubes Platform for Combined Chemo-Photodynamic Therapy Treatment of Cancer Cells. *RSC Adv,* 12, pp.33108–33123.

Onna, D., Fuentes, K. M., Spedalieri, C., Perullini, M., Claudia Marchi, M. C., Alvarez, F., Candal, R. J. and Bilmes, S. A., 2018. Wettability, Photoactivity, and Antimicrobial Activity of Glazed Ceramic Tiles Coated with Titania Films Containing Tungsten. *ACS Omega,* 3, pp.17629-17636.

Page, K. 2009. *Photocatalytic Thin Films.* Doctor of Philosophy, University College London.

Parastar, S., Nasseri S., Borji, H. S., Fazlzadeh., M., Mahvi, A., H.,, Javadi, A. H. and Gholami, M., 2013. Application of Ag-doped TiO$_2$ Nanoparticle Prepared by Photodeposition Method for Nitrate Photocatalytic Removal from Aqueous Solutions. *Desalination and Water Treatment,* 51, pp.7137-7144.

Pohan, L. A. G., Kambiré, O., Nasir, M. and Ouattara, L., 2020. Photocatalytic and Antimicrobial Properties of [AgTiO$_2$]:[Clay] Nanocomposite Prepared with Clay Different Ratios. *Modern Research in Catalysis,* 9, pp.47-61.

Prakash, J., Cho, J. and Mishra, Y. K., 2022. Photocatalytic TiO_2 Nanomaterials as Potential Antimicrobial and Antiviral Agents: Scope Against Blocking the SARS-COV-2 Spread. *Micro and Nano Engineering,* 14, pp.1-16.

Ramchiary, A., Samdarshi, S. K. and Shripathi, T., 2016. Hydrogenated Mixed Phase Ag/TiO_2 Nanoparticle - A Super-Active Photocatalyst Under Visible Radiation with Multi-Cyclic Stability. *Solar Energy Materials and Solar Cells,* 155, pp.117-127.

Ranogajec, J., Radeka, M., Backalic, Z., Škapin, A. and Zoric, D., 2010. Photocatalytic and Superhydrophilic Phenomena of TiO_2 Coated Clay Roofing Tiles. *Chemical Industry & Chemical Engineering Quarterly,* 16, pp.117-126.

Razak, K. A., Halin, D. S. C., Abdullah, M. M. A., Azani, A., Salleh, M. A. A. M., Mahmed, N. and Chobpattana, V., 2020. Self - Cleaning Property of Ag/TiO_2 Thin Film. *Materials Science Forum,* 1010, pp.397-404.

Regonini, D., Bowen, C. R., Jaroenworaluck, A. and Stevens, R., 2013. A Review of Growth Mechanism, Structure and Crystallinity of Anodized TiO_2 Nanotubes. *Materials Science and Engineering: R,* 74, pp.377-406.

Reinosa, J. J., Enríquez, E., Fuertes, V., Liu, S., Menéndez, J. and Fernández, J. F., 2022. The Challenge of Antimicrobial Glazed Ceramic Surfaces. *Ceramics International,* 48, pp.7393-7404.

Rejek, M., Damszel, J. G. and Schmidt, B., 2021. Synthesis, Characterization, and Evaluation of Degussa P25/Chitosan Composites for the Photocatalytic Removal of Sertraline and Acid Red 18 from Water. *Journal of Polymers and the Environment,* 29, pp.3660-3667.

Rheima, A. H., Hussain, D. H. and Abed, H. J. 2020. Fabrication of a New Photo-Sensitized Solar Cell Using TiO_2/ZnO Nanocomposite Synthesized Via a Modified Sol-Gel Technique. *2nd International Scientific Conference of Al-Ayen University.* IOP Publishing.

Rtimi, S., 2017. Indoor Light Enhanced Photocatalytic Ultra-Thin Films on Flexible Non-Heat Resistant Substrates Reducing Bacterial Infection Risks. *Catalysts,* 7, pp.1-17.

Sangchay, W., Phoempoon, P. and Ubonchonlakat, K., 2018. Effect of Ag Doped on Photocatalytic and Antibacterial Activity of TiO_2 Thin Films. *Kasem Bundit Engineering,* 8, pp.341-353.

Sangchay, W. and Rattanakun, T. 2018. Photocatalytic, Antibacterial and Self-Cleaning Properties of TiO_2 and Ag Doped. *The 4th Rajamangala University of Technology International Conference.*

Sangchay, W., Sikonga, L. and Kooptarnonda, K., 2012. Comparison of Photocatalytic Reaction of Commercial P25 and Synthetic TiO_2-AgCl Nanoparticles. *Procedia Engineering,* 32, pp.590-596.

Saraswati, M., Permadani, R. L. and Slamet, 2019. The Innovation of Antimicrobial and Self-Cleaning Using Ag/TiO_2 Nanocomposite Coated on Cotton Fabric for Footwear Application. *Materials Science and Engineering,* 509, pp.1-9.

Šauta, O. J., Lavrenčič, S. U. and Peter, B., 2008. Enhancement of Photocatalytic Activity of Sol-gel TiO_2 Thin Films with P25. *Acta Chimica Slovenica,* 55, pp.889-896.

Scandola, L., Latorrata, S., Matarrese, R., Cristiani, C. and Nova, I., 2019. Effect of Thickness and Cracking Phenomena on the Photocatalytic Performances of Ti/TiO_2 Photoanodes Produced by Dip Coating. *Materials Chemistry and Physics,* 234, pp.1-8.

Shakeri, A., Yip, D., Badv, M., Imani, S. M., Sanjari, M. and Didar, T. F., 2018. Self-Cleaning Ceramic Tiles Produced Via Stable Coating of TiO_2 Nanoparticles. *Materials Chemistry and Physics,* 11, pp.1-16.

Sharma, M., Pathak, M. and Kapoor, P., 2018. The Sol-Gel Method: Pathway to Ultrapure and Homogeneous Mixed Metal Oxide Nanoparticles. *Asian Journal Chemical,* 30, pp.1405-1412.

Sharma, M., Urone, P. P., Dirks, K. and Hoinrichs, R. 2012. *College Physics,* 1st ed. Texas, OpenStax College.

Sharma, R., Sarkar, A., Jha, R., Sharma, A. K. and Sharma, D., 2019. Sol-gel Mediated Synthesis of TiO_2 Nanocrystals: Structural, Optical, and Electrochemical Properties. *Applied Ceramics Technology,* 17, pp.1400-1409.

Shieh, Y., Huang, J. J. and Chen, J. H., 2015. Antibacterial Activity of Ag/TiO_2 Nanocomposite Films on Ceramic Plate. *Proceedings of the World Congress on New Technologies*, pp.1-8.

Silva, A. F. R., Mohallem, N. D. S. and Viana, M. M., 2017. Titanium dioxide (TiO_2) and Silver/Titanium Dioxide (Ag/TiO_2) Thin Films with Self-Cleaning Properties. *Advanced Materials Letters,* 8, pp.444-448.

Simona, D. N., Moreno, B. and Federica, B., 2013. Self-Cleaning and Antibacteric Ceramic Tile Surface. *International Journal of Applied Ceramic Technology,* 10, pp.949-956.

Singh, J., Sahu, K., Pandey, A., Kumar, M., Tapas Ghosh, T., Satpati, B., Som, T., Varma, S., Avasthi, D. K. and Mohapatra, S., 2017. Atom Beam Sputtered $Ag-TiO_2$ Plasmonic Nanocomposite Thin Films for Photocatalytic Applications. *Applied Surface Science,* 411, pp.347–354.

Smestad, G., Bignozzi, C. and Argazzi, R., 1994. Testing of Dye Sensitized TiO_2 Solar Cells I: Experimental Photocurrent Output and Conversion Efficiencies. *Solar Energy Materials and Solar Cells,* 32, pp.259-272.

Sobana, N., Muruganadhan, M. and Swaminathan, M., 2006. Nano-Ag Particles Doped TiO_2 for Efficient Photodegradation of Direct Azo Dyes. *J. Mol. Catalyst. A Chem.,* 258, pp.124-132.

Sreethawong, T., Ngamsinlapasathian, S. and Yoshikawa, S., 2014. Positive Role of Incorporating P-25 TiO_2 to Mesoporous-Assembled TiO_2 Thin Films for Improving Photocatalytic Dye Degradation Efficiency. *Journal of Colloid and Interface Science,* 430, pp.184–192.

Supriyanto, A., Saputri, D. G., Ahmad, M. K., Ramelan, A. H. and Ramadhani, F., 2021. Significant Efficiency Improvement of TiO_2:LEG4-Ag Layer Dye Sensitized Solar Cells by Incorporating Small Concentration of Ag. *Optik - International Journal for Light and Electron Optics,* 231, pp.1-9.

Suwarnkar, M. B., Dhabbe, R. S., Kadam, A. N. and Garadkar, K. M., 2013. Enhaned Photocatalytic Activity of Ag Doped TiO_2 Nanoparticles Synthesized by a Microwave Assisted Method. *Ceramics International,* 40, pp.5489-5496.

Suwei, Z., Bo-Ping, Z., Shun, L., Zhicheng, H., Chushu, Y. and Huiying, W., 2017. Enhanced Photocatalytic Activity in Ag-Nanoparticle-Dispersed $BaTiO_3$ Composite Thin Films: Role of Charge Transfer. *Journal of Advanced Ceramics,* 6, pp.1-10.

Sze-Mun, L., Jin-Chung, S., Ahmad Zuhairi, A. and Abdul, M., 2014. Photocatalytic TiO_2/Carbon Nanotube Nanocomposites for Environmental Applications: An Overview and Recent Developments. *Fullerenes, Nanotubes and Carbon Nanotubes,* 22, pp.471-509.

Tallósy, S. P., Janovák, L., Nagya, E., Deák, A., Juhász, A., Csapóc, E., Buzásd, N. I. and Dékányc, I., 2016. Adhesion and Inactivation of Gram-Negative and Gram-Positive Bacteria on Photoreactive TiO_2/Polymer and Ag–TiO_2/Polymer Nanohybrid Films. *Applied Surface Science,* 371, pp.139–150.

Teixeira, S. and Bernardin, A. M., 2009. Development of TiO_2 White Glazes for Ceramic Tiles. *Dyes and Pigments,* 80, pp.292-296.

Terohid, S. A. A., Heidari, S., Jafari, A. and Asgary, S., 2018. Effect of Growth Time on Structural, Morphological and Electrical Properties of Tungsten Oxide Nanowire. *Applied Physics A,* 124, pp.567.

Thamer, N. H. and Hatem, O. A., 2022. Synthesis and Characterization of TiO_2 – Ag-Cellulose Nanocomposite and Evaluation of Photocatalytic Degradation Efficiency for Congo Red. *Earth and Environment Science,* 1029, pp.1-11.

Thi-Tuyet, H. N., Thi-Kim, T. A., Van, S., N., and Nguyen, T. V., 2016. Antibacterial Activities of Gel-Derived Ag-TiO_2-SiO_2 Nanomaterials Under Different Light Irradiation. *AIMS Materials Science,* 3, pp.339-348.

Thi-Tuyet, H. N. and Van, S. N., 2015. Bactericidal Activities and Synergistic Effects of Ag-TiO_2 and Ag-TiO_2-SiO_2 Nanomaterials Under UV-C and Dark Conditions. *Int. J. Nanotechnol.,* 12, pp.367-379.

Thiruvenkatachari, R., Vigneswaran, S. and Moon Ii, S., 2008. A Review on UV/TiO_2 Photocatalytic Oxidation Process (Journal Review). *Korean Journal of Chemical Engineering,* 25, pp.64-72.

Tijani, J. O., Totito, T. C., Fatoba, O. O., Babajide, O. O. and Petrik, L. F., 2017. Synthesis, Characterization and Photocatalytic Activity of Ag Metallic Particles Deposited Carbon-Doped TiO_2 Nanocomposites Supported on Stainless Steel Mesh. *Journal of Sol-Gel Science and Technology,* 83, pp.207-222.

Tryba, B., Piszcz, M. and Morawski, A. W., 2010. Photocatalytic and Self-Cleaning Properties of Ag-Doped TiO_2. *The Open Materials Science Journa,* 4, pp.5-8.

Tsai, C. Y., Liu, C. W., Hsi, H. C., Lin, K. S., Lina, Y. W. and Lai, L. C., 2019. Synthesis of Ag-Modified TiO_2 Nanotube and Its Application in Photocatalytic Degradation of Dyes and Elemental Mercury. *J. Chem Technol Biotechnol,* 94, pp.3251-3262.

Tung-Yueh, L., Lay-Gaik, T., Chao-Kai, H. and Ying-Chieh, L., 2016. A Study of Roughness Improvement of Al$_2$O$_3$ Substrates Using Sol-Gel Method. *Procedia Engineering,* 141, pp.108-114.

Ubonchonlakat, K., Sikong, L. and Kooptarnond, K., 2008. Efffect of Calcinations Temperature on Photocatalytic Activity of Ag-doped TiO$_2$ Coated on Tile Substrate. *J. Nat. Sci.,* 7, pp.43-50.

Ulrike, D., 2003. The Surface Science of Titanium Dioxide. *Surface Science Reports,* 48, pp.53-229.

Vakhrushev, A. Y., Boitsova, T. B., Gorbunova, V. V. and Stozharov, V. M., 2017. Effect of Silver Additions on the Structural Properties and Phase Composition of TiO$_2$/Ag Composites. *Inorganic Materials,* 53, pp.171-175.

Vasileva, P., Donkova, B., Karadjova, I. and Dushkin, C., 2011. Synthesis of Starch-Stabilized Silver Nanoparticles and Their Application as a Surface Plasmon Resonance-Based Sensor of Hydrogen Peroxide. *Colloids and Surfaces A: Physicochemical and Engineering Aspects,* 382, pp.203-210.

Vitanov, P., Milanova, M., Dikov, H. and Petkov, N., 2023. Application of TiO$_2$/Ag/TiO$_2$ as an Ohmic Contact to an AlGaAs Layer in a GaAs Solar Cell. *Energies,* 16, pp.1-10.

Vladkova, T., Angelov, O., Stoyanova, D., Gospodinova, D., Gomes, L., Soares, A., Mergulhao, F. and Ivanova, I., 2020. Magnetron Co-Sputtered TiO$_2$/SiO$_2$/Ag Nanocomposite Thin Coatings Inhibiting Bacterial Adhesion and Biofilm Formation. *Surface & Coatings Technology,* 384, pp.1-7.

Wang, D. and Bierwagen, G. P., 2009. Sol–gel Coatings on Metals for Corrosion Protection. *Progress in Organic Coatings,* 64, pp.327-338.

Wang, G., Xu, L., Zhang, J., Yin, T. and Han, D., 2012. Enhanced Photocatalytic Activity of TiO$_2$ Powders (P25) Via Calcination Treatment. *International Journal of Photoenergy,* 2012, pp.1-9.

Wang, K., Janczarek, M., Wei, Z., Raja-Mogan, T., Endo-Kimura, M., Khedr, T. M., Ohtani, B. and Kowalska, E., 2019. Morphology-and Crystalline Composition-governed Activity of Titania-Based Photocatalysts: Overview and Perspective. *Catalysts,* 9, pp.1054.

Wu, L., Pei, X., Mei, M., Li, Z. and Lu, S., 2022. Study on Photocatalytic Performance of Ag/TiO$_2$ Modified Cement Mortar. *Materials,* 15, pp.4031.

Wu, X. 2021. Applications of Titanium Dioxide Materials. *Titanium Dioxide - Advances and Applications.* IntechOpen.

Xin, B., Jing, L., Ren, Z., Wang, B. and Fu, H., 2005. Effects of Simultaneously Doped and Deposited Ag on the Photocatalytic Activity and Surface States of TiO$_2$. *The Journal of Physical Chemistry B,* 109, pp.2805-2809.

Xinggang, H., Dong, M., Huiyan, M., Yukai, A., Xinlei, Z., Jianhua, D., Dejun, L. and Bin, L., 2015. Antibacterial Ability of Ag–TiO$_2$ Nanotubes Prepared by Ion Implantation and Anodic Oxidation. *Materials Letters,* 161, pp.309-312.

Xu, M., Gao, Y., Moreno, E. M., Kunst, M., Muhler, M., Wang, Y., Idriss H. and Wöll, C., 2011. Photocatalytic Activity of Bulk TiO$_2$ Anatase and Rutile Single Crystals Using Infrared Absorption Spectroscopy. *Physical Review Letters,* 106, pp.1-4.

Yazid, S. A., Rosli, Z. M. and Juoi, J. M., 2019. Effect of Titanium (IV) IIsopropoxide Molarity on the Crystallinity and Photocatalytic Activity of Titanium Dioxide Thin Film Deposited Via Green Sol–Gel Route. *Journal of Materials Research and Technology,* 8, pp.1434-1439.

Yiming, C., Yu, B., Qingjiang, Y., Yueming, C., Shi, L., Dong, S., Feifei, G. and Peng, W., 2009. Dye-Sensitized Solar Cells with a High Absorptivity Ruthenium Sensitizer Featuring a 2-(Hexylthio) Thiophene Conjugated Bipyridine. *The Journal of Physical Chemistry C,* 113, pp.6290-6297.

Ying, L., Shaohua, W. and Pengfeng, G., 2016. Effects of Ag on the Photocatalytic Activity of Multiple Layer TiO$_2$ Films. *Materials Technology,* 32, pp.46-51.

Yu, B., Man Leung, K. M., Guo, Q., Lau, W. M. and Yang, J., 2011. Synthesis of Ag–TiO$_2$ Composite Nano Thin Film for Antimicrobial Application. *Nanotechnology,* 22, pp.1-10.

Žerjav, G., Žižek, K., Zavašnik, J. and Pintar, A., 2022. Brookite vs. Rutile vs. Anatase: What`s Behind Their Various Photocatalytic Activities? *Journal of Environmental Chemical Engineering,* 10, pp.1-18.

Zhang, H. and Banfield, J. F., 1999. New Kinetic Model for the Nanocrystalline Anatase to Rutile Transformation Revealing Rate Dependence on Number of Particles. *American Mineralogist,* 84, pp.528-535.

Zhang, H. and Banfield, J. F., 2000. Understanding Polymorphic Phase Transformation During Growth of Nanocrystalline Aggregates: Insights from TiO_2. *Journal of Physical Chemistry B,* 104, pp.3481-3487.

Zhang, J., Tian, B., Wang, L., Xing, M. and Lei, J. 2018. *Chapter 6: Phase Control of TiO_2 Photocatalyst.*

Zhang, J. K., You, K. S., Huang, C. H., Pin-Jyun Shih, P. J. and Liu, D. S., 2022a. Investigations into the Photocatalytic and Antibacterial Activity of the Nitrogen-Annealed Titanium Oxide/Silver Structure. *Coatings,* 12, pp.1-19.
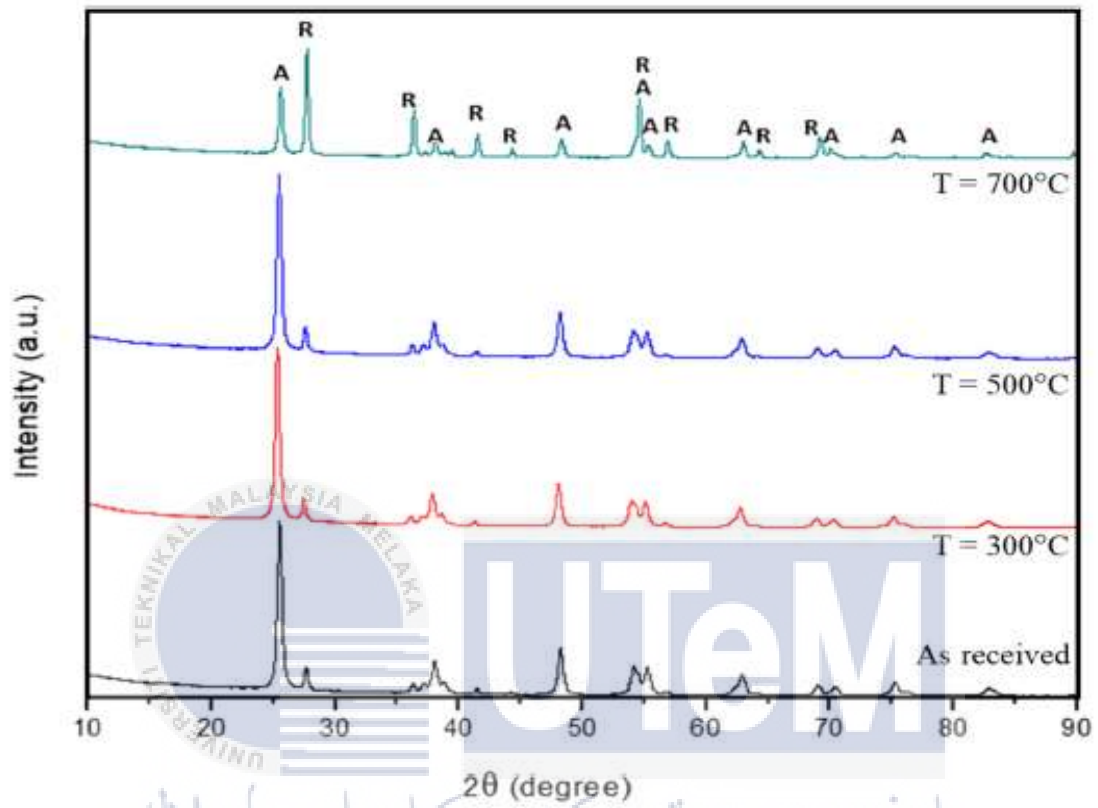
Zhang, Y., Xu, Z., Wu, S., Zhu, A., Zhao, X. and Wang, Y., 2022b. Enhanced Surface Plasmon by Clusters in TiO_2-Ag Composite. *Materials,* 15, pp.1-9.

Zhang, Y., Zhao, X., Fu, S., Lv, X., He, Q., Li, Y., Ji, F. and Xu, X., 2022c. Preparation and Antibacterial Activity of Ag/TiO_2-Functionalized Ceramic Tiles. *Ceramics International,* 48, pp.4897–4903.

Zheng, X., Zhang, D., Gao, Y., Wu, Y., Liu, Q. and Zhu, X., 2019. Synthesis and Characterization of Cubic Ag/TiO_2 Nanocomposite for the Photocatalytic Degradation of Methyl Orange in Aqueous Solutions. *Inorganic Chemistry and Communications,* 110, pp.1-7.

XRD of Pre-calcined Degussa P25 nanoparticles at for 1 hour at constant heatig rate of 10°C/min